University of Alberta

A Low Cost Electronic Nose for Multimedia Applications

by

Rafael Felipe Castro Rodriguez

©

A thesis submitted to the Faculty of Graduate Studies and Research in partial fulfillment
of the requirements for the degree of Master of Science

Department of Electrical and Computer Engineering

Edmonton, Alberta
Fall 2005

Library and
Archives Canada

Published Heritage
Branch

395 Wellington Street
Ottawa ON K1A 0N4
Canada

Bibliothèque et
Archives Canada

Direction du
Patrimoine de l'édition

395, rue Wellington
Ottawa ON K1A 0N4
Canada

0-494-09136-3

Your file Votre référence
ISBN:
Our file Notre reterence
ISBN:

NOTICE:
The author has granted a non-exclusive license allowing Library and Archives Canada to reproduce, publish, archive, preserve, conserve, communicate to the public by telecommunication or on the Internet, loan, distribute and sell theses worldwide, for commercial or non-commercial purposes, in microform, paper, electronic and/or any other formats.

The author retains copyright ownership and moral rights in this thesis. Neither the thesis nor substantial extracts from it may be printed or otherwise reproduced without the author's permission.

AVIS:
L'auteur a accordé une licence non exclusive permettant à la Bibliothèque et Archives Canada de reproduire, publier, archiver, sauvegarder, conserver, transmettre au public par télécommunication ou par l'Internet, prêter, distribuer et vendre des thèses partout dans le monde, à des fins commerciales ou autres, sur support microforme, papier, électronique et/ou autres formats.

L'auteur conserve la propriété du droit d'auteur et des droits moraux qui protège cette thèse. Ni la thèse ni des extraits substantiels de celle-ci ne doivent être imprimés ou autrement reproduits sans son autorisation.

In compliance with the Canadian Privacy Act some supporting forms may have been removed from this thesis.

While these forms may be included in the document page count, their removal does not represent any loss of content from the thesis.

Conformément à la loi canadienne sur la protection de la vie privée, quelques formulaires secondaires ont été enlevés de cette thèse.

Bien que ces formulaires aient inclus dans la pagination, il n'y aura aucun contenu manquant.

Canada

To my mother Emma

Abstract

Multimedia systems are widely used in consumer electronics environments today, where humans can work and communicate through multi-sensory interfaces. Unfortunately smell detection is not yet part of today's multimedia systems. On the other hand, the interest in electronic noses has grown enormously in the last decade and the smell devices have already reached the commercial market targeting several sectors of the world global economy. However, these devices are still too expensive for acquisition by general consumers.

In this thesis, we present a complete design, implementation and evaluation of a low cost electronic nose suitable for integration into multimedia systems and capable to discriminate a large sub-set of commonly occurring smells. The proposed electronic nose system consists of several hardware and software modules. The hardware modules comprise the mechanisms developed to sniff and detect commonly occurring smells. One software module is dedicated to control and interface with the hardware mechanisms and three software modules are dedicated to smell signal processing, smell pattern recognition and performance evaluation over different smell environments.

Acknowledgements

Thanks to all at the faculty of engineering who have made this study possible. First to Dr. Mandal for countless hours of reviews and revisions. Thanks also to the members of my committee Dr. John Feddes, Dr. Marek Reformat, and Dr. Jeremy Sit for their gracious assistance.

From the Department of Agriculture, Food & Nutritional Science, Dr. John Feddes who opened his lab to this work and shared his time. Thanks also to his lab assistant Dwayne Martineau who facilitated some of the smell samples tested in this thesis.

Fellow students Donald Kennedy, great friend from the Project Management course, for awakening my interest in academic writing and letting me know that the Power Plant was also a good place for sharing scientific ideas. Yufei Yuan, Biswaroop Palit and Meghna Singh for expending long companionable hours working in the MCCL lab together. Kenneth Chau from the Photonics lab, for his support and nice exchange of ideas. Thanks to teammates Peter Ajemba and Mujtaba Al Istihad, co-authors, together with Dr. Mandal of my first paper on electronic noses published in the *IEEE Transactions on Consumer Electronics* Journal.

Finally, thanks to my mother, Emma who has always believed in and supported me. To my wife Ruth for her continuous encouragement. To my children Elena, Laura, Pedro and Rafael junior. To my father who gave me a book by Jules Verne that awakened my interest for science. To Vern and Betty Schwab for their kindness and support.

Table of Contents

Chapter 1 Introduction 1

1.1 Objectives 2

1.2 Main Contributions 2

1.3 Outline 3

Chapter 2 Review of Machine Olfaction Systems 5

2.1 The Human Olfactory System 6

2.2 Smell Attributes 9

2.3 Smell Classification 10

2.4 Smell Sensing Materials 11

2.5 Smell Sensors 12

2.6 Electronic Nose Architecture 13

2.6.1 Smell Delivery System 14

2.6.2 Smell Sensing Chamber 17

2.6.3 Smell Sensors Array 18

2.6.4 Sensor Electronics 19

2.6.5 Analog to Digital Conversion Module 21

2.6.6 Selected Electronic Nose Systems 21

2.7 Summary 22

Chapter 3 Review of Smell Signal Processing Techniques 23

3.1 Smell Pattern Analysis Overview 24

3.2 Smell-Signal Transient Regions 28

3.3 Smell-Signal Preprocessing Stages 30

3.3.1 Baseline Manipulation 30

3.3.2 Feature Vector Extraction 31

3.3.3 Feature Vector Normalization 36

3.4 Reducing the Dimensionality of the Feature Space 38

3.4.1 Principal Components Analysis 39

3.5 Pattern Recognition Module 40

3.5.1 Nearest Neighbor Classifier 41

3.5.2 Nearest Mean Classifier 43

3.6 Performance Evaluation Criterion 44

3.6.1 Statistical Re-sampling 44
3.7 Summary 46
Chapter 4 The Proposed Electronic Nose 47
4.1 Introduction 48
4.2 The eNose Smell Space 49
4.3 Hardware System 49
4.3.1 Concentration Flask 51
4.3.2 Smell Delivery System 52
4.3.3 The smell sensors used 54
4.3.4 The smell sensor array 56
4.3.5 Temperature Sensors 59
4.3.6 Smell Sensing Chamber 62
4.3.7 Sensors Interface Board 63
4.3.8 Control Interface Board 65
4.3.9 Cooling Fan 68
4.3.10 Data Acquisition Board 68
4.3.11 The entire eNose hardware system 71
4.4 The Control Panel 72
4.5 The eNose Sniff Cycle 75
4.6 The Smart-Sniff Cycle 77
4.7 Summary 78
Chapter 5 The eNose signal processing system 79
5.1 The Smell-Signal Transient Regions 79
5.2 The Smell-Signal Preprocessing Techniques 82
5.2.1 Baseline Manipulation 84
5.2.2 Feature-Vector Extraction 86
5.2.3 Feature-Vector Normalization 99
5.3 The eNose Software System 99
5.3.1 Smell Signal Processing Module 101
5.3.2 Pattern Analyzer Module 103
5.3.3 Results Plotter 104
5.3.4 The eNose Data Flow 108

5.4 Summary 110
Chapter 6 Performance Evaluation 112
6.1 Experimental Setup 113
6.1.1 Proposed Smell Experiments 113
6.1.2 Smell-Database Collection Method 115
6.1.3 Smell Sampling Methods 116
6.1.4 The Smell Sniff Cycle Settings used 117
6.1.5 The Collected Smell-Databases 122
6.2 Results and Discussion 126
6.2.1 Evaluation Procedure 127
6.2.2 Performance of DIFF_SS_VNORM combination 127
6.2.3 Performance of other combinations 130
6.2.4 Graphical Analysis of different combinations 134
6.2.5 Conclusions 142
6.3 Summary 143
Chapter 7 Conclusions and Future Work 144
7.1 Summary of Contributions 145
7.2 Future Work 145
References 147

List of Figures

Figure 2-1 Schematic of the Human Olfactory System [3] 6
Figure 2-2 A simplified schematic of the smell signal path in the HOS (Adapted from [4]) 7
Figure 2-3 The Olfactory Epithelium with detail of the smell receptors [3] 8
Figure 2-4 Electronic Nose Basic Architecture 14
Figure 2-5 A typical metal-oxide sensor response to a VOM pulse 15
Figure 2-6 Smell Delivery System for a Robot Head [21] 16
Figure 2-7 Sensing chamber for inline arranged sensors 17
Figure 2-8 Sensing chamber design for parallel sensors arrangement [18] 18
Figure 2-9 Voltage Divider for interfacing Metal-Oxide Sensors 19
Figure 2-10 Interfacing circuit for Metal-Oxide Sensors (adapted from [24]) 20
Figure 3-1 Smell Data Analysis Architecture 24
Figure 3-2 Smell signal processing stages. $W_{e,s}[k]$ is the digitized output from the sensors 25
Figure 3-3 A typical smell sensor response showing the transient regions 29
Figure 4-1 Schematic of the proposed eNose 48
Figure 4-2 A simplified schematic of the eNose hardware 50
Figure 4-3 Parts of the Concentration Flask 51
Figure 4-4 Picture and schematic of the Smell Delivery System (top view) 53
Figure 4-5 Photograph of a few selected Figaro gas sensors 54
Figure 4-6 Electrical schematic and specifications of Figaro sensors 55
Figure 4-7 Picture and schematic of the smell sensors array 58
Figure 4-8 Evolution of the temperature inside the chamber during a smelling cycle 61
Figure 4-9 Schematic of the electrical circuit for the temperature sensors 61
Figure 4-10 Photograph of the opened Smell Sensing Chamber 63
Figure 4-11 Photograph of the Sensor Interface Board 64
Figure 4-12 Schematic of the sensors interface circuits 64
Figure 4-13 Control Interface Board 65
Figure 4-14 Schematics of the heater control circuit 66
Figure 4-15 Solenoid valves driver circuits 67
Figure 4-16 Data Acquisition board connections to the Sensor and Control Interface boards 68
Figure 4-17 Simplified schematic of the Data Acquisition board 69
Figure 4-18 The Low Cost Electronic Nose 71

Figure 4-19 The eNose Control Panel Interface 74
Figure 4-20 The structure of the eNose sniff-cycle 76
Figure 5-1 Smell signal transient regions for eNose 81
Figure 5-2 Power spectrum of TGS 880 sensor response to a VOM lemon sample 93
Figure 5-3 Array sensors response to the proposed modulation function 95
Figure 5-4 Power spectrum of the eight sensors signals responses to Coca Cola 98
Figure 5-5 Power spectrum of the eight sensors signals responses to Pepsi Cola 98
Figure 5-6 The Smell-Signal Processing Module 102
Figure 5-7 The Pattern Analyzer Module 103
Figure 5-8 The Results Plotter Module 106
Figure 5-9 Example of a bars-plot graph produced by the Results Plotter 108
Figure 5-10 The eNose Software System data flow 110
Figure 6-1 TM sniff-cycle (a) and standard sniff-cycle (b) responses to Coke VOM 121
Figure 6-2 Bars plot of the detection efficiencies achieved in Experiment #5 137
Figure 6-3 Bars plot of the detection efficiencies achieved in Experiment #1 138
Figure 6-4 Bars plot of the detection efficiencies achieved in Experiment #2 139
Figure 6-5 Bars plot of the detection efficiencies achieved in Experiment #3 140
Figure 6-6 Bars plot of the detection efficiencies achieved in Experiment #4 141

List of Tables

Table 2-1 Linnean's and Zwaardemaker's smells classifications [3] 10
Table 2-2 Lovell's smells classification [3] 11
Table 2-3 Typical material used as sensors [3] 12
Table 3-1 Baseline manipulation techniques 31
Table 4-1 eNose Smell Space 49
Table 4-2 Concentration Flask (parts description) 52
Table 4-3 Components of the smell delivery system 54
Table 4-4 List of the Selected Smell Sensors 57
Table 4-5 Temperature changes observed during a sniff cycle 60
Table 4-6 Sensor Interface board electronic specifications 65
Table 4-7 Control Signals Descriptions 67
Table 4-8 Data Acquisition board signals 70
Table 4-9 Details of the sniff-cycle structure 77
Table 5-1 Description of the eNose smell-signal transient regions 81
Table 5-2 Smell-signal preprocessing techniques used in this thesis 82
Table 5-3 The eNose baseline manipulation techniques 85
Table 5-4 Sniff Cycle settings for the proposed Temperature Modulation Function 96
Table 5-5 Example of a table printout produced by the Results Plotter 107
Table 6-1 Smell Experiments performed for the eNose performance evaluation 115
Table 6-2 Sniff Cycle Settings for the eNose experiments (times are expressed in seconds)119
Table 6-3 Smell Databases 123
Table 6-4 Database classes for Experiments #1 and #2 124
Table 6-5 Database classes for Experiment #3 124
Table 6-6 Database classes for Experiments #5 and #6 125
Table 6-7 Experiment Results 128
Table 6-8 Detailed Results of the eNose Performance Evaluation Experiments 130
Table 6-9 The best and worst performing combination for Experiments #1 and #2 133
Table 6-10 The best and worst performing combination for Exp. #3, #4 and #5 134

List of Abbreviations

ATD	Ascending Transient Derivatives. Features Extraction Tech.
DAS	Dimension Auto Scaling. Normalization Technique
DC	Direct Current
DFT	Discrete Fourier Transform
DIFF	Difference. Baseline Manipulation Technique
DTD	Descending Transient Derivatives. Features Extraction Tech.
eNose	The Electronic Nose proposed in this thesis
FRACT	Fractional Change. Baseline Manipulation Technique
GUI	Graphical User Interface
HOS	Human Olfactory System
LOG	Logarithmic. Baseline Manipulation Technique
LOO	Leave-One-Out. Re-sampling Technique
METS	Multi-Exponential Transient Spectroscopy
MOS	Metal Oxide Semiconductor
MOSFET	Metal-Oxide Field Effect Transistor
N-CV	N-Fold Cross Validation. Re-sampling Technique
N-MEAN	Nearest Mean. Pattern Recognition Algorithm
NN	Nearest Neighbor. Pattern Recognition Algorithm
NOBM	No Baseline Manipulation Technique was applied

NOFEXT	No Features Extraction
NOFSEL	No Features Selection
NONR	No Normalization Technique was applied
PCA	Principal Component Analysis
PFV	Prototype Feature-Vector
RAW	Raw Voltage Signal. Sensor Output Parameter
REL	Relative. Baseline Manipulation Technique
STD	Steady Transient Derivatives. Features Extraction Technique
SS	Steady State. Features Extraction Technique
TC	Time Constants. Features Extraction Technique
TM	Temperature Modulated
TMDFT	Temperature Modulated DFT. Features Extraction Technique
TMWSD	Temperature Modulated WSD. Features Extraction Tech.
VAS	Vector Auto Scaling. Normalization Technique
VNORM	Vector Array Normalization. Normalization Technique
VOM	Volatile Odorous Molecules
WSD	Whole Signal Derivatives. Features Extraction Technique

Chapter 1

Introduction

An electronic nose can be generally defined as an electronic instrument consisting of a multi-sensor array module and a pattern recognition module that is capable of recognizing simple or complex odors.

One of the earliest instruments able to produce electrical signals in the presence of a smell source was reported by Moncrief in 1961 [1]. He used a single coated thermistor as the smell-sensing unit but postulated that the use of an array of six differently coated thermistors would increase the range and discrimination between smells. Twenty years later, in 1987, J. W. Gardner used for first time the term "electronic nose" in a landmark paper titled "*Pattern recognition in the Warwick Electronic Nose* [2].

Electronic noses have reached the commercial market targeting several sectors of the world global economy such as food, perfumery, health and environmental applications. Human noses are also used in commercial applications. However, the measurements realized with human nose panels are much more expensive and can be affected by subjective factors such as the association of smell with pleasant or unpleasant memories.

The interest in electronic noses has grown enormously in the last decade and new researchers and merchants are joining the machine olfaction community. However, these devices are still too expensive for acquisition by the general consumer. As a result these noses are not yet suitable for integration with multimedia systems.

1.1 Objectives

This thesis aims to explore the feasibility of design and construction of the hardware and software modules for a low cost electronic nose. The electronic nose presented here can discriminate a large sub-set of commonly occurring smells such as foodstuffs, beverages, plants and perfumes. It can be made accessible to the general consumer, and it can be produced using inexpensive off-the-shelf components. More specifically the main objectives of this thesis are as follows:

- Review of the existing smell detection techniques and their limitations.

- Design and development of a low cost electronic nose, which is easy to assemble and will recognize at least ten different smells from commonly occurring odours.

- Design and development of a software system to allow the analysis and performance evaluation of several smell signal processing techniques and pattern recognition algorithms. The software system must be expandable allowing easy integration of more smell signal processing techniques and smell-pattern analysis methods into the current developed framework.

1.2 Main Contributions

In this thesis, we present a complete design, implementation and testing of an electronic nose suitable for integration into multimedia systems, which can be made accessible to general consumers at a very low cost.

There are four main contributions of this thesis into the area of machine olfaction:

- A low cost electronic nose suitable for integration with multimedia systems has been implemented and tested.

- A software system that serves as development infrastructure for further research in the area of smell detection has been implemented and tested (see Section 5.3).

- An efficient smell sniffing technique for machine olfaction applications has been proposed, implemented and tested (see Section 4.7).

- An efficient variant (STD) of the signal derivative technique used for feature-vector extraction has been proposed and tested with good results (see Section 5.2.2.3.3).

1.3 Outline

This thesis studies the feasibility of design and construction of a low cost electronic nose suitable for integration into multimedia systems. In Chapter 2, a review of the human olfactory system (HOS) and the machine olfaction systems is presented. The anatomy of the HOS and the biological processes to detect the volatile odorant molecules (VOM) is presented first, which is followed by a brief discussion on the sensing materials, smell sensor types and the simplified architecture of an electronic nose. Finally, a review of a few selected implementations of different machine olfaction systems is presented.

In Chapter 3, a comprehensive review of the smell signal processing techniques, pattern recognition algorithms and validation procedures commonly used in machine olfaction is presented. An exhaustive discussion of commonly used smell-signal processing techniques is presented first, which is followed by a detailed review of two simple but powerful pattern recognition techniques. Finally, the performance evaluation techniques commonly used in machine olfaction systems are introduced.

In Chapter 4, the proposed low cost electronic nose (eNose) design suitable for integration with multimedia systems is presented. A detailed explanation of the hardware modules and the software interface needed to control this hardware is first presented, which is followed by a detailed explanation of the eNose smell sniff-cycle characteristics. Finally, a novel smell sniff technique for machine olfaction applications is proposed.

In Chapter 5, the signal processing techniques and the GUI software system modules implemented in the proposed electronic nose are presented. The characteristics of the smell signals produced by the eNose hardware is first presented, which is followed by a detailed explanation of each smell-signal preprocessing techniques implemented in the eNose system.

Finally, the GUI software system that computes the signal processing and the analysis of the extracted smell-pattern are briefly reviewed.

In Chapter 6, the performance achieved by the proposed eNose in several machine olfaction application areas is presented. The working environments for testing and evaluation are first outlined followed by the description of the evaluation procedures. Finally, the performance achieved by the eNose in the outlined smell experiments and the influence of different combinations of signal processing techniques is presented and briefly discussed.

The conclusions and future work is presented in Chapter 7 followed by the References with the list of papers and books referenced in this thesis.

Chapter 2

Review of Machine Olfaction Systems

An ideal machine olfaction system is a system that closely mimics the human olfactory system. The current machine olfaction systems typically use an array of gas sensors to detect the presence of odorous substances and pattern recognition techniques to identify the smell produced by these substances.

In this chapter, we present a comprehensive review of the human olfactory system (HOS) and the machine olfaction systems. The organization of this chapter is as follows. In Section 2.1, we present the anatomy of the HOS and the biological processes to detect the volatile odorant molecules (VOM). Section 2.2 follows with a brief discussion on the parameters commonly used to characterize smells. In section 2.3, we present a few popular smell classification systems. In Sections 2.4 and 2.5, several sensing materials, sensing parameters and smell sensor types are briefly reviewed. In Section 2.6, we describe a simplified architecture of an electronic nose. In Section 2.6.6, we present a few selected implementations of different machine olfaction systems.

2.1 The Human Olfactory System

The human olfactory system includes more than five millions smell receptors and specialized neurons. A simplified schematic of a typical human olfactory system (HOS) is shown in Figure 2-1. The smell detection process is as follows. The odorant molecules reach the olfactory epithelium after following a spiral trajectory through the turbinated bones. When the smell receptors, which are embedded inside the olfactory epithelium, come into contact with the odorant molecules, an electrochemical signal is generated and sent to the olfactory bulb. In the olfactory bulb, the signal is first preprocessed and then sent to the forebrain systems (the thalamus and the hypothalamus) where the final smell recognition takes place.

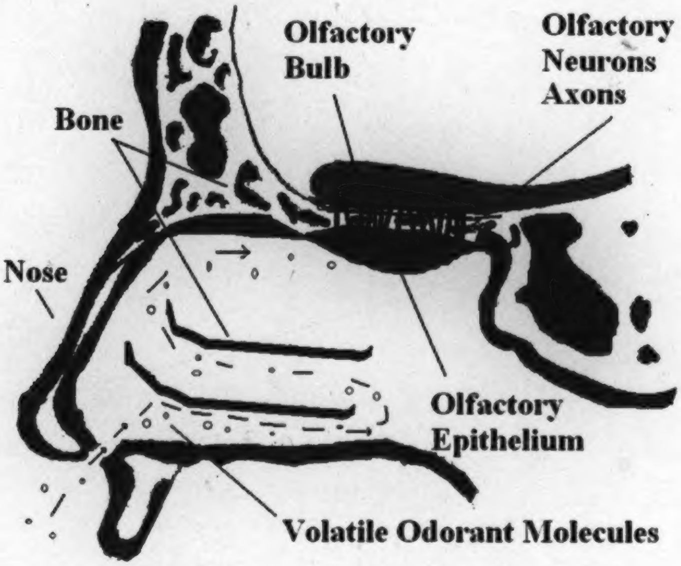
Olfactory
Bulb
Olfactory
Neurons
Axons
Bone
Nose
Olfactory
Epithelium
Volatile Odorant Molecules

Figure 2-1 Schematic of the Human Olfactory System [3]

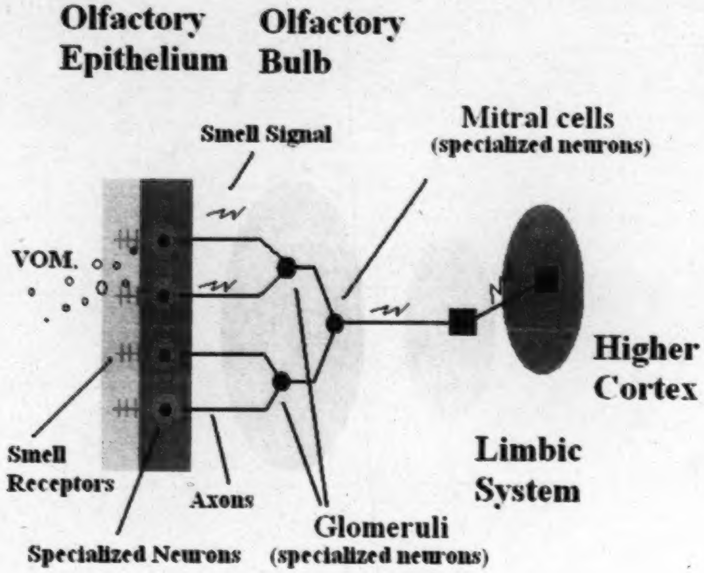
Olfactory Epithelium
Olfactory Bulb
Smell Signal
Mitral cells (specialized neurons)
VOM.
Higher Cortex
Limbic System
Smell Receptors
Axons
Glomeruli (specialized neurons)
Specialized Neurons

Figure 2-2 A simplified schematic of the smell signal path in the HOS (adapted from [4])

When a VOM excites the smell receptors (see Figure 2-2), the generated electrochemical signal travels along the axons and is transferred to the neurons in the olfactory bulb, where it travels through different layers of specialized neurons (for preprocessing) until it is outputted from the olfactory bulb to the forebrain. The *olfactory bulb* is located in the front of the brain and from it the smell signals are both relayed to brain's higher cortex (which handles conscious thought processes) and limbic system (in *central nervous system* which generates emotional feelings). This makes it possible for smells to evoke powerful emotional responses as well as convey factual information [3].

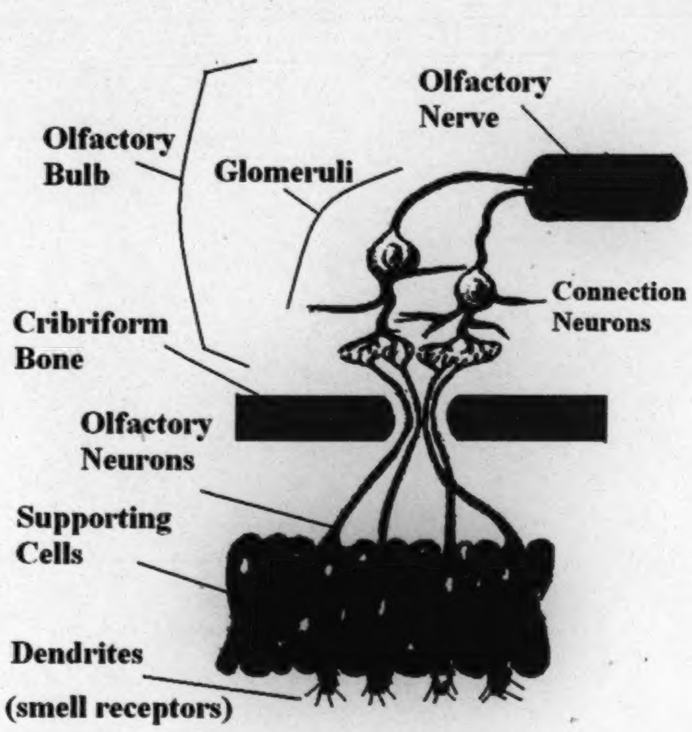
Olfactory Nerve
Olfactory Bulb
Glomeruli
Connection Neurons
Cribriform Bone
Olfactory Neurons
Supporting Cells
Dendrites
(smell receptors)

Figure 2-3 The Olfactory Epithelium with detail of the smell receptors [3]

A detailed schematic of an olfactory epithelium is shown in Figure 2-3. It is observed that the olfactory epithelium contains the olfactory receptors, which are the dendrites of a layer of first order specialized neurons. The olfactory neurons are arranged in parallel and have large axons that penetrate through the thin holes in the *cribriform bone*. The axons diverge but terminate on the surface of the olfactory bulb where there is a first layer of second order specialized neurons called *glomeruli*. The *glomeruli* neurons interconnect with the axons of the olfactory neurons carrying out some primary signal processing.

It is known that a typical HOS contains several millions receptors of approximately 1000 different types. These receptors together can detect up to 5,000 different smells with 98% accuracy. Human smell detection is based on a combinational scheme where a different number and type of smell receptors are activated in the presence of a particular smell. As a result, small changes in the chemical structure of a gas will activate a different combination of receptors. That is why octanol smells like oranges, while a similar compound, octanoic acid, smells like sweat. It has also been found that large amount of VOM affect larger number of receptors, which may change the smell perceived from this chemical. In other words, a small amount of VOM might smell flowery while a large amount of the same VOM might smell putrid

2.2 Smell Attributes

A smell is typically characterized by attributes such as Intensity, Character, Hedonic tone and Concentration [5].

These attributes are subjective and in most cases depend on the previous personal experience of an individual. Therefore, in order to measure these attributes accurately it is necessary to put together several human panels to evaluate and rank them. A brief explanation of each smell attribute is given below.

The *intensity* of a smell is difficult to measure as it is influenced by other attributes such as character, hedonic tone and concentration. The intensity is measured by comparing the intensity of a given odorous sample to the intensity of the reference odorant, which is usually n-butanol, at different concentrations.

The *character* is expressed using descriptors such as minthy, earthy and fishy. The character of a smell is the base of most smell classification systems.

The *hedonic tone* is subjective and related to the experience of the human subjects evaluating the smell. The hedonic tone is independent of the smell character and refers to the degree of pleasantness or unpleasantness. It is usually measured by using a 10 points scale (from –5 to +5).

The *concentration* is defined as the mass concentration of pure odorous substances or odor dilution required to reach the detection level. At the concentration of the detection level a given smell has a 50% detection probability.

2.3 Smell Classification

It is difficult to express a smell in terms of simpler smells as it is done with other perceptual attributes such as color. It is widely known that the human visual system has 3 types of cone cells (to detect three primary colors: red, green, and blue). As a result, an arbitrary color can be expressed in the form of these primary colors. However, no evidences have been found regarding any primary smell detected by the HOS. Therefore, several smell classification systems have been proposed in order to help the communication between individuals working in smell research areas and smell related industries.

Some of these smell classifications systems were proposed more than 200 years ago [6]. Linnaeus proposed one of the earliest smell classifications in 1752. He grouped smells into seven classes based on their appeal (see Table 2-1). Zwaardemaker's classification, made in 1895 expanded Linnaeus's classifications to include two classes: Ethereal and Empyreumatic.

Table 2-1 Linnean's and Zwaardemaker's smells classifications [3]

LINNAEAN AND ZWAARDEMAKER CLASSES	EXAMPLES
Aromatic	Camphor, spices, anise, citron, almond
Fragrant	Flowers, vanilla, balsam
Ambrosiac	Musk, amber
Alliaceous	Onion, garlic, acetylene, iodine
Hircine	Goaty smells, cheese, sweat, chestnuts
Foul	Narcotics, and some bugs
Nauseous	Carrion, carrion flower, faeces
Ethereal	The fruity ethers of perfumes, beeswax, ether
Empyreumatic	Roasted coffee, tobacco smoke, naphthalene

In 1923, Lovell proposed another smell classification (see Table 2-2) where smells were divided into eight groups based on smell sources. Although this classification is incomplete since it does not cover all the commonly occurring smells, it meets the requirements of most consumers such as beekeepers, agriculturalists and naturalists.

Table 2-2 Lovell's smells classification [3]

LOVELL CLASSES	EXAMPLES
Sweet Flowers	Honey, apricot
Fruit	Apple, pear
Aromatic or Spicy	Cloves, ginger
Musk	Musk mallow
Onion and Alliaceous	Onion, garlic
Rank	Goat smell
Foul	Bugs, opium.
Nauseous	Urine, putrid fish

The classifications mentioned above are neither detailed nor complete enough to cover most commonly occurring smells. Several classifications, mostly from the standpoint of perfumery, have been developed in the last few decades. There are individual differences in human smell perception and the debate on the right classification will continue. However, for the multimedia applications, classification of smells into 50-200 groups will be easily manageable, while achieving a reasonably good accuracy.

2.4 Smell Sensing Materials

As smells are typically generated and transmitted by gaseous molecules, gas sensors are used for their detection. Gas sensors are generally developed with materials whose properties also change when exposed to smell-producing gas. The following properties are typically exploited in smell detection [7]:

a) Capacitance

b) Mass difference

c) Frequency dependent optical absorption or reflection

d) Voltage, temperature and frequency dependent conductivities and complex impedances

e) Frequency dependent electrochemical potential differences and currents.

Several materials are used in the fabrication of sensors and these include metals, semiconductors, ionic compounds, and organic compounds such as enzymes and polymers. Table 2-3 shows various types of materials typically used for smell sensors.

Table 2-3 Typical material used as sensors [3]

TYPE OF MATERIAL	EXAMPLES
Metals	Pt, Pd, Ni, Ag, Au, In, Ga, Rh, Sb
Semiconductors	Si, GaAs, InP, $NiFe_2O_4$
Electronic conductors	SnO_2, TiO_2, Ta_2O_5
Mixed conductors	Ga_2O_3, WO_3, IrO_x
Ionic conductors	ZrO_2, LaF_3, CeO_2, CaF_2, Na_2CO_3
Crystals	PbPc, $LuPc_2$, $(PcAlF)_n$
Polymers	Phthalocyanines, polydiacetylenes

2.5 Smell Sensors

Although, there are several types of sensors, in industrial gas sensing applications, the semiconductor and metal sensors are widely used. P-type semiconductor is effective in sensing oxidizing gases whereas the n-type semiconductors are generally used to detect gases such as hydrogen and methane.

The metal-oxide semiconductor (MOS) based sensors are also very popular because of their low cost and availability. They have been used in several industrial and research applications such as beverages, perfumery and food industries. Olaffsson et al [8] used an array of 4 MOS sensors to determine the freshness of fish (e.g., cod, haddock). Tan *et al.* [9] used 6 MOS sensors to discriminate various kinds of sausage meats. Aishima applied 6 MOS to discriminate café arabica and café robusta [10] and also to discriminate various types of alcoholic drinks [11]. Gardner *et al.* [12] applied 12 MOS sensors to discriminate between different blends and roasts of coffee.

The semiconductor-based gas sensors can be manufactured using microtechnology. The sensors manufactured with this technology have several advantages over other bulky sensors, such as high productivity, low cost and low power consumption [13]. Note that most gas sensing materials have a narrow sensing range for gases. Therefore, many systems designed to detect more than one smell producing gases use arrays of micro-sensors instead of a single sensor.

Polymer based smell sensors are also of widespread use in machine olfaction systems [14], [15], [16]. These sensors are attractive because they do not need to be heated at high temperatures as the MOS sensors do. Moreover, polymer sensors have high sensitivity to different polar compounds in contrast to MOS sensors, which respond poorly to these compounds. The main disadvantage of polymer sensors is their high sensitivity to minor changes in the ambient humidity, their poor fabrication reproducibility from batch-to-batch and generally slower response times than MOS sensors.

2.6 Electronic Nose Architecture

Electronic noses make use of gas sensor arrays and well-known pattern recognition techniques in order to detect and identify the smells. The sensors in the array have broad and overlapping selectivities, which allows for detection of a wide range of smells. The sensor array response is preprocessed and used by the pattern recognition system as an electronic fingerprint to characterize the smell.

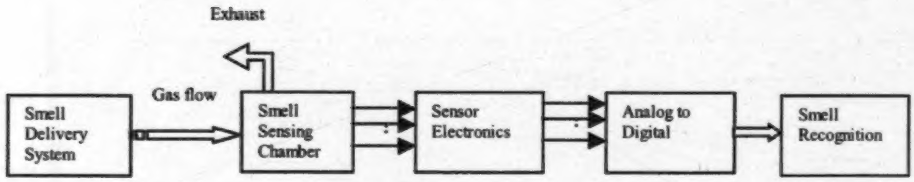

Figure 2-4 Electronic Nose Basic Architecture

The basic architecture of a typical electronic nose system is depicted in Figure 2-3. The Smell Delivery system takes the VOM- example from the smell-source and brings it into contact with the array of smell sensors within the smell-sensing chamber. When the VOM-example impacts upon the surface of the s different sensors in the array, the chemical reactions between the odorant molecules and the active surface of the sensors modify some physical property of the sensing materials (e.g., electrical resistance). The signal generated by the sensor is then modified and converted into a useful electrical signal $V(t)$ by the sensor electronics. The signal $V(t)$ is proportional to the sensing parameter changes (see Figure 2-5). The analog electrical signal is then converted into a digital signal $W[k]$ in the analog to digital module, which permits for rapid computation and recording of the sensor response parameters. Finally, in a computerized stage, the digitized smell-signals are preprocessed and fed into the selected pattern recognition algorithm for the final smell recognition.

2.6.1 Smell Delivery System

The delivery system brings the VOM-examples into the sensor chamber. The delivery systems can be divided into two broad categories: *sample flow* systems and *static sampling*. In the sample flow systems the sensors are placed in the vapor flow, which allows a rapid chemical exchange of the vapor in the sensor surfaces. In static sampling systems, there is no vapor flow around the sensors and the sensors are usually exposed to vapor at constant concentration.

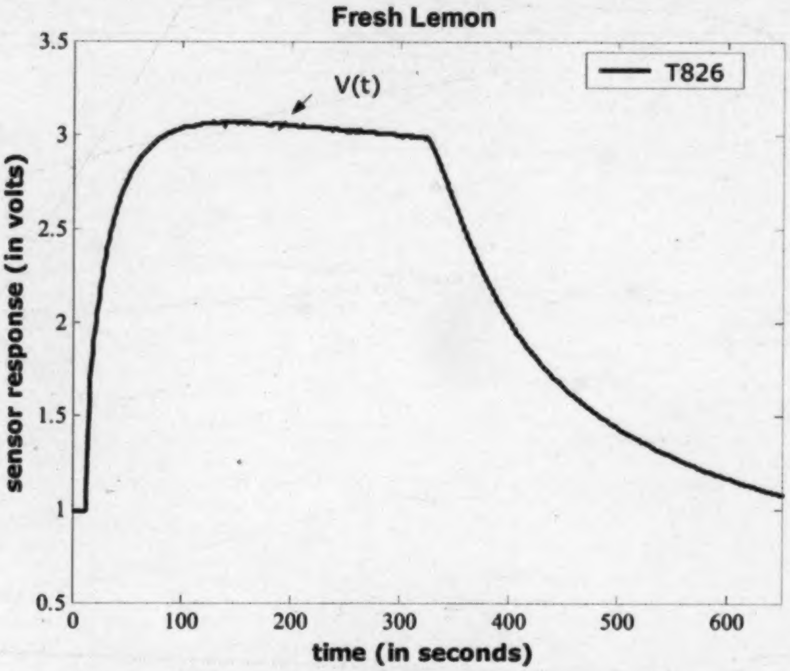

Figure 2-5 A typical metal-oxide sensor response to a VOM pulse

The *Sample flow system* is the most popular smell delivery system method. A generic sample flow delivery system may use an automated pump with flux volume, speed control and humidity and temperature regulation. These will ensure the repeatability of the measurements and minimize sensor's drifts. Several sample flow system methods such as headspace sampling, bubbler and sampling bag methods have been developed. In this thesis, we have mostly used headspace sampling method and bubbler methods. However, for a few experiments, it was necessary to use the sampling bag method (see Section 6.1.3).

The headspace sampling method is an easy method to implement [17], [18]. Here, a carrier gas is passed through a concentration vessel containing the smell sample and then into the sensor chamber. The carrier gas (usually an inert gas, such as nitrogen) will drag the VOM and transport them into the sensor's chamber. The distance between the smell source surface and the tubes that carry out the smell and the carrier gas must be kept constant because the vapor concentration inside the concentration flask varies according to its distance from the source surface. The bubbler method is very similar to headspace sampling but the carrier gas is forced through the liquid smell source and the vapor is generated by bubbling and taken away by the carrier gas into the smell sensor chamber. The sampling bag method is usually employed when the smell source cannot be brought close to the electronic nose. In this method, a bag made of an inert material such as Tedlar keeps a large volume of VOM that was previously extracted from the smell source. The bag is connected to the smell inlet of the delivery system and the VOM examples are then drawed directly from the bag. In this method no carrier gas is used.

In *static sampling* a few micro liters of the liquid smell source is taken manually with a syringe and injected into the sensor chamber [19], [20]. A small fan stirs the air inside the sensor chamber in order to guarantee uniformity in the mix. The sensor chamber volume is much larger than the volume of sample used, typically in the order of a few liters. Static measures (steady-state) of the sensor response are taken after the liquid has totally evaporated and the equilibrium has been reached. The static sampling smell delivery system approach is time consuming, and may not be very precise.

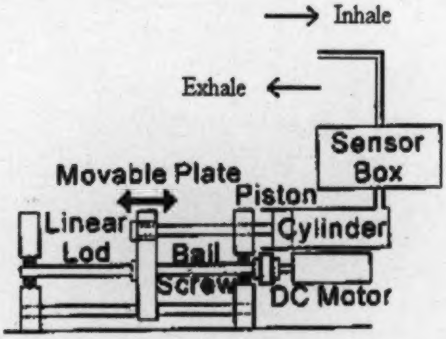

Figure 2-6 Smell Delivery System for a Robot Head [21]

A simple implementation of a sample flow smell delivery system design that was proposed by Miwa et al. [21] is shown in Figure 2-6. Here, they mimicked the human respiratory system in their implementation of a smell delivery system for their robot head. A small DC motor and a ball screw mechanism (similar to that of an old floppy drive unit). The smell delivery component consists of four sets of pistons that make the air move into the nose passing through the sensors-box and arrives to the lung. The air is then directly breathed out through the same input path. The lung volume is 3700 cm^3 and the airflow rate is 6100 cm^3 per second.

2.6.2 Smell Sensing Chamber

The smell-sensing chamber is one of the most important parts of the smell delivery system. Its design determines the response time of the sensors because a sensor response is influenced by its position within the chamber relative to the smell sample flow. The internal volume of a smell-sensing chamber should be as small as possible in order to minimize the effects due to the sensors position. However, when the sensor response is slow enough, the impact of sensor's position can be ignored. Two widely used types of sensing chamber designs are shown in Figure 2-7 and Figure 2-8.

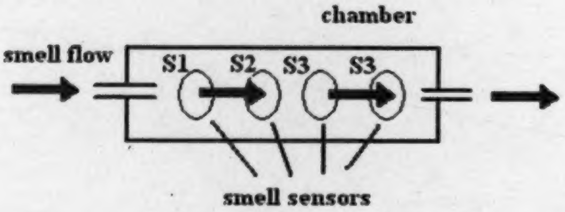

Figure 2-7 Sensing chamber for inline arranged sensors

A very popular inline arrangement of the smell sensor within the smell-sensing chamber is shown in Figure 2-7. The smell sampled from the concentration vessel flows over the sensors surfaces. Theoretically, sensor S1 will produce a response before sensors S2 and S3. However, it also depends on the response time of sensor S1 compared to that of the sensors S2 and S3.

The materials used to build the sensing chamber should be inert to the gases being tested to avoid interference in the measurements. The most popular choices are stainless steels, Teflon derivatives and glass. Each of these materials has its pros and cons. For example, stainless steel is very difficult to machining but it is a good heat conductor and inert to almost all chemicals.

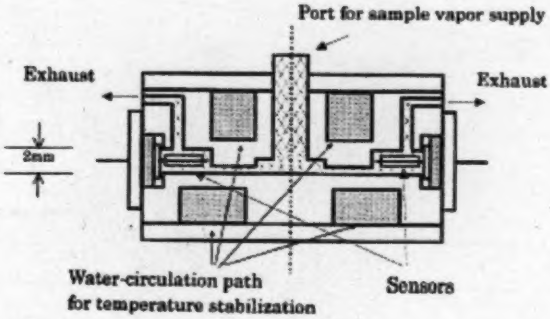

Figure 2-8 Sensing chamber design for parallel sensors arrangement [18]

An implementation of a sophisticated smell sensing chamber (see Figure 2-8) was developed by Nakamoto et al. [18]. Here, both sensors will receive the odorant molecules at the same time. Note the small active volume inside the chamber. This characteristic guarantees fast response time because all smell molecules are efficiently blown over the sensors surfaces. In addition, the dead volume, which is responsible for performance degrading turbulences, is minimized. In this design, a flow of water through special paths embedded in the chamber is used to keep the sensors at a controlled temperature.

2.6.3 Smell Sensors Array

The smell-sensing unit of an electronic nose is built around an array of several gas sensors placed together inside the smell-sensing chamber. This is necessary because the gas sensors have partial sensitivities and respond broadly to a range of gases rather to a specific one. Therefore, by using several sensors the selectivity of the smell recognition system can be improved and the system will accurately discriminate among a wider range of smells.

2.6.4 Sensor Electronics

The sensor electronic circuits are responsible for interfacing and conditioning the sensor response. The purpose of the sensor interfacing is to produce an electrical signal that reflects the changes in the sensor parameters being measured. The conditioning electronics are responsible for buffering, amplification and filtering of the electrical signal produced by the interfacing circuitry.

One parameter per sensor type is typically selected by the interfacing electronic in order to simplify the circuitry. The conductivity, resistance and frequency changes are the most commonly chosen sensing parameters used by electronic noses. However, larger smell-spaces can be represented if several smell sensors of different types are combined together in the sensor array or if more than one sensing parameter per smell sensor is chosen for measuring by the interfacing electronic. However, this can lead to an extremely complex electronic circuitry [22], [23].

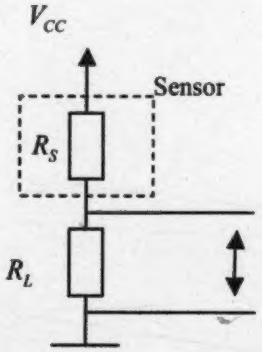

Figure 2-9 Voltage Divider for interfacing Metal-Oxide Sensors

A standard circuit for measuring large resistance changes is the voltage divider, which is widely used with metal-oxide gas sensors due to its simplicity. In this circuit (see Figure 2-8) the unknown sensor internal resistance R_s is connected in serial connection with a known load resistance R_L through a constant voltage supply V_{CC} and ground. Therefore, the current through the sensitive element and the load resistance becomes:

$$I_s = \frac{V_{CC}}{R_s + R_L} \tag{2-1}$$

Changes in the sensor resistance are then proportional to the V_L (the voltage across the load resistor R_L). Therefore, by measuring V_L and applying Ohm's law $(V = IR)$ we can calculate the changes produced in the sensing resistance by the odorant under test. Some sensors need additional interfacing circuitry in order to control vital operation parameters, such as the work-temperature operating point in metal-oxide gas sensors.

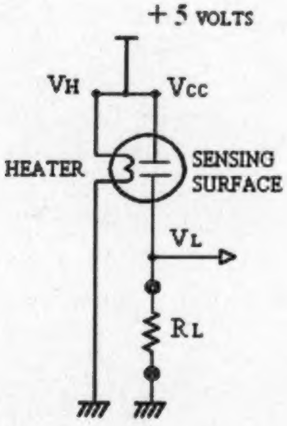

Figure 2-10 Interfacing circuit for Metal-Oxide Sensors (adapted from [24])

A schematic of the metal-oxide interfacing electronics including the sensors heater circuit recommended by the manufacturer [24] is shown in Figure 2-10. Metal-oxide sensors are commonly operated in the isothermal mode, in which the work-temperature is kept constant during exposure to smells. The simplest method is to implement a pseudo isothermal control, in which the sensors heater (a heating resistance buried into the sensing surface) is kept at a constant voltage V_H. However, in some implementations where modulation of this voltage is achieved a more sophisticated interfacing circuits is used.

2.6.5 Analog to Digital Conversion Module

In this module, the analog voltage signals produced by the sensor interfacing electronics are sampled (quantized and digitized) in order to feed them into the computerized modules where further digital signal preprocessing and final smell recognition is performed.

Here, the signal $V(t)$ produced by sensor s in response to a given VOM-example e (see Figure 2-5) is converted into the digital signal $W[k]$ such that $t = kT_0$ and $1 \leq k \leq N_k$, where T_0 is the selected sampling interval in seconds and N_k is the number of data points acquired per VOM-example.

Sampling rates between one sample-per-second ($T_0 = 1s$) to one sample-every-ten-seconds ($T_0 = 10\,s$) are typically used by the analog-to-digital conversion modules of most machine olfaction systems. This is because, the response voltage signals delivered by the sensor interfacing electronics change at slow rates since they reflect the slow chemical processes that take place between the odorant molecules and the smell sensing surfaces.

2.6.6 Selected Electronic Nose Systems

A few smell-sensing instruments have been developed in narrow applications. Moncrief [1] developed one of the first smell detection instruments in 1961 for agricultural application, where he used a single coated thermistor as the smell sensor. In 1964, Wilkens and Hartman [25] developed a smell detector where an array of eight electrochemical sensors was used.

The first intelligent electronic smell sensing systems appeared in late 1980's. Gardner [26] used pattern recognition techniques to discriminate the output of electronic smell sensors. Hatfield *et al* [19] described an integrated circuit based device that performs data acquisition from a miniature array of 32 conducting polymer gas sensors. David *et al* [27] designed a circuit capable of measuring signals from arrays of resistive and piezoelectric sensor types in the same board. Chueh and Hatfield [28] presented a sensor electronics circuit coupled with a hand-held computer that allows real-time field measurement of gas smells.

Miwa et al. [21] built a robot head that displays a reaction in the presence of some smells (e.g., alcohol and cigarette smoke). The sensor array comprises only 4 metal oxide gas sensors. The recognition algorithm uses a look-up table that contains sensor outputs and their derivatives. Mizsei and Ress [29] developed a system that converts the output signals of a gas sensor array into pixel elements displayed as a 2-D image. The sensor electronics is based on a scanning version of a vibrating capacitor (Kelvin probe). The sensor array comprised of several receptors material strips on a ceramic subtract that are asymmetrically heated.

2.7 Summary

In this chapter, we first presented the anatomy of the human olfactory system and the biological processes involved in smell sensing. It was followed by a brief discussion on odorant substances, the parameters commonly used to characterize smells and a few smell classification systems. The smell sensing materials and the sensing parameters were then reviewed before describing the basic architecture of an electronic nose. Finally, a few implementations of different machine olfaction systems were presented.

Chapter 3

Review of Smell Signal Processing Techniques

In the previous chapter we presented the anatomy of the human olfactory system and the basic architecture of an electronic nose. In this chapter, we present a comprehensive review of the smell signal processing techniques, pattern recognition algorithms and validation procedures used in the machine olfaction field. These techniques have been used to discriminate between various smells, different concentrations of the same smell and to identify individual odorant components in a specific blend of volatile odorous molecules.

The organization of this chapter is as follows. In Section 3.1, we present an overview of a typical electronic nose signal processing modules. We also define here, some of the mathematical notation that will be used in the rest of this thesis. In Section 3.2, we present the typical sensor response focusing on its transient regions. Section 3.3 presents an exhaustive discussion of the most commonly used smell-signal preprocessing techniques. A brief review of the Principal Component Analysis technique, which is used to remove the collinearity between the selected features, is presented in Section 3.4. In Section 3.5, we present details of two simple but powerful pattern recognition techniques: the nearest-mean and the nearest-neighbor. Finally, in Section 3.6, the performance evaluation techniques commonly used in machine olfaction systems are briefly reviewed.

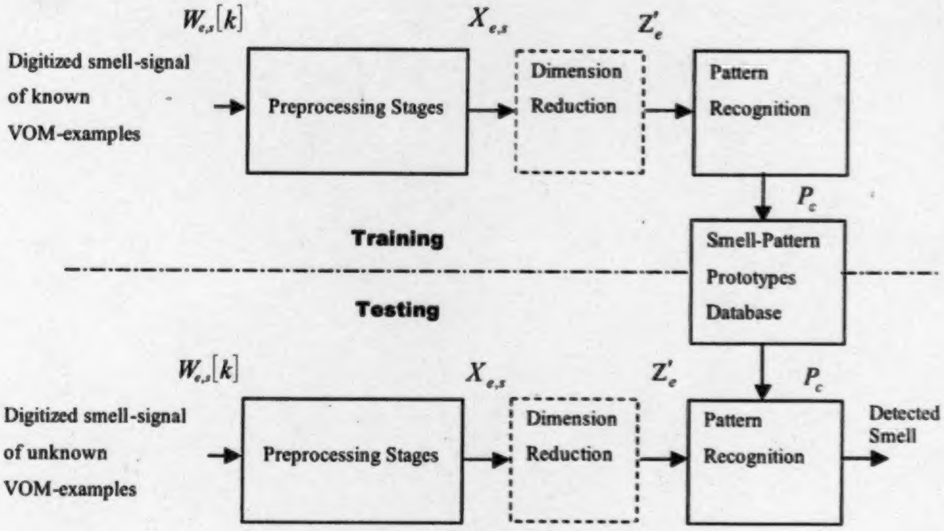
$W_{e,s}[k]$
$X_{e,s}$
Z'_e
Digitized smell-signal of known VOM-examples
Preprocessing Stages
Dimension Reduction
Pattern Recognition
P_c
Training
Smell-Pattern Prototypes Database
Testing
$W_{e,s}[k]$
$X_{e,s}$
Z'_e
P_c
Digitized smell-signal of unknown VOM-examples
Preprocessing Stages
Dimension Reduction
Pattern Recognition
Detected Smell

Figure 3-1 Smell Data Analysis Architecture

3.1 Smell Pattern Analysis Overview

The general architecture of the smell data analysis process for machine olfaction is shown in Figure 3-1. In general, machine olfaction systems work in one of two operation modes: the training (learning) mode and the classification (testing) mode. In the learning mode, the system is programmed to recognize the set of smell-classes that are specific to a given smell environment. In the classification mode, the system classifies the unknown incoming smells into one of the previously learned smell-classes.

Training an electronic nose in a new smell environment is a three-step process. First, a database containing many smell-examples from the smell-classes defined in the smell environment is collected. Here, a smell-example is a data file containing the digitized smell sensor response signals $W_{e,s}[k]$ corresponding to one sample of the VOM from a given smell-source. Second, each example in this database is preprocessed in order to obtain its smell-pattern (feature-vector) Z_e. Optionally, an additional processing stage can be applied to reduce the dimensionality of each feature-vector. Third, the pattern recognition system is trained using these smell-patterns. The pattern prototypes that characterize each smell-class in the given smell environment are obtained in this step. These class prototypes P_c are saved for later use in the classification process.

The classification of an unknown smell is a three step process that is typically applied after the electronic nose has been trained in the given smell environment. In the first step, the unknown VOM-example is sniffed and converted into a digitized VOM-example $W_{e,s}[k]$ by the electronic nose. In the second step, this digitized output ($W_{e,s}[k]$) is sent to the preprocessing module where it is processed in order to produce its smell- pattern. The same preprocessing techniques that were applied during the training process (including the same dimensionality reduction technique) are applied in this step. Finally, the unknown smell-pattern is sent to the pattern recognition module where it is processed according to the specific pattern recognition algorithm and classified into one of the previously learned class prototypes or rejected as a dubious smell.

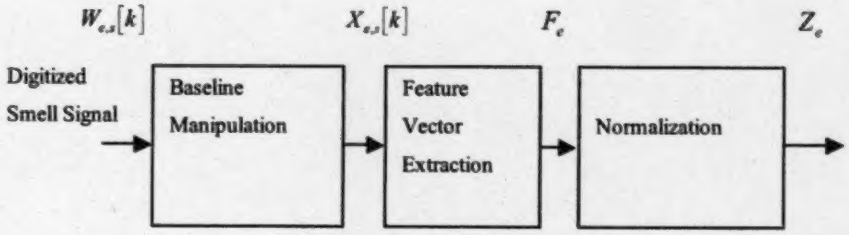

Figure 3-2 Smell signal processing stages. $W_{e,s}[k]$ is the digitized output from the sensors

The most commonly used smell-signal preprocessing techniques for machine olfaction systems are shown in Figure 3-2. The digitized sensor responses $W_{e,s}[k]$ undergo a three-step preprocessing stage before being fed into the pattern recognition module. These signals are first pre-processed relatively to their baselines in the Baseline Manipulation module. The most informative features are then extracted from the smell-signal and the feature-vector F_e is assembled in the Feature-Vector Extraction module. Normalization procedures are finally applied to ensure that the magnitudes of all the features are limited to a specific range of values appropriated for input into the selected pattern recognition algorithm. The dimensionality of the normalized feature-vector Z_e can then optionally be reduced to a smaller size by a feature-extraction technique such as Principal Component Analysis (PCA) or Linear Discriminant Analysis (LDA) obtaining the feature-vector Z'_e.

In order to facilitate the mathematical formulation for each of the different signal processing techniques that will be reviewed, we use the following notation:

N_e: The number of samples (measurements) contained in a smell-database

N_s: The number of sensors in the proposed electronic nose

N_k: The number of data points acquired per VOM-example

T_0: The sampling interval in seconds

$V_{e,s}(t)$: The electrical signal generated by sensor s, $(1 \leq s \leq N_s)$ in response to the given VOM-example e, $(1 \leq e \leq N_e)$

$W_{e,s}[k]$: Digitized version of $V_{e,s}(t)$, where $t = kT_0$ and $(1 \leq k \leq N_k)$

$X_{e,s}[k]$: The output of the baseline manipulation preprocessing stage, which is the baseline-relative version of $W_{e,s}[k]$

N_f: The number of features extracted from the response of a sensor s

N_m: The number of features extracted from the array response $X_{e,s}[k]$, where $N_m = N_f \times N_s$

$F(e,m)$: The m^{th} feature extracted from the array response $X_{e,s}[k]$ to the smell example e, such that $(1 \le m \le N_m)$

F_e: The row feature-vector extracted from smell example e, such that $F_e = [F(e,1), F(e,2), \ldots, F(e,N_m)]$

F: The $(N_e \times N_m)$ matrix of the feature-vectors extracted from all the available examples N_e, such that:

$$F = \begin{bmatrix} F(1,1) & F(1,2) & . & . & F(1,N_m) \\ F(2,1) & F(2,2) & . & . & F(2,N_m) \\ . & . & . & . & . \\ . & . & . & . & . \\ F(N_e,1) & F(N_e,2) & . & . & F(N_e,N_m) \end{bmatrix}$$

$Z(e,m)$: Normalized version of $F(e,m)$ (see Section 3.3.3)

Z_e: Normalized version of F_e (see Section 3.3.3)

Z: The normalized version of F, such that Z is a $(N_e \times N_m)$ matrix of the normalized feature-vectors extracted from all the available examples N_e

N_l: The number of new features used to map Z_e in a new coordinated system L defined by a Feature Extraction transformation function such as PCA (see 3.4.1)

$Z'(e,l)$: The l^{th} new feature needed to map Z_e in a new coordinated system L, such that $(1 \le l \le N_l)$

Z'_e: The image of row vector Z_e mapped into the new coordinated system L, such that $Z'_e = [Z'(e,1), Z'(e,2), \ldots, Z'(e,N_l)]$ and $N_l < N_m$ (see 3.4.1)

Z': The $(N_e \times N_l)$ matrix of the feature-vectors images mapped into the new coordinated system L, such that $N_l < N_m$ and:

$$Z' = \begin{bmatrix} Z'(1,1) & Z'(1,2) & . & . & Z'(1,N_l) \\ Z'(2,1) & Z'(2,2) & . & . & Z'(2,N_l) \\ . & . & . & . & . \\ . & . & . & . & . \\ Z'(N_e,1) & Z'(N_e,2) & . & . & Z'(N_e,N_l) \end{bmatrix}$$

3.2 Smell-Signal Transient Regions

The smell signal can be divided into three characteristic transient regions: ascending transient, steady state and descending transient. In the ascending transient region the sensors output rapidly increase in response to the input of a VOM-example. It typically follows an exponential like curve of the type $y = \beta - \alpha e^{-\gamma t}$. The steady-state region follows the ascending transient, here the signal rising rate slows down and becomes an elbow shaped curve as the chemical reactions between the sensor surface and the odorant molecules slowly reach the equilibrium state in which the curve finally flattens. The descending transient is initiated when the VOM-example is pumped out of the sensor chamber and replaced by clean air (e.g. dry and filtered air) or any other reference gas. The descending transient follows a logarithmic like curve of the type $y = \beta e^{-\eta t}$.

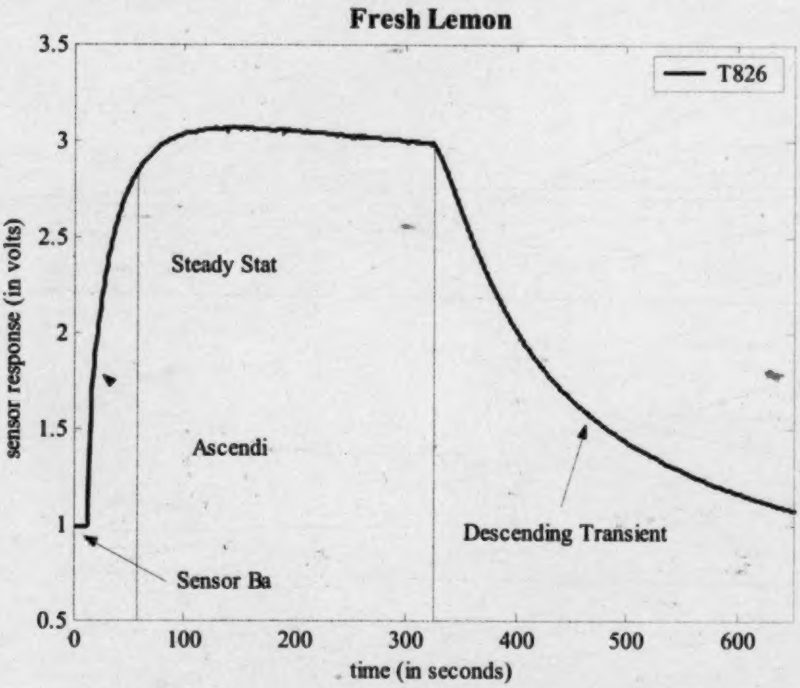

Figure 3-3 A typical smell sensor response showing the transient regions

In general, the ascending and descending transients have strong dependency on the smell delivery system (i.e., type of carrier, flow rate, relative position of the smell input pipe and the sensors, etc.) but also on the smell type, smell concentration, nature of the sensing materials and the reaction kinetics. On the other hand, the steady state regions of the sensor response depends almost only on the nature of the smell and sensing materials used and it is influenced by the characteristics of the smell delivery system [26]. However, there are strong evidences that smell-patterns extracted from the response transient regions also carry enough information for a successful smell classification task [30], [31], [32], [33].

3.3 Smell-Signal Preprocessing Stages

The digitized response of a sensor array to a VOM-example undergoes a sequence of transformations that are realized in order to prepare the multivariate response in a format that improves the performance of the subsequent modules. Three main transformations stages can be identified that have been used extensively in machine olfaction systems. First, a baseline manipulation technique is applied to reduce the effects of sensor drifts and temperature sensitivity dependences by processing the sensor responses relative to their baselines or initial states. Secondly, a feature-vector extraction technique is applied to calculate features that will efficiently discriminate different smells. Finally, a third transformation performs local and global normalization procedures that prepare the feature vector for subsequent analysis.

3.3.1 Baseline Manipulation

The baseline of a smell sensor is the stable state reached by the sensor when it has been in contact with a reference gas for certain amount of time. Normal air, filtered air and dry air are the reference gases commonly used in electronic noses.

It is a common practice to compute the final value of the sensor response based on their initial or baselines values in an attempt to reduce the effects of the short-term drifts by canceling the signal shifts before extracting the features [14], [34]. Here, we present four most popular baseline manipulation techniques (see Table 3-1): Difference (DIFF), Relative (REL), Fractional change (FRACT) and logarithm technique (LOG).

The DIFF technique subtracts the baseline response $W_{e,s}[1]$ (i.e., $W_{e,s}[k]$ at $k=1$) from the actual sensor response $W_{e,s}[k]$ to a VOM-example (see Equation 3-1). The REL technique divides the actual sensor response by the baseline response (see Equation 3-2). The FRACT combines the two previous procedures: first it subtracts the baseline response from the actual sensor response and secondly, it divides this result by the baseline response (see Equation 3-3). The LOG technique computes the logarithm (to base 10) of the ratio of the actual sensor response and the baseline response (see Equation 3-4).

The DIFF technique has been reported to provide the best performance in general. Osuna and Nagle [34] found that the DIFF technique performed better than the REL and FRACT for detecting smells of canned fruit juices and pops. Gardner at al. [35] studied nine different ad hoc baseline procedures, and found that the DIFF technique performed better on several bacteria cultures.

Table 3-1 Baseline manipulation techniques

BASELINE TRANSFORMATION	FORMULA	
DIFF	$X_{e,s}[k] = W_{e,s}[k] - W_{e,s}[1]$	(3-1)
REL	$X_{e,s}[k] = \frac{W_{e,s}[k]}{W_{e,s}[1]}$	(3-2)
FRACT	$X_{e,s}[k] = \frac{W_{e,s}[k] - W_{e,s}[1]}{W_{e,s}[1]}$	(3-3)
LOG	$X_{e,s}[k] = \log \frac{W_{e,s}[k]}{W_{e,s}[1]}$	(3-4)

3.3.2 Feature Vector Extraction

The goal of the feature vector extraction module is to find a small set of features that can represent efficiently the smells under analysis. Reducing the number of features from the response signal is necessary in order to reduce the computational complexity.

Numerous feature-vector extraction techniques and ad-hoc procedures have been implemented in machine olfaction applications. These techniques exploit different characteristics of the smell-signal. The earlier techniques exploit the stationary information conveyed by the smell-signal. More recent techniques aim to exploit the dynamic information contained in the transient regions of the smell-signal. The dynamic information is typically obtained in the time domain or in the frequency domain. Here, we have identified and grouped these techniques in the six following categories:

1) Signal Decimation Techniques

2) Signal Steady State Techniques

3) Signal Dynamics Techniques

4) Signal Spectral Techniques

5) Signal Modeling Techniques

6) Temperature Modulation Techniques

Signal Decimation is the simplest approach to reduce the dimensionality of feature-vectors. Here, equally spaced sample points are randomly extracted from the quantized and digitized original signal and used to assemble each feature-vector. However, some valuable information could be lost with this approach since the physical-chemical characteristics of the sensing materials are not taken into account.

The *Signal Steady State* (SS) technique has been widely used by the machine olfaction community since 1980's and it is still being used extensively [26]. This method exploits the stationary information conveyed by the smell signal. One value is extracted from each sensor in the array and this is the sensor response measured when the sensors reached their steady state in response to a VOM-example. In some implementations, this value is simply the final sampled point extracted from the sensor response signal (i.e., before pumping out the VOM-example). Besides being a simple technique, it has the additional advantage that the smell information extracted with the SS technique depends almost only on the nature of the smell and sensing materials used and it is less influenced by the characteristics of the smell delivery system [25] than other techniques. This characteristic have made it very attractive for the machine olfaction community because it eliminates the errors introduced by any variability in the smell delivery system

The *Signal Dynamics* techniques aim to exploit the dynamic information contained in the transient regions of the smell-signal response working in the signal time domain. These techniques work directly in the time domain by extracting various signal derivatives values, rise-decay time values, maximum and minimum signal values and signal values from ad-hoc selected test points [30], [36], [37].

In the *Signal Spectral* techniques, transforms of the smell-signal such as Fourier and Wavelet are calculated. Appropriated features are then extracted from the transform coefficients [20]. As the wavelet transform can represent the non-stationary signals better than the Fourier transform, it generally provides a superior performance for smell recognition [38], [33].

The *Signal Modeling* techniques model the sensor response instead of extracting features from the signal waveform. The model-parameters are then used as the features that characterize the smell. Samitier et al. [39] proposed a novel method, that they called METS (multi-exponential transient spectroscopy), to find the time-constant distribution in the exponential-like decay response that is typical of smell sensors. They tested several combinations of three different alcohols: ethanol, methanol and 2-propanol at different concentrations. Osuna et al. [40] reviewed four multi-exponential models (including METS) applied to samples from six different odorants: water, ethanol, acetic acid, perfume, fruit juice and coffee mixtures. Eklöv et al. [36] applied three curve-fitting techniques: polynomial functions, exponential functions and auto-regressive curve fitting algorithms to the responses of 4 MOSFET (metal-oxide field effect transistors) smell sensors. They tested hydrogen and ethanol at different concentrations ranging between 0 to 50 ppm.

In the *Temperature Modulation* techniques, the work-temperature is modulated while capturing the sensor output in order to improve the detection performance. These techniques are commonly applied to metal-oxide gas sensors because these sensors need to be heated at very high temperatures in order to detect VOM. Metal-oxide gas sensors detect reducing gases because those gases decrease the concentration of oxygen species in the sensing surface. This detection process is temperature dependent for two reasons. First, the surface oxygen species have differing stabilities at different temperatures. Secondly, the optimum oxidation temperature is different for different reducing gases. Therefore, one single sensor becomes equivalent to an array of n different sensors if the sensor response is measured at n different temperature steps. Hence, widening the range of smells that can be detected and at the same time producing n times more discriminative information [41]. Sears *et al.* [42] were able to discriminate between substances such as propane, carbon monoxide, hydrogen and alcohols by applying thermal cycling to a single Figaro sensor TGS 819. Heilig *et al.* [43] used a 50 mHz square function to modulate the voltage applied to the heater of a single custom-made metal-oxide sensor. They were able to discriminate between several blends of CO, NO_2 and ambient air at different concentrations ranging from 1 to 150 ppm by applying the Discrete Fourier transform (DFT) to the transients induced. Huang *et al.* [44] used a rectangular function at several frequencies (ranging from 20 mHz to 50 mHz) to modulate the heater voltages of metal-oxide sensors. The authors also used the DFT and were able to detect thrichlorophon and acephate gases at 0.1 ppm concentration.

3.3.2.1 Selected Feature-Vectors Implementations

Time Constants. Tomas Eklöv et al. studied the detection performance of features extracted in the time domain [45]. They measured several time intervals based on the rise time and fall time of the smell signal. Let $T_{on}X$ represent the time for the smell-signal to reach $X\,\%$ of its maximum value after the VOM input is ON and $T_{off}X$ represent the time for the smell-signal to fall to $X\,\%$ of its maximum value after the VOM purging is ON. The authors measured $T_{on}X$ for $X = \{60,90\}$ and $T_{off}X$ for $X = \{40,10\}$. These parameters are then used to discriminate smells.

Signal Derivatives. In this method the derivative of the digitized smell-signal is computed and averaged over few selected time intervals. These averages are then used to discriminate smells.

Since the acquired smell-signal is a discrete signal, we compute the derivative using an approximation method based on the Taylor series. Starting with the first order Taylor series we have that $f(k_{n+1}) = f(k_n) + f'(k_n)(k_{n+1} - k_n)$ and from here we obtain the Equation 3-5, which approximates the derivative for any point k_i of a given discrete signal

$$f'(k_n) = \frac{f(k_{n+1}) - f(k_n)}{k_{n+1} - k_n} \tag{3-5}$$

Cosimo et al. [33] studied the responses of five metal-oxide sensors that were sampled at 32 seconds intervals during 20 minutes for a total of 75 sampling points per sensor response. The mean derivative was computed over intervals of 10 sampling points over the entire response signal obtaining 7 features per sensor or a total of 35 features per smell-pattern. They used neural networks for the final smell identification obtaining 95 % recognition rate over seven combinations of acetone, hexanal and pentanone mixed with dry air and at 50% humidity.

Second Derivative of the smell-signal. The smell-signal second derivative has also been used in order to extract discriminative features. Rousel et al. [30] studied the smell discrimination performed by the signal first and second derivatives. The authors used the responses of five metal-oxide sensors to modeled mixtures representing wine with different grades of tart or vinegar flavor. The sensor responses were sampled at one-second intervals during 15 minutes for a total of 900 sampling points per sensor response. The authors measured four parameters from the first and second derivatives of the ascending and descending transients. The parameters extracted were: the maximum value, the time interval to the maximum value, the minimum value and the time interval to the minimum value. They concluded that the most discriminative features were: the ascending transient maximum derivative, the descending transient minimum derivative, the time interval of the descending transient second derivative maximum and the signal maximum.

3.3.3 Feature Vector Normalization

In the previous section, several features have been proposed for smell recognition. Some of these features such as the steady state sensor response parameters, which are voltage values, are not comparable to features of the time-interval types such as $T_{on}X$ (see Section 3.3.2.1). Therefore, some kind of scaling is needed in order to put together such a different magnitude. A simple technique is to scale the different feature types according to its mean value and variance. This technique clearly makes different feature types comparable because each feature type is now measured relatively to its mean and variance.

The function of the Normalization module is to adjust the magnitude of the individual features such that all the features magnitudes are comparable. The normalization techniques are also used to limit the range of values that the features can take.

Normalization techniques are generally grouped into two classes: global and local techniques. Global normalization techniques are generally applied to ensure that the magnitudes of the different features are comparable. These techniques adjust each individual dimension (feature) of the smell-pattern across all the smell-patterns in the training database. Local techniques are generally applied to compensate sample-to-sample variations due to small changes of the analyte concentration and sensor drifts. These techniques adjust all the dimensions (features) locally within each smell-pattern without accounting for the rest of patterns in the database.

In this thesis, we have implemented three widely used normalization techniques [46]: dimension auto-scaling (DAS), vector auto-scaling (VAS) and vector normalization (VNORM). The DAS is a global normalization technique that adjusts each individual dimension (feature) to have zero mean and unit variance across all the smell-patterns in the training database. The VNORM and the VAS locally adjust all the dimensions (features) at the smell-pattern level. VNORM adjusts each individual smell-pattern such as it will lie in a hyper-sphere of radius unit while VAS adjusts each individual smell-pattern such as the magnitude of each of its features will have zero mean and unit variance computed relatively to all the feature values of this particular smell-pattern.

In the DAS technique the normalized feature-vector coordinates are calculated using the following equation

$$Z(e,m)=\frac{F(e,m)-\mu_m}{\sigma_m} \qquad \forall e,m \qquad (3\text{-}6)$$

Where the mean $\mu_m=\frac{1}{N_e}\sum_{e=1}^{N_e}F(e,m)$ and the variance $\sigma_m=\sqrt{\frac{1}{N_e}\sum_{e=1}^{N_e}\left(F(e,m)-\mu_m\right)^2}$ are computed for each dimension along all the smell-patterns in the database. Note that this technique focuses in the global relationship among all the features values within each dimension along the entire database.

In the VAS technique, the normalized feature-vector coordinates are calculated using the following equation.

$$Z(e,m)=\frac{F(e,m)-\mu_e}{\sigma_e} \qquad \forall e,m \qquad (3\text{-}7)$$

The mean $\mu_e=\frac{1}{N_m}\sum_{m=1}^{N_m}F(e,m)$ and variance $\sigma_e=\sqrt{\frac{1}{N_m}\sum_{m=1}^{N_m}\left(F(e,m)-\mu_e\right)^2}$ are computed across the different coordinates per each smell-pattern. Note that this technique focuses on the local relationship between all features values within each smell-pattern.

In the VNORM technique, the normalized feature-vector is calculated using the following equation.

$$Z(e,m) = \frac{F(e,m)}{\sqrt{\sum_{m=1}^{N_m} F^2(e,m)}} \qquad (3\text{-}8)$$

Note that each vector F_e is normalized relative to its norm $\sqrt{\sum_{m=1}^{N_m} F^2(e,m)}$ to ensure that it will lie in a hyper-sphere of radius unit.

3.4 Reducing the Dimensionality of the Feature Space

The feature-vector extraction techniques proposed in the literature for machine olfaction are generally ad-hoc techniques based on different physical-chemical characteristics of the smell-signals. These techniques typically produce a large number of features due to the multiplicative effect of the "*n*" sensors in the array. For example, if five derivatives are extracted from each sensor response and there are eight sensors in the array, the resultant feature-vector will have 40 features. Redundant and noisy features can easily hide in such a large features sets producing unexpected bad performance of the pattern recognition system. It is well-known in the pattern recognition field that there is an optimal set of features that produce the peak performance and beyond this number the system classification performance degrades instead of improving. This effect is known as the "curse of dimensionality" [47].

In general, reducing the number of extracted features from a very large feature set can improve the system performance for two reasons. First, the performance of a classifier degrades when the number of training examples is small compared to the number of features extracted [47], [48]. Secondly, the features used in machine olfaction applications due to different sensors are typically highly correlated [14]. Therefore, screening out these redundant features will reduce the noise and improve the performance of the classifier.

Feature extraction is a dimensionality reduction technique where a given set of candidate features is reduced to a smaller set. Feature extraction techniques typically apply a given transformation function that maps the original set into a new coordinates system. The best-known technique used for feature extraction is the Principal Component Analysis (PCA) [49].

The PCA has also been used as an unsupervised pattern recognition algorithm in several electronic nose systems.

3.4.1 Principal Components Analysis

The PCA is a dimensionality reduction technique widely used in image and signal processing. It has also been applied in smell-signal processing [50], [51]. The PCA is a linear transformation technique that aims to find a new set of orthogonal axis (principal components) for the input space given by the smell-patterns. The new axes are aligned in the direction of maximum variances of the input space variables. The first axis (first PC eigenvector) is in the same direction of the highest variance found in the input data. The second axis is in the same direction of the second maximum variance and so on. The PCA transformation of a given input space of feature-vectors Z into the new feature space Z' is calculated using the following equation [47]

$$Z' = Z \times H \tag{3-9}$$

In Equation 3-9, the matrix Z, is the $(N_e \times N_m)$ matrix containing the N_e input feature-vectors and the matrix Z', is the $(N_e \times N_l)$ matrix containing the images of the feature-vectors Z_e in the new coordinated system of dimension N_l such that $N_l \leq N_m$.

The transformation matrix H is an orthonormal $(N_m \times N_l)$ matrix, where N_m is the dimension of the input space and N_l is the dimension of the new representation space such that $N_l \leq N_m$. The columns of H are the N_l largest eigenvectors computed from the $(N_m \times N_m)$ covariance matrix S of the N_e input feature-vectors in the input space (smell-database). The columns of H are also known as the principal components and define the axes of the new coordinated system. The elements in each column-vector are the cosines of the angles between each new axis and all the old axes.

3.5 Pattern Recognition Module

The analysis of the data generated by the electronic nose focuses in finding hidden relationships between a set of independent variables (i.e., the features extracted from the array response) and a set of dependant variables (i.e., smell class or component concentration). Three major techniques can be identified: Regression, Clustering and Classification [46]. In regression analysis techniques the objective is to predict some selected properties of an analyte such as the different components of a mix. The clustering techniques aim to find structural relationships among different smells. The classification techniques focus on the identification of an unknown sample from a set of learned smells. In this thesis, we have used the classification techniques to detect smells. Therefore, we present a brief overview of two selected classification techniques.

In order to facilitate the mathematical formulation of the classifiers that will be reviewed, we add the following notation to the list defined earlier in this chapter (see 3.1):

N_c : The number of smell-classes contained in the training set

N_j : The number of examples for each smell-class such that $N_e = N_c \times N_j$, where N_c is the number of smell-classes. We assume that there is identical number of smell-pattern examples in each smell-class in order to simplify computation.

N_u : The number of unknown examples contained in the testing set

Z'_u : The feature-vector of an unknown VOM-example, which has been fully preprocessed and mapped into the new coordinated system L, such that $Z'_u = [Z'(u,1), Z'(u,2), \dots, Z'(u,N_l)]$, $(1 \le u \le N_u)$ and $N_l < N_m$

$P(c,l)$: The l^{th} coordinated the Prototype Feature-Vector for smell class c computed by the Nearest Mean Classifier, such that $(1 \leq l \leq N_l)$ and $(1 \leq c \leq N_c)$

P_c: The Prototype Feature-Vector for smell class c computed by the Nearest Mean Classifier, such that $P_c = [P(c,1), P(c,2), ..., P(c,N_l)]$

P: The $(N_c \times N_l)$ matrix of all the Prototype Feature-Vectors for the smell classes N_c contained in the training set (computed by Nearest Mean Classifier) such that:

$$P = \begin{bmatrix} P(1,1) & P(1,2) & . & . & P(1,N_l) \\ P(2,1) & P(2,2) & . & . & P(2,N_l) \\ . & . & . & . & . \\ . & . & . & . & . \\ P(N_c,1) & P(N_c,2) & . & . & P(N_c,N_l) \end{bmatrix}$$

3.5.1 Nearest Neighbor Classifier

The Nearest Neighbor (NN) rule is a powerful classifier that can be used to generate highly nonlinear classifications with small sized data sets [52].

In the training phase, all the training smell-examples are allocated in a list in memory. All examples belonging to a given class c are placed together and the smell classes are sorted in ascending order.

In the testing phase, the feature-vector of an unknown VOM-example is compared to all the feature-vectors allocated in the lookup table assembled during the training phase. The unknown VOM-example is then classified into the same smell-class of its closest feature-vector. The Euclidean distance is typically used as proximity measure since it calculates the minimum distance between two vectors in a multidimensional feature space. The distance between an unknown feature-vector Z'_u and the feature-vector Z'_e of a given example e in the lookup table is calculated using the following equation.

$$d_{u,e} = \sqrt{\sum_{l=1}^{N_l} \left(Z'(u,l) - Z'(e,l)\right)^2} \quad \forall u,e \qquad (3\text{-}10)$$

The class label c_u for the unknown feature-vector Z'_u is computed using the following equation.

$$c_u = Arg_e(Min(d_{u,e})), \quad for \ \left(1 \le e \le N_e\right) \ for \ any \ "u" \qquad (3\text{-}11)$$

In Equation 3-11, the function *Min*(.) returns the minimum distance value computed between the unknown example u and each of the N_e examples in the training set and the function Arg_e(.) returns the class label number of the example e, which produced the smallest distance value to the unknown example u. For the implementation of this classifier the first column of each feature-vector in the training and data sets are filled with the class label number of this example.

Although the NN classifier appears to be a heuristic classifier, it is in fact a formal nonparametric approximation of the Bayes decision rule. It has been theoretically demonstrated that the probability of error for the NN classifier will not be worse than twice the Bayes error, which is the best any classifier can achieve [53]. The main disadvantages limiting the use of NN in machine olfaction applications are its large storage requirements and high computational cost. The NN classifier must keep the entire training data set in memory while in testing mode because the array of feature-vectors in each class constitutes the smell-class Feature-Vector Prototype (PFV). Every time that a new example is analyzed a full search and sorting through all the PFVs (in the case of NN this is the entire training set) is necessary in order to find the closest neighbor to the incoming example.

3.5.2 Nearest Mean Classifier

The Nearest Mean classifier (N-MEAN), which is also known as the minimum distance classifier, is a simple classification technique that can be successfully used when the smell-patterns are well separated [54],

In the N-MEAN classifier, the Prototype Feature-Vector (PFV) for a given smell-class c is represented by the mean feature-vector computed along all the feature-vectors that share the given smell-class. Hence, during the training phase the mean feature-vector for each smell class c in the training set is computed. The coordinates of the Prototype Feature-Vector P_c for a given smell-class c are calculated using the following equation.

$$P(c,l) = \frac{1}{N_j} \sum_{e=(c-1)\times N_j+1}^{(c)\times(N_j)} Z'(e,l) \quad for \quad 1 \le l \le N_l \quad for\ any\ "c" \qquad (3\text{-}12)$$

$\forall e$ such that $((c-1)\times N_j + 1) \le e \le (c \times N_j)$ where
c is the class label number
N_j is the number of examples in class c
N_l is the number of features
N_c is the number of smell-classes in the training set
$N_e = N_c \times N_j$ is the number of examples in the training set

In the testing phase, the classification is performed by calculating the Euclidean distance between an unknown feature-vector and each of the Prototype Feature-Vectors computed from the training database. The unknown smell-pattern is then assigned to the class label number of its closest PFV. The Euclidean distance is commonly used as proximity measure since it calculates the minimum distance between two vectors in a multidimensional feature space. The distance between an unknown feature-vector and a given PFV is calculated using the following equation.

$$d_{u,c} = \sqrt{\sum_{l=1}^{N_l} \left(Z'(u,l) - P(c,l)\right)^2} \quad \forall u,c \tag{3-13}$$

3.6 Performance Evaluation Criterion

In the previous sections, we have reviewed several signal processing and pattern recognition techniques that are commonly used in machine olfaction. In this section we present the evaluation criterion typically used to evaluate the performance of the smell recognition subsystem of an electronic nose.

The smell recognition subsystem of an electronic nose is defined here as the system constituted by a given combination of smell-signal preprocessing techniques (see Section 3.3) and a given pattern recognition technique (see Section 3.5).

The smell recognition systems are generally evaluated using the *detection efficiency* (also known as predictive accuracy) criterion [34], which is defined as follows

$$\eta = \left(\frac{\textit{Number of correctly classified examples}}{\textit{Number of examples in the Testing Set}} \right) \times 100 \tag{3-14}$$

A simple method to calculate the detection efficiency η of a given smell recognition system consists of three steps. First, all the available examples are split into two sets: the training set and the testing set. Second, the training set is used to design (train) the classifier. Third, the detection efficiency is calculated over the testing set using the Equation 3-14.

3.6.1 Statistical Re-sampling

In the previous section, we presented a simple method to calculate the detection efficiency η of a given smell recognition system but we did not mention that the size of the testing set and training sets affect the reliability of the detection efficiency η estimation [47]. However, the number of available examples collected in machine olfaction applications is typically very small. Therefore, statistical re-sampling methods such as cross-validation (N-CV) are commonly used to reliably estimate the detection efficiency of a given recognition system [55],[56].

The N-fold cross-validation (N-CV) re-sampling method splits the available examples into $N = N_p$ partitions. One of the partitions is put aside for testing while the remaining $(N_p - 1)$ partitions are pasted together and used to design (train) the classifier. This process is repeated until all the N_p partitions have been used to evaluate the classifier. The detection efficiency is then computed as the average of correctly classified examples obtained over the N_p partitions tested.

A particular case of the N-CV method is the Leave-one-out (LOO) re-sampling method. In LOO, $N_p = N_e$ (where N_e is the number of examples in the database) and the size of the testing partition is to one. Both methods produce similar results when the number of available examples is large but for small number of examples LOO produces a more reliable estimation of the detection efficiency. In this thesis, we used N-CV with those smell-databases having more than 50 examples in each smell-class and LOO otherwise.

The following equation is used to calculate the detection efficiency for N-CV or LOO re-sampling methods

$$\eta = \left(\frac{1}{N_p} \sum_{p=1}^{p=N_p} \frac{C_p}{N_t} \right) \times 100 \ , \qquad (3\text{-}15)$$

where $N_t = \dfrac{N_e}{N_p}$ is the number of examples in each testing partition "p",

and C_p is the number of correctly classified examples in the test partition "p"

3.7 Summary

In this chapter, we first presented an overview of the signal processing and pattern analysis stages usually implemented in machine olfaction systems. Following was the presentation of a typical smell sensor response signal and an exhaustive review of the most commonly used smell-signal processing techniques. Next, an introduction to the popular dimensionality reduction technique Principal Component Analysis and a review of two powerful pattern recognition techniques were presented. Finally, a methodology for the validation and performance evaluation of electronic nose was briefly discussed.

Chapter 4

The Proposed Electronic Nose

In chapters two and three, we have presented a comprehensive review of olfaction systems, signal processing techniques, pattern recognition algorithms and validation procedures used in machine olfaction. A majority of the commercial electronic noses are designed for narrow applications such as wastewater analysis, quality control of foodstuffs and detection of spilled chemicals in industry. These systems have usually very high cost. As a result these noses are not suitable for integration with multimedia systems.

In this chapter, we present a low cost electronic nose design suitable for integration with multimedia systems. The organization of this chapter is as follows. In Section 4.1 we briefly introduce the different modules of the proposed electronic nose (eNose). Section 4.2 presents the smell space targeted by the eNose. Section 4.3 provides a detailed explanation of the eNose hardware modules. In Section 4.4, we present a graphical user interface that allows controlling and interfacing the eNose hardware modules. Section 4.5 describes the eNose sniff-cycle characteristics and Section 4.6 proposes a novel sniff technique, which is followed by the summary.

4.1 Introduction

The proposed electronic nose (eNose) consists of two main subsystems: the hardware subsystem and the software subsystem.

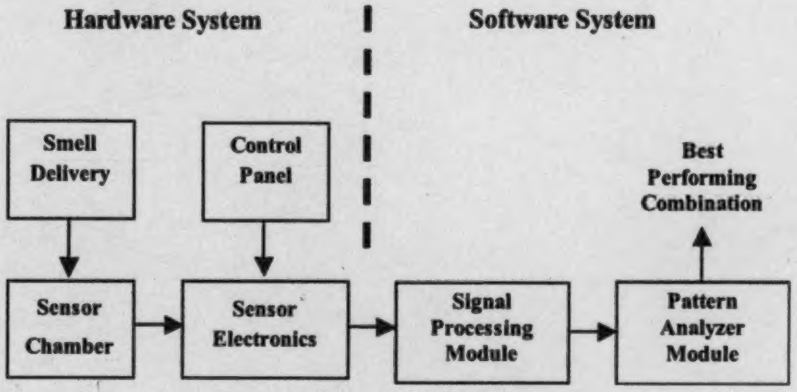
Hardware System
Software System
Smell Delivery
Control Panel
Best Performing Combination
Sensor Chamber
Sensor Electronics
Signal Processing Module
Pattern Analyzer Module

Figure 4-1 Schematic of the proposed eNose

Figure 4-1 shows a simplified schematic of the proposed electronic nose. The hardware subsystem consists of three modules: Smell Delivery system, Sensor Chamber and the Sensor Electronics. The Control Panel is a graphical user interface program that allows the controlling and interfacing of the all hardware modules. The software subsystem consists of three modules: Signal Processing, Pattern Analyzer and Results Plotter. The Signal Processing module is a graphical user interface program that can compute many combinations of signal processing techniques on a given smell-database. The Pattern Analyzer is a graphical user interface program that computes the smell detection efficiencies of the different signal processing combinations. The Results Plotter module is used offline to produce comparative bars plots and tables with the detection efficiencies scored by the different combinations.

4.2 The eNose Smell Space

The goal of the proposed eNose is to detect and discriminate a sub-set of natural occurring smells from common items such as foodstuffs, beverages, plants, perfumes and essential oils. It was noted in Section 2.3, that natural occurring smells are complex smells, which are constituted for more than one type of odorant molecule. Various areas of application of electronic noses were considered when selecting the smells for testing: perfumery, food and beverages industry, environmental, and agricultural sectors. Finally, a temporary smell space was conceived in order to test the general performance of e-nose. The smell space proposed for the low cost eNose prototype presented here expands over a wide range of smells aiming to the possible use of the eNose in the above-mentioned areas.

Table 4-1, shows the smell space defined to train and evaluate the performance of the proposed eNose. The smell space used here expands over a wide range of smells aiming to evaluate the possible use of the eNose in different applications such as perfumery, food and beverages industry, environmental, and agricultural applications.

Table 4-1 eNose Smell Space

SMELL	SOURCE
Fragrant smells	Essential oils
Aromatic smells	Spices, coffees
Fishy smells	Cod oil, sardines
Fruity smells	Fruit juices
Hircine smells	Cheese
Beverages smells	Pops, colas, beers
Nauseous smells	Livestock manure

4.3 Hardware System

In this section, we describe the hardware components used in the design of the proposed electronic nose. The primary design goal was to keep the costs low while achieving maximum smell detection efficiency.

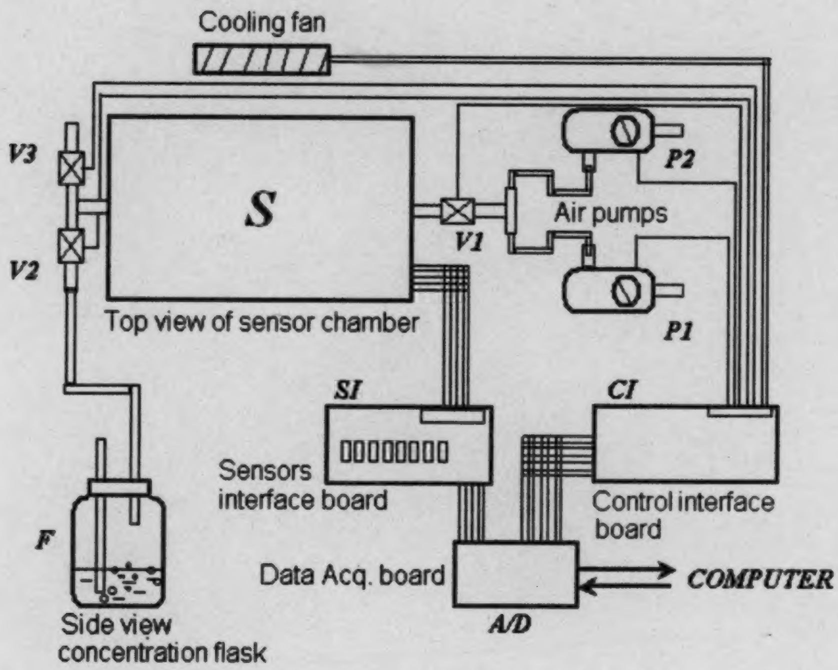
Cooling fan
V3
V2
S
V1
Air pumps
P2
P1
Top view of sensor chamber
SI
CI
Sensors interface board
Control interface board
F
Data Acq. board
COMPUTER
A/D
Side view concentration flask

Figure 4-2 A simplified schematic of the eNose hardware

Figure 4-2 depicts the hardware parts of the eNose and the interconnection between them. The main eNose hardware components are: Concentration flask (**F**), Smell Delivery System (solenoid valves: **V1**, **V2**, **V3**; sensor chamber: **S**; air pumps: **P1**, **P2**), Smell Sensors Array (located inside the chamber **S**), Sensor Interface Board (**SI**), Control Interface Board (**CI**) and the Data Acquisition Board (**A/D**).

The smell detection operation is as follows. The source of VOM is placed in the concentration flask **F** from where a small air sample is drawn by the smell delivery system and brought into the sensor chamber **S**. The smell sensors inside the chamber generate output voltages depending on the VOM. These output voltages are received in the Sensors Interface board **SI** and digitized by the Data Acquisition board (**A/D**). These digitized sensor responses are then saved on disk or processed further depending on the eNose operation mode.

4.3.1 Concentration Flask

The function of the concentration flask is to isolate and create a proper headspace for the smell source under test. Figure 4-3 shows a picture and the schematics of the jars used as concentration flasks and Table 4-2 contains the detailed description of the concentration flask parts.

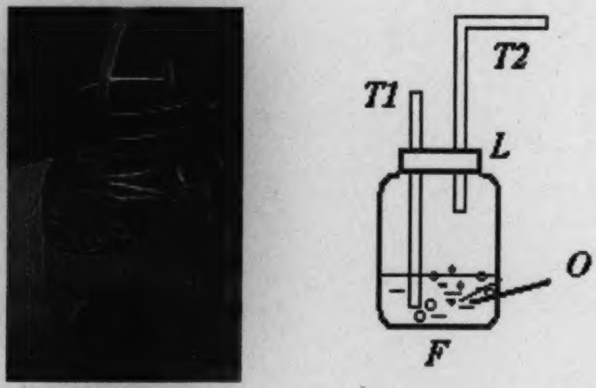

Figure 4-3 Parts of the Concentration Flask

Regular food storage 500 ml glass jars are used as concentration flasks [57]. Two orifices, with ¼ inches diameter each, were made to the metallic top lid of every flask. A 15 cm vinyl tube is introduced through one of the orifices up to two centimeters above the bottom. The second orifice is connected to the eNose smell inlet by a 30 cm long vinyl tube. When a liquid smell source is being sampled, the ambient air is fed through pipe **T1** producing a bubbling effect in the smell source. The stirring caused by the bubbles increase the release of VOM from the smell source. Similar stirring effect is also produced for a grounded smell source substance such as ground coffee.

Table 4-2 Concentration Flask (parts description)

LABEL	DESCRIPTION	SPECIFICATIONS
F	Glass Flask (Home Canning)	Volume = 500 cm^3, Height = 13 cm,
T1	Air Input Vinyl Tube	Length = 15 cm, Diameter = ¼ inches
T2	Odorant Vapors Output Vinyl Tube	Length = 25 cm, Diameter = ¼ inches
O	Odorant Source Substance	Volume ~ 160 cm^3
L	Airtight Metallic Lid	Diameter = 70 mm

4.3.2 Smell Delivery System

The smell delivery system has two important functions. It brings the VOM from the smell source into the smell-sensing chamber. In addition, it flushes the smell out cleaning the chamber for the next sample of VOM. A picture of the Smell Delivery System and a detailed schematic are depicted in Figure 4-4 and a description with the specifications of the main components is presented in Table 4-3.

The Smell Delivery System has been built with two air pumps, three solenoid valves, two T-shaped brass connectors, ¼ inches external diameter (0.170 inches internal diameter) vinyl tubing and nine short hand-made Teflon couplings. The Teflon couplings were used to interconnect all the components of the Smell Delivery System. Teflon material was selected because it is non-reactive to most chemicals and is odorless. The vinyl tubes were placed in those sections of the Smell Delivery System where the memory of a previous smell could not affect the performance of the tests. For example, all the smell exhaust connections to the air pumps were made of vinyl tubing.

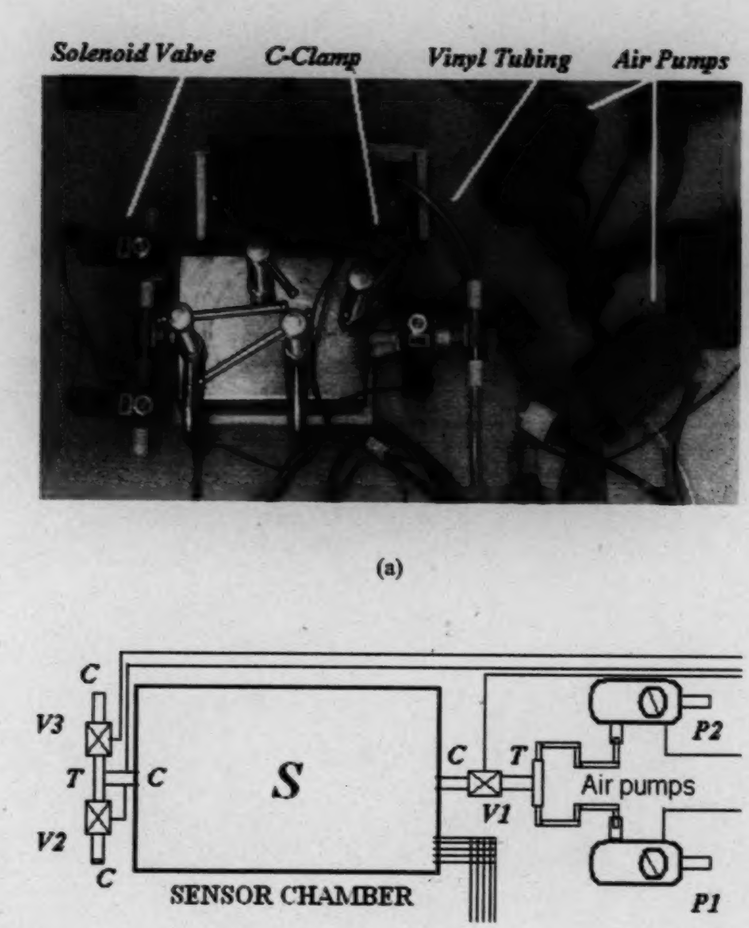
Solenoid Valve
C-Clamp
Vinyl Tubing
Air Pumps
C
V3
T
C
S
V2
C
SENSOR CHAMBER
C
T
V1
Air pumps
P2
P1

(a)

(b)

Figure 4-4 Picture (a) and schematic (b) of the Smell Delivery System (top view)

The air pumps **P1** and **P2** are used to create a vacuum in the smell-sensing chamber **S** and the vacuum is transmitted to the Concentration Flask **F** through the pipeline system. Therefore a sample of VOM is inhaled from the smell source and it is blown over the smell sensor heads. The solenoid valves are used to keep the VOM isolated inside the chamber giving time for the sensors to reach their steady states. Two of these valves are connected to the inlet pipe. One valve is used to bring the VOM inside the chamber while the other valve is used to bring inside the clean ambient air used to purge the smell out of the chamber. Note that the function of the two air pumps is identical and they are used together to create a stronger vacuum.

Table 4-3 Components of the smell delivery system

LABEL	COMPONENT DESCRIPTION	SPECIFICATIONS
S	Sensor Chamber	Aluminum Box Volume = 495 cm^3
V1, V2, V3	Miniature Solenoid Valves [60]	Model Burkert 6011 Port Diameter = ¼ inches
C, T	Couplings: Teflon coupling, T-Brass coupling	External Diameter = ¼ inches
P1, P2	Air Pumps Model Elite799 [61]	Home aquarium pumps. Each pump flow-rate is 1000 cm^3/min. System flow-rate is 33 cm^3/s.

4.3.3 The smell sensors used

Several types of sensors were considered for the eNose. However, the Taguchi metal-oxide gas sensors were selected as these sensors are commercially available at a reasonable price, and they can detect a wide range of gases. The Taguchi gas sensors are primary produced for industrial applications such as toxic gas detection, combustible gas detection and smoke detectors. Taguchi gas sensors are also known as Figaro sensors as they are manufactured and commercialized by the Japanese company Figaro Engineering Inc. [24]. The pictures of four Figaro sensors are shown in Figure 4-5.

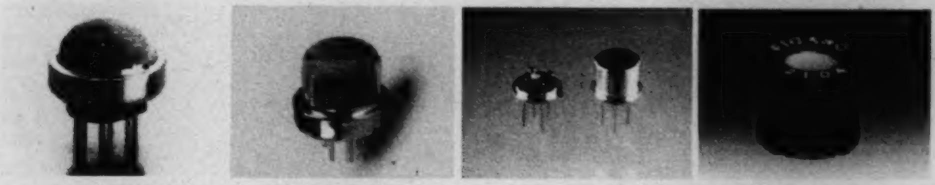

TGS 825 TGS 880 TGS 2602 TGS 2104

Figure 4-5 Photograph of a few selected Figaro gas sensors

Figaro (Taguchi) sensors are generally sensitive to reducing gases such as CO, NH_3 and H_2S. It has been found that many of these sensors are also sensitive to many volatile vapors from organic compounds (VOC), solvents, food, and different species of alcohol. Figaro sensors are also capable of detecting polluting smells such as cigarette smoke and the exhaust of (gasoline and diesel) automobiles.

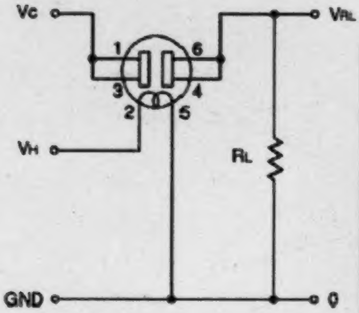

Label	Description	Specs	
		TGS 8xx	TGS 2xxx
V_C	Circuit Voltage	Max 24V	Max 5V
V_H	Heater Voltage	Max 5V	
R_L	Load Resistor	Min. 450 Ω	
I_H	Heater Current	130mA	55mA

Figure 4-6 Electrical schematic and specifications of Figaro sensors (adapted from [24])

Figure 4-6 shows the electrical schematic and the specification of two types of Figaro gas sensors. These sensors need high temperatures in the range of $400^{\circ}C$ in order to sense gases and they are built with a heater resistance embedded into the sensing surface that allows them to reach these temperatures. The exact temperature at which a specific sensor works vary according to the gasses targeted. The sensor response can be obtained connecting a voltage divider resistor R_L in serial connection with the sensing surface of the sensor (see Section 2.6.4).

Figaro sensors detect reducing gases. Reducing gases are those gases that have affinity to oxide themselves. When the sensors are heated in the presence of clean air, different species of oxygen such as O_2^-, O^- and O^{2-} are adsorbed onto the tin dioxide surface withdrawing electron density from the semiconductor material [41]. As a result the electrical resistance of the semiconductor increases and the sensor reaches its baseline state. A given reducing gas that comes in contact with the sensors surface can be detected because this gas will combine with the oxygen species adsorbed on to the sensing surface. As a result the electron density of the semiconductor material is increased and consequently the electrical resistance of the semiconductor is decreased.

The relationship between sensor resistance and concentration of a given reducing gas is expressed by the following equation.

$$R_S = A[C]^{-\alpha} \quad (4\text{-}1)$$

where R_S represents the electrical resistance of the semiconductor, A is the sensitivity constant of the sensor to the given reducing gas, C is the concentration of the gas under test and α represents the slope of the R_S curve.

4.3.4 The smell sensor array

In this thesis we have used eight different Figaro metal-oxide gas sensors to build the sensors array. The picture and schematics of the sensors array board is shown in Figure 4-7. The sensors in the array, and their targeted gases are listed in Table 4-4. The labels shown in the first column of this table correspond to the labels shown in the schematics of Figure 4-7. The third column of this table shows the gases to which the sensor in column two is more sensitive. The third column of this table shows the smells that can be associated with the gases targeted by the sensor in column two.

Sensors **TGS 826** and **TGS 825** are chosen because of their high sensitivity to fishy and sulfurous smells, respectively. These sensors have a very specific and narrow smell detection range. The sensor **TGS 2620** is sensitive to a narrow range of smells that include wood fermentation and alcohols.

The sensor **TGS 2602** has high sensitivity to various odorous gases and volatile organic compounds. Its smell space overlaps the smells detected by the above-mentioned sensors (ammonia, sulfur, alcohols and wood fermentation smells). We expect that the wide smell range of sensor **TGS 2602** will complement the information gathered by the data processing module improving the characterization of a given smell.

Table 4-4 List of the Selected Smell Sensors

LABEL	SENSOR	TARGETED GASES	SMELLS LIKE
S1	TGS 880	Volatile vapors from food	Food (while cooking)
S2	TGS 2620	Volatile org. vapors	Aromatic solvents, alcoholic beverages
S3	TGS 825	Hydrogen sulfide (H2S)	Rotten-egg
S4	TGS 2602	Air contaminants	Responsive to many smells
S5	TGS 826	Ammonia (NH3)	Old rotten urine and fish
S6	TGS 2104	Gasoline exhausts	Irritating and suffocating smells
S7	TGS 883T	Water vapors from food	Soups, brewed coffee
S8	TGS 2610	Hydrocarbons in general	Smell of ripening of fruits

Sensors **TGS 826** and **TGS 825** are chosen because of their high sensitivity to fishy and sulfurous smells, respectively. These sensors have a very specific and narrow smell detection range. The sensor **TGS 2620** is sensitive to a narrow range of smells that include wood fermentation and alcohols.

The sensor **TGS 2602** has high sensitivity to various odorous gases and volatile organic compounds. Its smell space overlaps the smells detected by the above-mentioned sensors (ammonia, sulfur, alcohols and wood fermentation smells). We expect that the wide smell range of sensor **TGS 2602** will complement the information gathered by the data processing module improving the characterization of a given smell.

The sensor **TGS 2610** is chosen because of its high sensitivity to hydrocarbons. The smell that we perceive from ripe fruits is the combined effect of volatile organic compounds emitted during the ripening process [58], especially hydrocarbon derivative groups like propanol and butanol. Therefore, such smells can be detected easily using this sensor.

The sensors **TGS 880** and TGS **883T** are chosen as they are sensitive to volatile and water vapors that are produced by food while cooking.

Sensor TGS **2201** targets smell produced in city streets and bars (e.g., gasoline and cigarettes smoke) that are commonly occurring smells in daily life.

The Figaro gas sensors come in two different encapsulation formats named **TGS 26xx** and **TGS 8xx**. The size of **TGS8xx** sensor type is generally bigger and consumes more power than type **TGS 26xx**.

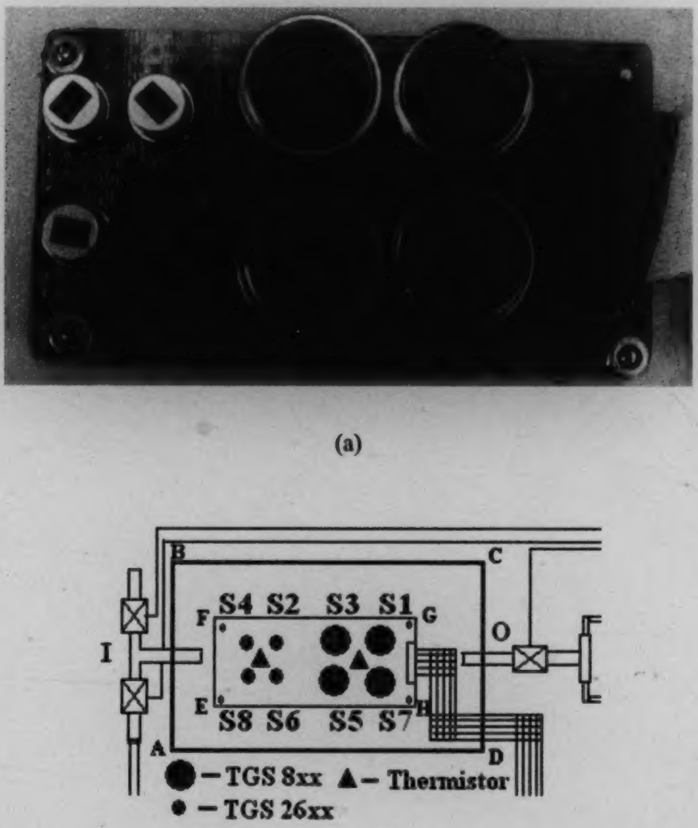
B
C
S4 S2 S3 S1
F
G
O
I
E
S8 S6 S5 S7
H
A
D
● – TGS 8xx
▲ – Thermistor
• – TGS 26xx

(a)

(b)

Figure 4-7 Picture (a) and schematic (b) of the smell sensors array

Figure 4-7 shows a picture (a) and the schematics (b) of the sensor array board. The schematics (b) represent a top view of the sensing chamber. The chamber has been opened to show the sensor array inside it. The rectangle ABCD represents the top view of the sensing chamber. The rectangle EFGH represents the printed circuit board (PCB) shown in Figure 4-7 (b). There are eight Figaro smell sensors (**S1, S2…S8**) plus two temperature sensors (represented by the two triangles) mounted on the board. The dimensions of the sensors array board are (10×4) cm^2. The smell sensors are arranged in two parallel rows that are inline with the air current that carries the VOM. The VOM inlet (**I**) is in the left of the schematic. This inlet tube also carries the clean air that is blown to purge the smell out of the sensing chamber. The pumps (not shown here) are connected to the outlet tube (**O**) and they draw the air from the sensing chamber when a smelling cycle is activated.

Solderless bases are used to allow for easy interchangeability of the sensors. The sensors are clustered into two groups according to their encapsulation type. A temperature sensor was soldered in the center of each of these clusters (see Figure 4-9). The sensors load resistances and heater control circuits are placed in the sensors interface and control interface boards. There are two reasons for placing these circuits outside the smell sensors array board. The first reason is to adjust the smell sensor baselines without opening the chamber. The second reason is to avoid contamination with the smell that the electronic components may produce when they are working in a hot environment.

4.3.5 Temperature Sensors

It is well documented that the response of metal-oxide gas sensors is affected by minor changes in the ambient temperature [14]. Three temperature sensors are included in the eNose circuits in order to monitor and record the temperatures inside/outside the chamber. The temperatures in the laboratory and inside the chamber are recorded together with each smell sampled. However, temperature was not an issue because all the smell experiments were realized in stable laboratory conditions.

Table 4-5 shows the temperatures recorded during a sniff cycle. The ambient temperature during this experiment was $24^{\circ}C$. The temperatures were recorded at the end of each event.

Table 4-5 Temperature changes observed during a sniff cycle

EVENT	TEMPERATURE	
	TGS 8XX CLUSTER	TGS 26XX CLUSTER
One hour resting, no smell inhaled	$52^{\circ}C$	$43^{\circ}C$
Ten seconds inhaling a smell	$49^{\circ}C$	$42^{\circ}C$
Five minutes flushing the smell out	$41^{\circ}C$	$38^{\circ}C$

Recording the inside and ambient temperatures may be useful in smell experiments outside the laboratory. These temperatures can be added to the feature-vector aiming to compensate the drifts produced by the ambient temperature changes.

Figure 4-8, shows the evolution of the temperature of the TGS 8xx smell sensors cluster during a sniff cycle. The VOM inhaling period lasted 10 seconds and the smell-purging period lasted 300 seconds.

The temperature sensors were built using disk thermistors type 5K-5 produced by Semitec [59]. Thermistors are devices that change their electrical resistance depending on the temperature. The temperature measured by a thermistor can be calculated using the following equation

$$r_1 = R_2 \times \exp\left(B \times \left(\frac{1}{t_1} - \frac{1}{T_2}\right)\right) \qquad (4\text{-}2)$$

where

r_1 is the thermistor resistance at temperature "t_1"

$R_2 = 5.0$ KΩ is the thermistor resistance at 25 °C temperature ($T_2 = 298$ kelvin)

$B = 4.1$ KΩ is a constant

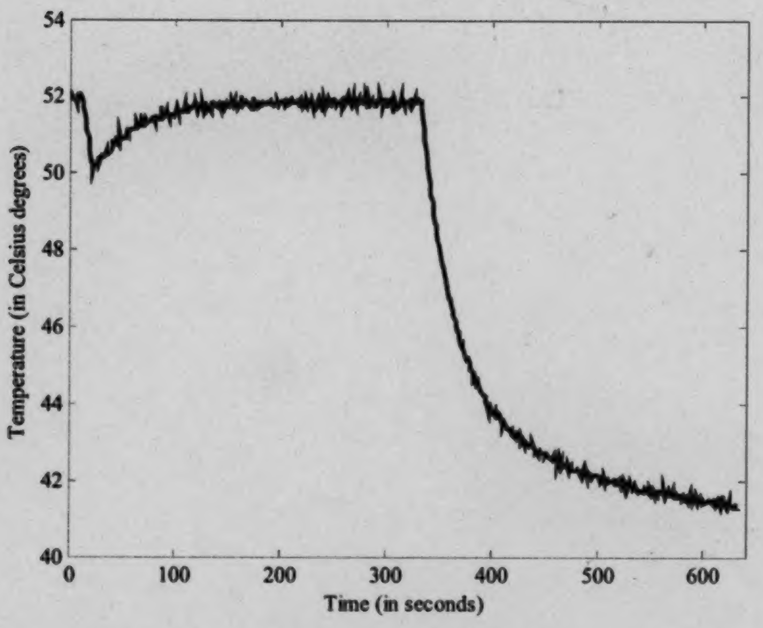

Figure 4-8 Evolution of the temperature inside the chamber during a smelling cycle

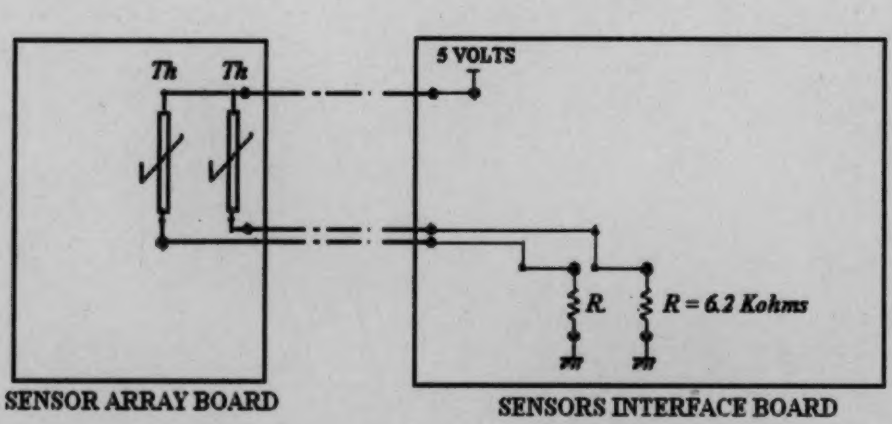
Th
Th
5 VOLTS
R
R = 6.2 Kohms
SENSOR ARRAY BOARD
SENSORS INTERFACE BOARD

Figure 4-9 Schematic of the electrical circuit for the temperature sensors

Figure 4-9 shows the schematic of the two temperature sensors (**Th**) mounted in the sensor array board. The temperature sensors were built using disk thermistors type 5K-5 produced by Semitec [59].

4.3.6 Smell Sensing Chamber

The function of the smell-sensing chamber is to keep the smell sensors isolated from any undesirable smell occurring in the neighborhood of the electronic nose. In our eNose, the Smell Sensing Chamber is built on a $(11\times9\times5)$ cm^3 rectangular aluminum box (i.e., with a total volume of $495\,cm^3$). An aluminum lid is screwed to the bottom of the box. A custom made Teflon gasket is sandwiched between the lid and the box to make the chamber airtight. Four big C-Clamping screws were added in order to ensure the air tightness of the smell-sensing chamber. Teflon was selected for the gasket because it is an odorless material with some plasticity and a very smooth surface that makes it very hard for the smell molecules to stick on it producing contamination and consequently affecting the results of further testing.

Figure 4-10 shows a picture of the inside view of the Smell Sensing Chamber. The chamber is shown upside down with the bottom lid removed. The inlet pipe (**I**) and the outlet pipe (**O**) are aligned and in opposite sides. The smell sensor array is screwed to the bottom lid (not shown in the figure) and in line with these pipes. The sample of VOM is introduced in the chamber from the inlet pipe (**I**) when the pumps draw the air inside the chamber from the outlet pipe (**O**). The VOM are blown over the top of the smell sensors.

A metallic box was chosen for two reasons. Machined metals have smoother surfaces than most plastics and hence it is easier to flush all the smell molecules out of the chamber. The second reason is that temperature differences between the incoming smell and the hot air inside the chamber can be minimized, as a metallic material is better as heat conductor than plastic or glass. Among the metals, the steel has a very smooth surface. Unfortunately, it is very hard and costly to do machining on it and the steel boxes are not easily found over the counters. In this thesis, we have used aluminum as base material for the smell-sensing chamber because it is cheaper and easier to get.

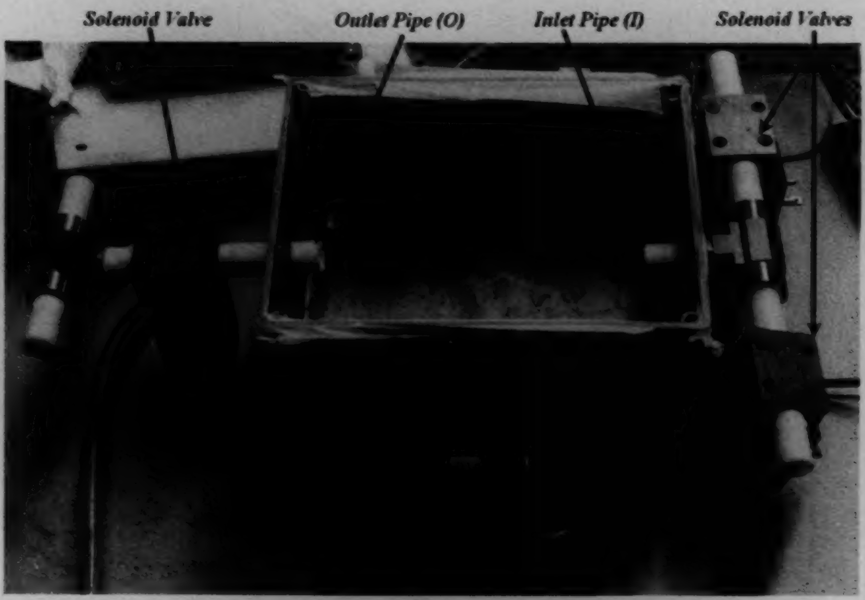

Figure 4-10 Photograph of the opened Smell Sensing Chamber

4.3.7 Sensors Interface Board

The main function of the Sensor Interface Board is to supply load resistors, ground reference and constant voltage to the output circuits of the smell sensors. There is one load resistor per each smell sensor in the array. Having the load resistors placed outside the chamber permits to adjust sensors baselines while keeping the sensors resting in stable conditions.

Figure 4-11 shows a photograph of the Sensor Interface board. The ribbon cable (gray color) in the upper left brings the ground references through the load resistors to all the smell sensors outputs. The external thermistor is assembled in this board, it can be noted in the right of the ribbon cable connector. The multicolor ribbon cable connects the sensors outputs to the analog inputs of the data acquisition board.

Figure 4-11 Photograph of the Sensor Interface Board

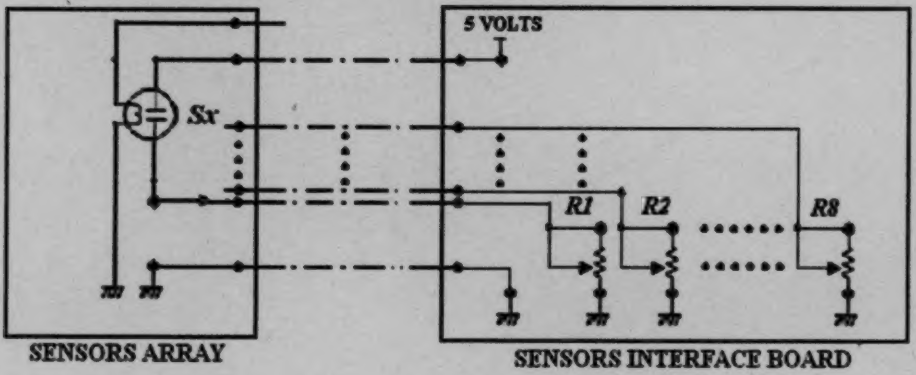
5 VOLTS
Sx
R1
R2
R8
SENSORS ARRAY
SENSORS INTERFACE BOARD

Figure 4-12 Schematic of the sensors interface circuits

Figure 4-12 shows the simplified schematic of the sensor interface circuits and their interconnection with the sensors array board. Table 4-6 shows the descriptions and specifications of the electronic components used in the design of the sensors interface circuits.

Table 4-6 Sensor Interface board electronic specifications

LABEL	DESCRIPTION	VALUE (IN KOHMS)
Sx	A given sensor "*x*" from the sensors array	
R1*	Load for Sensor TGS 880	5.53
R2	Load for Sensor TGS 2620	2.94
R3	Load for Sensor TGS 825	8.82
R4	Load for Sensor TGS 2602	3.58
R5	Load for Sensor TGS 826	5.61
R6	Load for Sensor TGS 2104	4.86
R7	Load for Sensor TGS 882	20.3
R8	Load for Sensor TGS 2610	7.62

* All resistors are implemented using 50 Kohms potentiometers

4.3.8 Control Interface Board

The function of the Control Interface Board is to interface and to amplify the output signals from the Data Acquisition Board. The output signals from the Data Acquisition Board are used to control the Smell Delivery System and the sensors heater circuits.

Figure 4-13 Control Interface Board

Figure 4-13 shows a picture of the Control Interface board. The multicolor ribbon cable in the lower part of the picture brings in the control signals from the computer. The marked area in the left (blue) corresponds to the electronic components that drive the solenoid valves. The marked area in the right (green) corresponds to the components that drive the sensors heaters voltages. The pumps are switched by an external relay (not showed in the figure). For security reasons, this relay is embedded in the pumps' power cable. An open collector chip (SN7416) buffers the control signal for this relay.

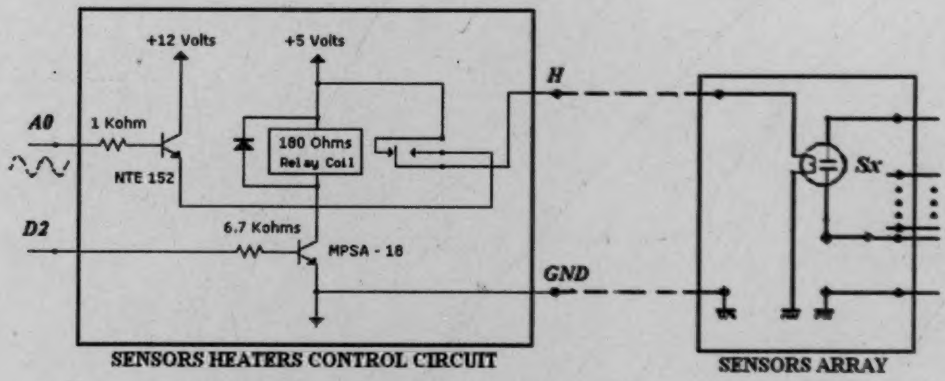

Figure 4-14 Schematics of the heater control circuit

Figure 4-14 shows the schematic of the sensors heaters control circuit. In normal operation a 5 volts constant voltage drives the sensor heaters. In this mode, the signal **(D2)** is logic "0", the transistor **(MPSA-18)** if switched OFF, the relay coil is not activated and the 5 volts constant voltage source is connected to the sensors heaters through pin **(H)**. In the heater modulation mode, the signal **(D2)** is logic "1", the transistor **(MPSA-18)** if switched ON, the relay coil is activated and the medium power transistor **(NTE 154)** drives the sensors heaters. This transistor amplifies the current of the function signal generated by the data acquisition board.

Table 4-7 Control Signals Descriptions

LABEL	DESCRIPTION	SIGNAL TYPE
A0	Function Generator Signal	Analog signal
D2	Heater Relay Control Input	Digital signal
H	Sensor Heaters Driver Signal	Analog signal
D3 – D6	Solenoid Valve Control Input for Valves: V1, V2, V3, V4	Digital signal
V1 – V4	Solenoid Valve Driver Signals	Analog signal

Table 4-7 shows detailed description of the control signals used in the sensor-heater control circuits and the solenoid valves driver circuits. Figure 4-15 shows the drivers for the solenoid valves. The solenoid valves used have 12 volts coils that work at 350 mA direct current.

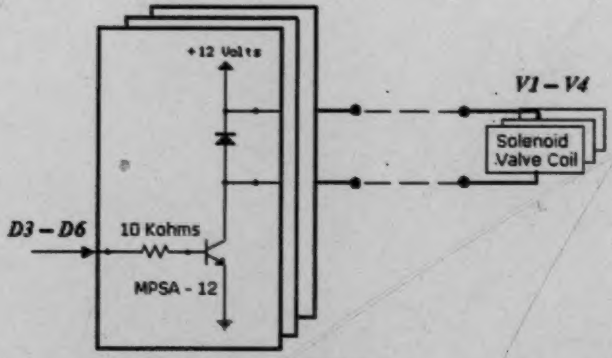

SOLENOID VALVE CIRCUIT x 4

Figure 4-15 Solenoid valves driver circuits

4.3.9 Cooling Fan

The cooling fan reduces the high temperatures produced by the sensor heaters inside the smell-sensing chamber. A four inches diameter fan type that is typically used in personal computers was selected. The cooling fan is situated perpendicular to the longest axe in the left hand side of the chamber and at about ten centimeters from its wall. The fan creates a forced constant air current that dissipates the heat out of the chamber walls and consequently reduces the temperature inside the chamber. The internal temperature drops from $70^{\circ}C$ to $52^{\circ}C$ when using the cooling fan.

4.3.10 Data Acquisition Board

The primary function of the Data Acquisition board is to acquire and digitize the analog sensors response signals and the temperature sensors signals. It also produces the analog voltage signal used to modulate the work temperature of the smell sensors. Finally, it produces the digital signals that control the operation of the smell delivery system.

CI
SI
RB-1
RB-2
RB-3
A/D

CI: Control Interface Board

SI: Sensors Interface Board

RB: Ribbon Cables (1,2,3)

A/D: Connection Plate

Figure 4-16 Data Acquisition board connections to the Sensor and Control Interface boards

Figure 4-16 shows the interconnections of the Data Acquisition Board (not showed here), the Sensor Interface board (**SI**) and the Control Interface board (**CI**) through the connection plate (**A/D**) of the Data Acquisition board. The ribbon cable (**RB-1**) brings in the sensors response from the Sensors Interface board (**SI**) to the Data Acquisition board. The ribbon cable (**RB-2**) connects the sensor output pins to the load resistors in the Sensor Interface board (**SI**). The ribbon cable (**RB-3**) carries the control signals emitted by the Data Acquisition board to the Control Interface board (**CI**).

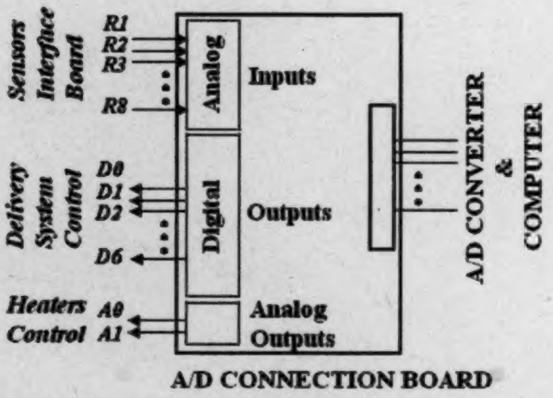
Sensors Interface Board
R1
R2
R3
R8
Analog
Inputs
Delivery System Control
D0
D1
D2
D6
Digital
Outputs
Heaters Control
A0
A1
Analog Outputs
A/D CONVERTER & COMPUTER
A/D CONNECTION BOARD

Figure 4-17 Simplified schematic of the Data Acquisition board

Figure 4-17 shows the simplified schematic of the input/output pin-out system of the Data Acquisition board. In Table 4-8, there is a detailed description of the input and output signals referenced in the schematic of Figure 4-17.

The multifunction board model NI PCI-6014 [62] was selected for the proposed eNose because this board offers great performance at a reasonable price. This board handles up to 16 analog inputs, 2 analog outputs and 8 digital bi-directional lines. The manufacturer also offers full compatibility with Matlab that was the framework selected to develop the software systems for the proposed eNose.

Table 4-8 Data Acquisition board signals

LABEL	DESCRIPTION
R1— R8	Sensors Response
D0	Air Pumps Control
D1	Air Blower (not used in this eNose prototype)
D2	Heater Relay Control
D3	Solenoid Valve #1
D4	Solenoid Valve #2
D5	Solenoid Valve #3
D6	Solenoid Valve #4 (not used in this eNose prototype)
A0	Function Generator Output
A1	Peltier Pump Control (not used in this eNose prototype)

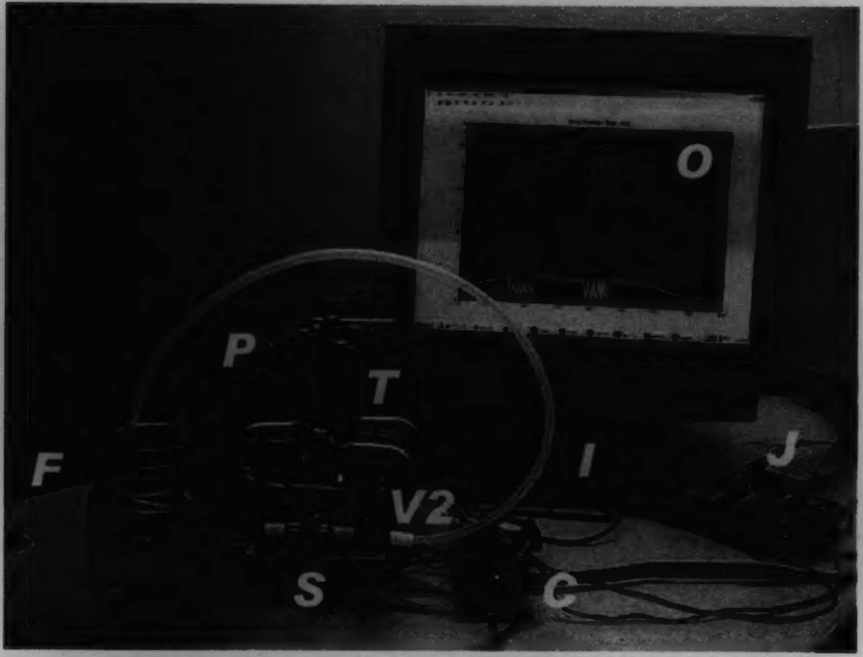

Figure 4-18 The Low Cost Electronic Nose

4.3.11 The entire eNose hardware system

Figure 4-18 shows a photograph of the low cost electronic nose implemented in this thesis. The picture shows the concentration flask (F), the smell-sensing chamber (S), one of the air pumps (P), the two input solenoid valves, the four 4 inches carpenter clamps (T), the control interface board (C), the sensors interface board (I) and the connection plate of the A/D data acquisition board (J). The solenoid valve (V2) controls the VOM input from the concentration flask (F). The solenoid valve in the left of V2 controls the input of fresh air needed to flush the VOM out of the chamber. The pumps (P) draw the air from the sensing chamber (S) trough solenoid valve (V1), which cannot be seen in this picture. The computer screen (O) shows a magnified offline view of the smell-signals. In this case two consecutive trains of a square signal control the sensors heater voltages during the steady state response of the sensors.

4.4 The Control Panel

The Control Panel is a graphical interface software application designed to allow controlling and interfacing with the hardware subsystem of the eNose (See Figure 4-19). The graphical interface consists of several virtual gadgets such as edit and list boxes, push buttons, multiple-choice buttons, checkmarks, and a virtual oscilloscope. These gadgets are organized in independent sub-modules. Each sub-module controls a specific function of the eNose hardware. This software module was developed using MATLAB visual environment and contains 6000 source code lines.

Figure 4-19 shows the Control Panel. In this picture, colored frames are drawn over this picture to highlight each sub-module. The most important sub-modules are: Sensors Viewer **(1)**, Data Acquisition control **(2)**, Smell Delivery control **(3)**, Sensor Heaters control **(4)**, Sniff Cycle control **(5,6,7,8)**.

In the **Sensors Viewer (1)** sub-module we have simulated an oscilloscope screen where the sensors responses can be viewed as they are being acquired. Below the Sensors Viewer are the controls to show magnified views of the sensors signals.

In the **Data Acquisition control (2)** sub-module we can set the sampling frequency (0.01Hz – 5000Hz) and duration (0.1 second – 2 hours) for the signal acquisition engine. The sensors to be sampled must be first selected using the list box (**Select Sensors**) in the center. The sensors responses are saved in a memory variable but they can also be saved in a disk file. The directory path and name of this file can be set through a standard Windows interface.

The **Smell Delivery control (3)** sub-module is used to manually activate the components of the smell delivery system (see Section4.3.2). Checkmark gadgets represent these components, checking the gadget turns the component on and otherwise the component is off. The temperature sensors readings are displayed in the three edit boxes located in the central part of this sub-module.

The **Sensor Heaters control (4)** sub-module controls the voltage source for the sensors heaters. In this sub-module, we have embedded a function generator program. A gamut of functions such as sinusoidal, square, sawtooth, triangle and step are currently implemented in this software. The function parameters such as the frequency, duty cycle and amplitudes are set using the edit boxes in this sub-module. The signal produced by this software is sent out to the sensors heaters through pin **A0** of the Data Acquisition board (see Figure 4-14, Table 4-7, Figure 4-16, Table 4-8 in Sections 4.3.8and 4.3.10).

The **Sniff Cycle control (5,6,7,8)** sub-module also known as **Programming Module** is used to set the parameters needed to perform automatic sniff cycles. The Programming Module was designed as a synchronic state machine with programmable state-duration. In the column of edit boxes **(5)**, we set the duration (in seconds) of each of the seven states of the sniff cycle. In the checkmarks columns **(6)**, we define the activation and the deactivation states for the data acquisition engine and the sensors heaters control sub-module.

In the **Automatic Sniff control (7)**, we define the number of consecutive sniff cycles (smelling cycles) that the eNose will automatically perform. In multiple cycles, the eNose will execute as many cycles as indicated in the edit box. This operation mode has been implemented to allow the collection of large smell-databases without user intervention.

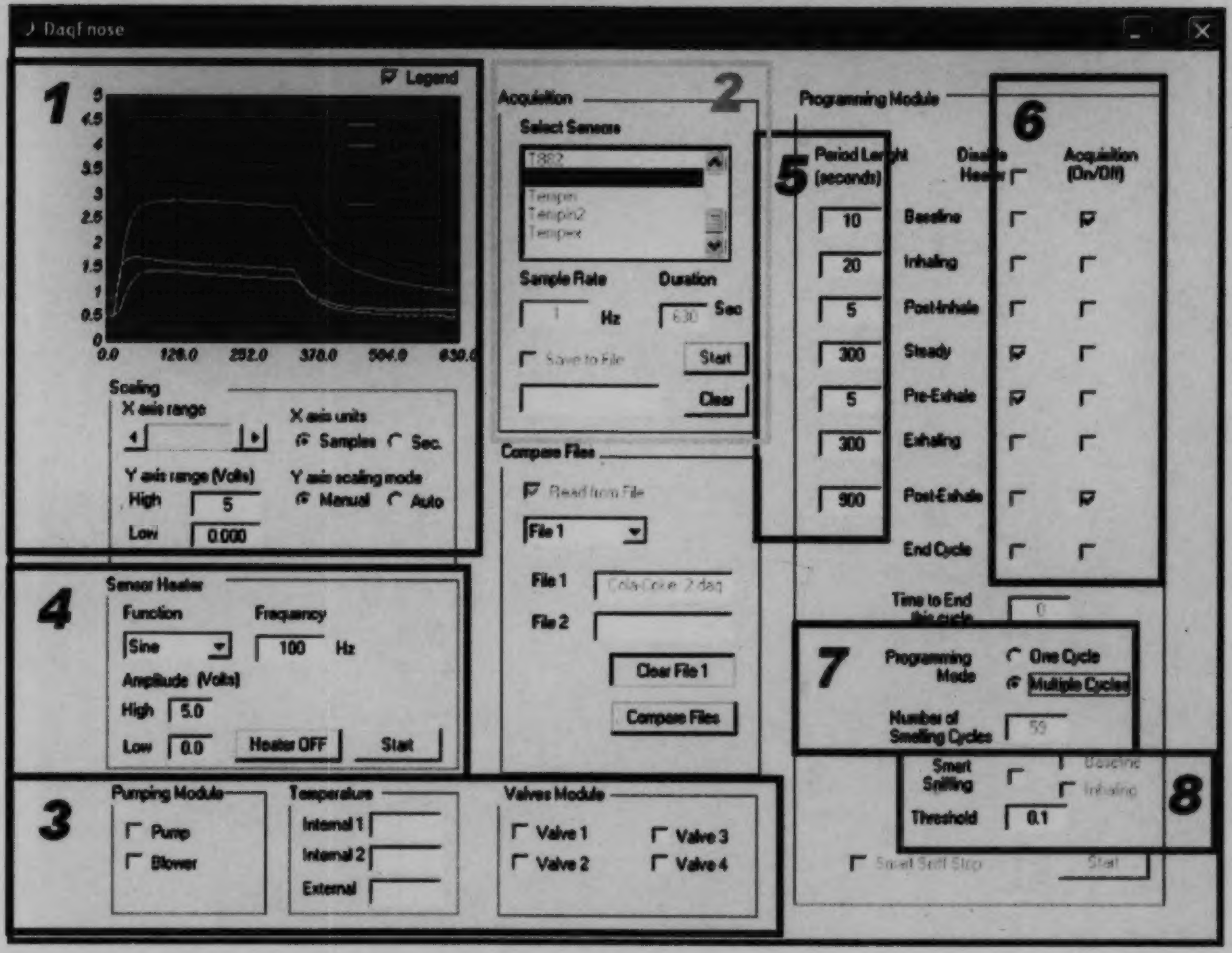
DaqEnose
1
2
3
4
5
6
7
8
5
4.5
4
3.5
3
2.5
2
1.5
1
0.5
0
0.0
126.0
252.0
378.0
504.0
630.0
Scaling
Acquisition
Compare Files
Programming Module
Sensor Heater
Pumping Module
Temperature
Valves Module
Start
Clear
Clear File 1
Compare Files
Heater OFF
Start
Internal 1
Internal 2
External

☑ Legend

X axis range

X axis units ● Samples ○ Sec.

Y axis range (Volts) High 5 Low 0.000

Y axis scaling mode ● Manual ○ Auto

Select Sensors: TB82, Tempin, Tempin2, Tempex

Sample Rate 1 Hz

Duration 630 Sec

☐ Save to File

☑ Read from File

File 1

File 1: Cola-Coke 2.daq

File 2

Function: Sine

Frequency: 100 Hz

Amplitude (Volts) High 5.0 Low 0.0

☐ Pump

☐ Blower

☐ Valve 1

☐ Valve 2

☐ Valve 3

☐ Valve 4

	Period Lenght (seconds)	Disable Heater	Acquisition (On/Off)
		☐	
Baseline	10	☐	☑
Inhaling	20	☐	☐
Post-Inhale	5	☐	☐
Steady	300	☑	☐
Pre-Exhale	5	☑	☐
Exhaling	300	☐	☐
Post-Exhale	900	☐	☑
End Cycle		☐	☐

Time to End this cycle: 0

Programming Mode ○ One Cycle ● Multiple Cycles

Number of Smelling Cycles: 59

Smart Sniffing ☐ ☐ Baseline ☐ Inhaling

Threshold 0.1

☐ Smart Sniff Stop

Figure 4-19 The eNose Control Panel Interface

4.5 The eNose Sniff Cycle

In the previous sections we have presented the design of the hardware and software interface subsystem of the proposed eNose. In this section we present the sniff-cycle proposed for our eNose. In this thesis, we define a sniff-cycle as the set of consecutive operations needed in order to physically obtain and electronically measure a sample of VOM from a given smell source.

This thesis proposes a novel and fully programmable sniff-cycle. The proposed sniff-cycle is divided into seven states (see Figure 4-20). The duration time of each state as well as most of the operations performed by the eNose in each state are fully programmable. This is an important feature that permits the use of the eNose in many different smell environments.

Four programmable operations are included in the proposed sniff-cycle. The data acquisition engine and function generator can be fully programmed to activate/deactivate in any state. The sniff-cycle can be programmed to stop the Inhale state when the sensors reach certain threshold voltage (see Section 4.6). This operation can only be programmed for the Inhale state. The sniff-cycle can be also programmed to restart a new sniff-cycle immediately after the Recovery state has ended. This operation can only be programmed in the Recovery state.

Figure 4-20 shows the structure of the proposed sniff cycle in relation to a hypothetical response signal. In this schematic we have used arbitrary units to describe the duration of each state. The number of sampling points recorded from the sensor response signal in each state can be calculated using the following equation

$$N_X = T_X \times F_{sampling} \qquad (4\text{-}3)$$

where

$X \in \{BL, I, SS, E, R\}$

N_X is the number of sampling points acquired during the sniff - cycle state "X"

T_X is the duration time of the sniff - cycle state "X"

$F_{sampling}$ is the sampling rate or frequency of the data *acquisition* process.

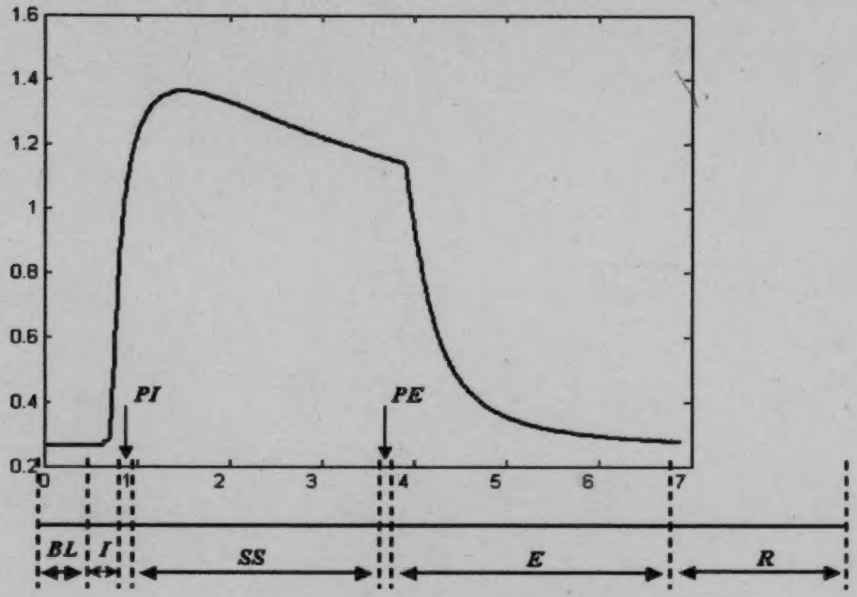

Figure 4-20 The structure of the eNose sniff-cycle

In the smell experiments realized we used the sampling rate of 1 Hz (i.e., one sample-per-second). This sampling frequency was good enough for recording the responses of the metal-oxide sensors used in the proposed eNose without loosing important information. Hence, calculating the number of sampling points in each eNose sniff-cycle state is a straightforward operation that equals to the duration time programmed for each state.

Table 4-9 describes the details of the sniff-cycle structure and the names and operations performed in each state. In Table 4-9, the first column refers to each of the sniff-cycle states labeled in the schematic of Figure 4-20. The third column of this table presents the default operations that are performed in the given state. These default operations cannot be modified.

Table 4-9 Details of the sniff-cycle structure

LABEL	STATE NAME	DEFAULT OPERATIONS AND DEFAULT STATE DURATIONS	COMMENTS
BL	Baseline	No default operations. Duration: 10s. It can be shortened up to 1 second.	Sensors baselines must be recorded before starting the inhalation of a new smell.
I	Inhale	Valves (V1, V2, see Section 4.3.2) and the air pumps are switched ON. Duration: 10s	In ten seconds, eNose inhales 330 ml of VOM from the concentration flask. The volume of the sensing chamber is 500 ml. (see Sections 4.3.2 and 4.3.6).
PI	Post-inhale	All valves and air pumps are switched OFF. Duration: 5s	
SS	Steady	No default operations. Duration: 300s	It was observed that the slowest sensors reach their saturation in around 200s after the VOM input. Therefore, $T_{SS} = 300s$ was chosen in all our experiments.
PE	Pre-exhale	No default operations. Duration: 5s	
E	Exhale	Valves (V1, V3, see Section 4.3.2) and the air pumps are switched ON. Duration: 300s	
R	Recovery	All valves and air pumps are switched OFF. Duration: 900s	

4.6 The Smart-Sniff Cycle

The **Smart-Sniff-Cycle** is a novel sniffing technique proposed in this thesis. The objective of this special sniff cycle is to avoid the poisoning of the sensors that was observed in some smell experiments. The sensors and the smell delivery system can be poisoned when certain VOM from strong smell sources such as ground pepper and some essential oils are inhaled. The VOM of these substances (when inhaled for more than two or three seconds) produce over saturation of the smell sensors and it is difficult to recover their baselines afterwards. These VOM also stick on the sensing chamber walls aggravating the problem and it usually takes very long time (in some cases hours) to clean the system from these smells.

In this thesis, we propose a simple solution to this problem. In the Inhaling state, the sensors signals are monitored and compared in real time to a given threshold voltage. The threshold default value is set to 0.1 volts but it can be changed to any value in the range 0-5 volts. As soon as any of the sensors reach this threshold (above its baseline voltage) the Inhaling state is terminated and the eNose switch to the next state of the sniff cycle. The Inhaling state is also terminated if its programmed duration time is reached before any of the sensors reaches the threshold.

4.7 Summary

In this chapter, we presented the design and implementation of a low cost electronic nose suitable for integration with multimedia systems. We presented a brief discussion about the general architecture including the hardware and software modules of the proposed eNose. We then provided a description of the smell-space used in this thesis. This was followed by the detailed explanation of the hardware modules of the eNose. The software application that allows for controlling and interfacing these hardware modules was also discussed in great detail. Finally, we presented the eNose smell sniff-cycle and a novel smell sniff technique.

Chapter 5

The eNose signal processing system

In the previous chapter, we presented the hardware design of a low cost electronic nose that is suitable for integration with multimedia systems. In this chapter we present the signal processing techniques and the GUI processing software framework developed for this electronic nose.

The organization of this chapter is as follows. Section 5.1 describes the different transient regions of the smell signals produced by the eNose hardware. Section 5.2 presents a detailed explanation of the signal preprocessing techniques implemented in the eNose software system. Section 5.3 describes the GUI software system that computes the signal processing and smell-pattern analysis in the eNose, which is followed by the summary.

5.1 The Smell-Signal Transient Regions

In this section we define the transient regions of the smell-signal response that are used by the proposed signal preprocessing techniques in order to extract the static and dynamic features from the smell signal. A typical smell-signal response can be divided into three transient regions: the ascending transient, the steady state transient and the descending transient (see Figure 5-1).

Figure 5-1 shows a schematic comparing the timing structure of the eNose sniff-cycle versus the smell-signal transient regions. The ascending transient region (AT) is defined as the sensors responses recorded during the 60 seconds after the smell inhaling state (**I**) started. In this region the sensors are responding rapidly to the input of VOM. The steady state transient region (**ST**) is defined as the sensors responses recorded from sampling point $(N_{BL}+61)$ to the end of the Pre-exhale state (**PE**). In this region the dynamics of the chemical interactions between the sensor and the odorant tend slowly to stabilize producing a distinctive elbow in the smell-signal. The proposed descending transient region (**DT**) is defined as the response enclosed from the beginning of the exhaling period to the end of this period. In this region, the sensors responses decay rapidly during the first third and then slowly tend to reach a horizontal line. Two actions are combined here, the rapid extraction of the VOM out of the chamber and the strong current of clean air blowing over the sensor. The first action clearly diminishes the sensors responses voltages because the concentration of VOM is dramatically reduced. The second action tries to increase the sensors responses voltages because an air current is blown over the sensor heads, see the reference manuals at Figaro web site [24].

In Figure 5-1, the "x" axis represents sample points instead of seconds because in the eNose experiments, we used the sampling frequency $F_S = 1\ Hz$ (i.e.. one-sample-per-second). Therefore, converting from duration-time to number-of-samples-points is a straightforward one-to-one operation.

Table 5-1 describes the labels used to represent each transient region depicted in Figure 5-1 and the formulas for calculating the starting sampling-point and ending sampling-point for each of these three proposed transient regions. These formulas are based in the duration times of the proposed sniff-cycle states. The variable N_X represents the number of signal sampling points recorded in the X state of the eNose sniff-cycle. For example, N_{BL} is the number of sampling points recorded in the Baseline state (**BL**).

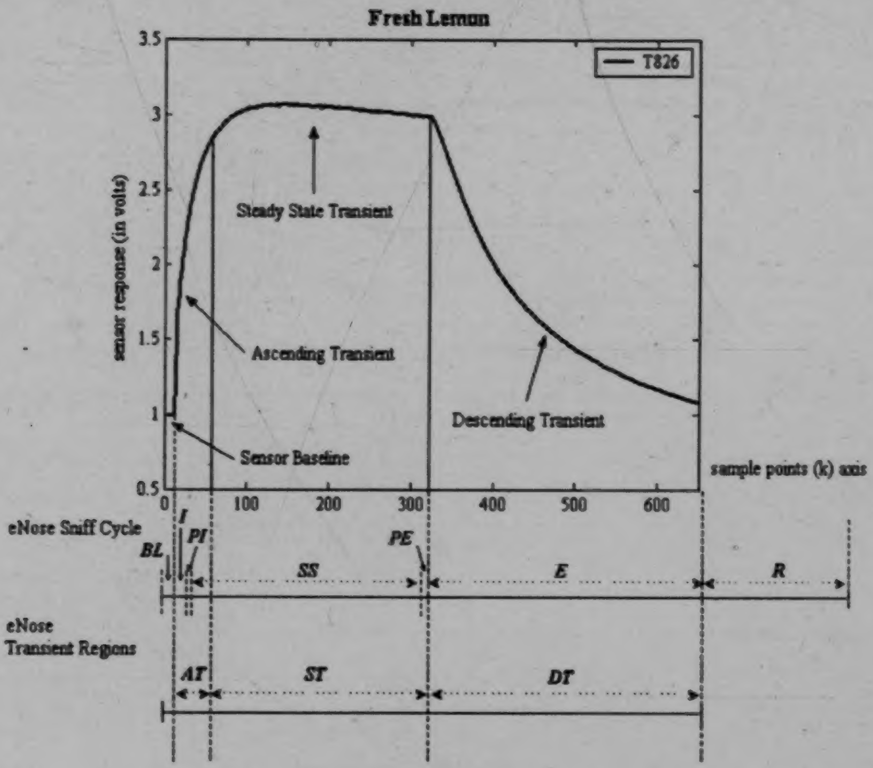

Figure 5-1 Smell signal transient regions for eNose

Table 5-1 Description of the eNose smell-signal transient regions

LABEL	REGION NAME	STARTING SAMPLE	ENDING SAMPLE
AT	Ascending Transient	$(N_{BL}+1)$	$(N_{BL}+60)$
ST	Steady-State Transient	$(N_{BL}+60+1)$	$(N_{BL}+N_I+N_{PI}+N_{SS}+N_{PE})$
DT	Descending Transient	$(N_{BL}+N_I+N_{PI}+N_{SS}+N_{PE}+1)$	$(N_{BL}+N_I+N_{PI}+N_{SS}+N_{PE}+N_E)$

5.2 The Smell-Signal Preprocessing Techniques

In this section, we present the implementation details of the different signal preprocessing techniques proposed in this thesis. These techniques can be divided into three broad categories: baseline manipulation, feature-vector extraction and feature-vector normalization (see Section 3.3).

In baseline manipulation, the sensor responses are processed relatively to their baselines. In the feature-vector extraction stage, the more relevant features are extracted from the sensors responses and a vector constituted by these features is assembled to represent the response to the given smell. Lastly, in the feature-vector normalization stage, the coordinates (features) of feature-vector assembled in the previous stage are adjusted and scaled such that all the features magnitudes are comparable. Table 5-2 shows the smell-signal preprocessing techniques implemented in the eNose software system

Table 5-2 Smell-signal preprocessing techniques used in this thesis

BASELINE MANIPULATION	FEATURE-VECTOR EXTRACTION	NORMALIZATION
Difference (DIFF)	Steady-State (SS)	Vector Array (VNORM)
Relative (REL)	Time Constants (TC)	Vector Auto-scaling (VAS)
Fractional (FRACT)	Whole Signal Derivatives (WSD)	Dimension Auto-scaling (DAS)
Logarithmic (LOG)	Ascending Transient Derivatives (ATD)	
	Steady State Transient Derivatives (STD)	
	Descending Transient Derivatives (DTD)	
	Discrete Fourier Transform (DFT)	
	Temperature Modulated Whole Signal Derivatives (TMWSD)	
	Temperature Modulated Discrete Fourier Transform (TMDFT)	

In order to facilitate the mathematical formulation for the different signal processing techniques, we use the following notation:

N_e: The number of measurements from VOM- examples contained in a smell-database

N_s: The number of sensors in the proposed electronic nose

N_k: The number of data points acquired from each VOM-example

$V_{e,s}(t)$: The electrical signal generated by sensor s, $(1 \leq s \leq N_s)$ in response to the given VOM-example e, $(1 \leq e \leq N_e)$

$W_{e,s}[k]$: Digitized version of $V_{e,s}(t)$, where $t = kT_0$ and $(1 \leq k \leq N_k)$

${W^{BL}}_{e,s}$: The mean value of the baseline response of sensor s, $(1 \leq s \leq N_s)$, recorded during sniff-cycle started to sniff the VOM of example e, $(1 \leq e \leq N_e)$

$X_{e,s}[k]$: The output of the baseline manipulation preprocessing stage, which is the baseline-relative version of $W_{e,s}[k]$

N_f: The number of features extracted from the response of a sensor s

N_m: The number of features extracted from the array response $X_{e,s}[k]$, where $N_m = N_f \times N_s$

$F(e,m)$: The m^{th} feature extracted from the array response $X_{e,s}[k]$ to the smell example e, such that $(1 \leq m \leq N_m)$

F_e :	The row feature-vector extracted from smell example e, such that $F_e = [F(e,1), F(e,2), ..., F(e, N_m)]$
T_X :	The duration time (in seconds) programmed for the X state of the eNose sniff-cycle (see Section 4.5)
N_X :	The number of signal sampling points recorded in the X state of the eNose sniff-cycle (see Section 4.5). For example, N_{BL} is the number of sampling points recorded in the baseline state (**BL**) of the eNose sniff-cycle.
F_S :	The sampling frequency for the data acquisition process. $F_S = 1 Hz$ (i.e., one-sample-per-second).

5.2.1 Baseline Manipulation

The sensors baselines are the sensor responses to a reference smell. The reference smell used in our eNose was the laboratory normal ambient air. The baseline manipulation techniques use the baseline values of the sensors (always recorded before each sample of VOM is inhaled) to preprocess the whole response signals. This preprocessing stage aims to compensate for occasional sensors drifts caused by small variations in the ambient temperature from one sniff to the next (see Section 3.3.1). The smell sensor response to a given smell is in general fixed and relative to the initial baseline value when the baseline drifts is caused by minor temperature changes. The baseline manipulation techniques do not effectively compensate for large variations in the sensors baselines.

The first state of the eNose sniff-cycle is the Baseline State. In this state the sensors respond to the reference air that was used to purge the VOM inhaled in the previous sniff. In this implementation, each sensor baseline value is calculated as the average of these sensor response values recorded in the Baseline State of the eNose sniff-cycle. The following equation is used to calculate the sensor array baseline mean values

$$W_{e,s}^{BL} = \frac{1}{N_{BL}} \sum_{1}^{k=N_{BL}} W_{e,s}[k] \qquad \forall e,s \tag{5-1}$$

where N_{BL} is the number of sampling points acquired in the baseline state BL.

In the eNose software system, we implemented the four Baseline Manipulation techniques presented in Section 3.3.1: Difference (DIFF), Relative (REL), Fractional change (FRACT) and Logarithmic (LOG). Table 5-3 shows the equations used to describe the four choices of preprocessing techniques implemented in this stage. The selected technique is applied to the digitized sensors signals $W_{e,s}[k]$ and the resultant preprocessed signal $X_{e,s}[k]$ is used as the input to the next preprocessing stage (i.e., the feature-vector extraction stage).

Table 5-3 The eNose baseline manipulation techniques

BASELINE MANIPULATION	FORMULA
DIFF	$X_{e,s}[k] = W_{e,s}[k] - W^{BL}{}_{e,s}$
REL	$X_{e,s}[k] = \frac{W_{e,s}[k]}{W^{BL}{}_{e,s}}$
FRACT	$X_{e,s}[k] = \frac{W_{e,s}[k] - W^{BL}{}_{e,s}}{W^{BL}{}_{e,s}}$
LOG	$X_{e,s}[k] = \log \frac{W_{e,s}[k]}{W^{BL}{}_{e,s}}$

5.2.2 Feature-Vector Extraction

The goal of the feature vector extraction module is to find a small set of features that can represent efficiently the smells under analysis. These techniques exploit relevant characteristics of the smell-signal such as the stationary information present in the signal steady state and the dynamic information contained in the signal transient regions.

In this thesis, seven different feature-vector extraction techniques were implemented in the eNose software system. These techniques aim to extract the stationary and dynamic smell information from the sensors responses to a VOM-example. The proposed techniques are grouped in four categories: the Signal Steady State techniques, the Signal Dynamics Techniques, Signal Spectral Techniques and the Temperature Modulation Techniques (see Section 3.3.2).

5.2.2.1 Steady-State Technique

The Steady-State (SS) technique extracts the stationary information from the signals given when the sensors acquire a stable state in response to a VOM input. In our experiments, the slowest sensors reached their saturation in around 200 seconds after the VOM input. Based in these results, we propose to calculate the SS as the mean value of the sensors responses recorded over the last sixth of the steady state of the eNose sniff-cycle.

The number of features N_f extracted by the SS technique from each sensor is equal to one (i.e., $N_f = 1$). Consequently, total number of features N_m obtained from each observation of the eight sensors array is eight. These eight features are put together in order to assemble a feature-vector F_e. The feature-vector F_e is said to have dimensionality eight because it has eight coordinates (features). The coordinates of the feature-vector F_e produced by the SS preprocessing technique are calculated using the following equation

$$F(e,m) = \frac{6}{N_{ss}} \sum_{k=a}^{k=b} X_{e,s}[k] \quad \forall e,s \tag{5-2}$$

where $m = s$, $a = \left(N_{BL} + N_I + N_{PI} + \frac{5N_{SS}}{6} + 1 \right)$, $b = \left(N_{BL} + N_I + N_{PI} + N_{SS} \right)$.

5.2.2.2 Time Constants Technique

The Time Constants (TC) technique extracts time values measured from the smell-signal rising and falling curves. In this thesis, we implement the TC technique proposed by Tomas Eklöv et al. (see Section 3.3.2.1). In this technique, the number of features N_f extracted from each sensor is equal to four (i.e., $N_f = 4$). Consequently, the total number of features N_m obtained from each observation of the $N_s = 8$ sensors array is $N_m = 32$. These 32 features are put together in order to assemble a feature-vector F_e. The features (coordinates) of the feature-vector F_e produced by the TC preprocessing technique are obtained using the following algorithm.

The feature $T_{on}Y$ represents the time for the smell-signal to reach $Y\,\%$ of its maximum value after the VOM input is ON. Two values of $Y\,\%$ are proposed, $Y = 60\%$ and $Y = 90\%$. The following equation is used to calculate these two features $T_{on}Y$

$$T_{on}Y = Arg_{a \le k \le b}\left(\left(\frac{Y}{100} Max\left(X_{e,s}[h] \right) - X_{e,s}[k] \right) = 0 \right) \quad \forall_{e,s} \tag{5-3}$$

where $a = \left(N_{BL} + 1 \right)$ and $b = \left(N_{BL} + N_I + N_{PI} + N_{SS} + N_{PE} \right)$, $\left(1 \le h \le N_k \right)$.

The feature $T_{off}Y$ represent the time for the smell-signal to fall to $X\,\%$ of its maximum value after the VOM purging is ON. Two values of $Y\,\%$ are proposed, $Y = 40\%$ and $Y = 10\%$. The following equation is used to calculate these two features $T_{off}Y$

$$T_{off}Y = Arg_k\left(\left(\frac{Y}{100}Max(X_{e,s}[h]) - X_{e,s}[k]\right) = 0\right) \quad \forall_{e,s} \qquad (5-4)$$

where $k \in DT_{region}$ and $(1 \leq h \leq N_k)$

In Eq. 5-3 and Eq. 5-4, the function $Max(\cdot)$ returns the maximum value reached by each of the sensors in the array in response to a given VOM-example e. The function $Arg_k(\cdot)$ returns the time (in seconds) for each sensor signal $X_{e,s}[k]$ to reach the percentage Y % of its maximum value.

5.2.2.3 Signal Derivatives Techniques

In Signal Derivatives techniques, the slope of the smell-signal is computed over several time intervals (see Section 3.3.2.1). These slope values are then used to discriminate smells. The major steps in this technique are summarized in the following algorithm.

SD algorithm

Step - 0, the size of the time interval k_n and the value of constant k_0 are defined in this step. These parameters are in general different for each particular implementation of the signal derivatives technique. These parameters must be calculated according to each particular implementation of the signal derivatives technique and given to this algorithm as input parameter values.

Step - 1, the derivative of the whole smell-signal is computed using an approximation method based on the Taylor series (see Section 3.3.2.1). The following equation is used to compute the smell-signal derivative $X'_{e,s}[k]$

$$X'_{e,s}[k]=\frac{X_{e,s}[k+1]-X_{e,s}[k]}{k+1-k}=X_{e,s}[k+1]-X_{e,s}[k] \quad \forall_{e,s} \qquad (5\text{-}5)$$

where $1 \le k \le N_k$.

Step - 2, the signal derivative $X'_{e,s}[k]$ is divided into N_f identical time intervals and the average derivative over each interval is calculated using the following equation

$$W^h_{e,s}=\frac{1}{k_n}\sum_{k=a}^{k=b}X'_{e,s}[k] \quad \forall_{e,s} \qquad (5\text{-}6)$$

with $a=k_0+(h-1)k_n+1$ and $b=k_0+hk_n$ such that $1 \le h \le N_f$

where

$W^h_{e,s}$ is the average value of each sensor signal derivative $X'_{e,s}[k]$ over time interval "h"

N_f is the number of features to be extracted from each sensor signal

a is the starting sampling point of interval "h"

b is the ending sampling point of interval "h"

k_n is the size of the interval given in number of sampling points

k_0 is a constant that depends on the feature - extraction technique used

Step - 3, the feature-vector F_e is assembled using the N_f parameters that were extracted from each sensor signal. The following equation is used

$$F_e=\left[\; W^1_{e,s} \;\; W^2_{e,s} \;\; \ldots \;\; W^{N_f}_{e,s} \;\right] \quad \forall_{e,s} \qquad (5\text{-}7)$$

where N_f is the number of features extracted from each sensor signal.

5.2.2.3.1 Whole Signal Derivatives Technique

In this thesis, we have implemented the derivative technique proposed by Cosimo et al. (see Section 3.3.2.1). Henceforth, this technique is referred to as WSD (Whole Signal Derivatives) as the derivative is calculated over the whole signal. The major steps in this technique are explained as follows.

The Whole Signal Derivative (WSD) technique divides the smell-signal into seven intervals of equal size and calculates the average of the derivatives computed over each of the seven intervals. The size of each interval k_n is calculated using the following equation

$$k_n = \frac{(N_k - 1 - N_{BL})}{N_f} \tag{5-8}$$

where N_f is the number of features to be extracted from each sensor signal.

In the WSD technique, the number of features N_f extracted from each sensor response is equal to seven (i.e., $N_f = 7$). Consequently, the total number of features N_m obtained from each observation of the $N_s = 8$ sensors array is $N_m = 56$. These 56 features are put together in order to assemble a feature-vector F_e. The features (coordinates) of the feature-vector F_e produced by the WSD preprocessing technique are calculated using the **SD algorithm** (see Section 5.2.2.3) with the value of parameter $k_0 = N_{BL}$.

The WSD technique has the disadvantage of producing a feature-vector of large dimensionality (large number of features). This large number of features could degrade the performance of the pattern recognition system if the number of examples per class is not large enough (see Section 3.4). Therefore, in this thesis, we propose three modified versions of the WSD technique that reduce the number of features extracted by dividing the smell-signal in the three transient regions defined in Section 5.1. The comparative performance of the Signal Derivative method applied in each different transient region can also help to define which transient region is best for the smell discrimination. The next three sections present these three proposed modifications of the WSD method.

5.2.2.3.2 Ascending Transient Derivatives Technique

The Ascending Transient Derivatives (ATD) technique computes the average of the derivative over three equally sized intervals from the ascending transient region (AT). The size of the interval k_n is calculated using the following equation

$$k_n = \frac{N_{AT}}{N_f} \qquad (5\text{-}9)$$

where N_f is the number of features to be extracted from each sensor signal, and N_{AT} is the number of sampling points in the Ascending Transient (AT) region.

In the ATD technique, the number of features N_f extracted from each sensor response is equal to three (i.e., $N_f = 3$). Consequently, the total number of features N_m obtained from each observation of the $N_s = 8$ sensors array is $N_m = 24$. These 24 features are put together in order to assemble a feature-vector F_e. The features (coordinates) of the feature-vector F_e produced by the ATD preprocessing technique are calculated using **SD algorithm** (see Section 5.2.2.3) with the value of parameter $k_0 = N_{BL}$

5.2.2.3.3 Steady State Transient Derivatives Technique

The Steady State Transient Derivatives (STD) technique computes the average of the derivative over two equally sized intervals from the steady state transient region (ST). The size of the interval k_n is calculated using the following equation

$$k_n = \frac{N_{ST}}{N_f} \tag{5-10}$$

where N_f is the number of features to be extracted from each sensor signal, and N_{ST} is the number of sampling points in the Steady State Transient (ST) region.

In the STD technique, the number of features N_f extracted from each sensor is equal to two (i.e., $N_f = 2$). Consequently, the total number of features N_m obtained from each observation of the $N_s = 8$ sensors array is $N_m = 16$. These 16 features are put together in order to assemble a feature-vector F_e. The features (coordinates) of the feature-vector F_e produced by the STD preprocessing technique are calculated using **SD algorithm** (see Section 5.2.2.3) with the value of parameter $k_0 = (N_{BL} + 60 + 1)$.

5.2.2.3.4 Descending Transient Derivatives Technique

The Descending Transient Derivatives (DTD) technique computes the average of the derivative over three equally sized intervals from the descending transient region (DT) only. The size of the interval k_n is calculated using the following equation

$$k_n = \frac{N_{DT}}{N_f} \tag{5-11}$$

where N_f is the number of features to be extracted from each sensor signal, and N_{DT} is the number of sampling points in the Descending Transient (DT) region

In the DTD technique, the number of features N_f extracted from each sensor is equal to three (i.e., $N_f = 3$). Consequently, the total number of features N_m obtained from each observation of the $N_s = 8$ sensors array is $N_m = 24$. These 24 features are put together in order to assemble a feature-vector F_e. The features (coordinates) of the feature-vector F_e produced by the DTD preprocessing technique are calculated using **SD algorithm** (see Section 5.2.2.3) with the value of parameter $k_0 = (N_{BL} + N_I + N_{PI} + N_{SS} + N_{PE} + 1)$.

5.2.2.4 Discrete Fourier Transform Technique

In this technique a feature-vector is represented by its DFT coefficients. In this thesis, the first ten coefficients were selected because almost all the signal power is concentrated in these coefficients (see Figure 5-2).

Figure 5-2 shows the plot of the first 100 coefficients obtained with the application of the DFT transform to the response signal of Figaro sensor T880. A sample of VOM from fresh lemon is used in this eNose experiment. Note, that the first few coefficients have the greatest power values. This characteristic pattern is observed in all the different smell experiments realized with our eNose.

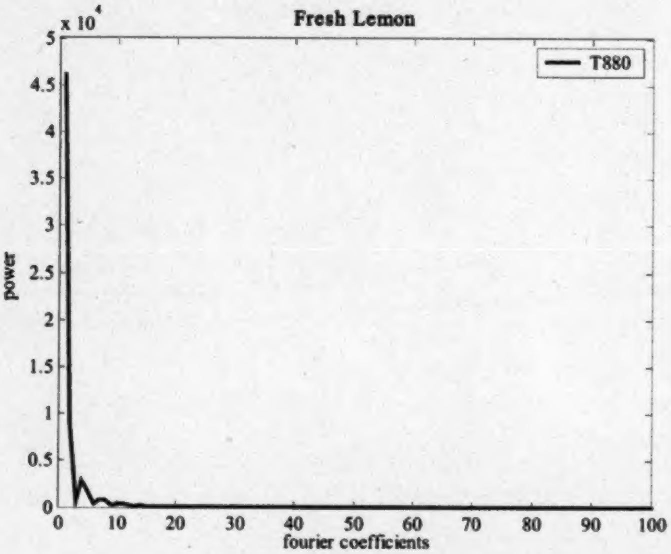

Figure 5-2 Power spectrum of TGS 880 sensor response to a VOM lemon sample

In the DFT technique, the number of features N_f extracted from each sensor is equal to ten (i.e., $N_f = 10$). Consequently, the total number of features N_m obtained from each observation of the $N_s = 8$ sensors array is $N_m = 80$. These 80 features are put together in order to assemble the feature-vector F_e.

5.2.2.5 Temperature Modulation Techniques

In the *Temperature Modulation* (TM) techniques, the work-temperature is modulated while capturing the sensor output in order to improve the detection performance. These techniques are commonly applied to metal-oxide gas sensors because these sensors need to be heated at very high temperatures in order to detect VOM (see *Temperature Modulation* techniques in Section 3.3.2).

Modulation Function used in the eNose smell experiments

In this thesis, we propose a simple work-temperature modulation function. The objective of the proposed function is to turnoff the heating circuit after most of the sensors have already reached the steady state (see Figure 5-3). The proposed function consists on a zero volts pulse of 20 seconds duration. The zero pulse is applied 150 seconds after the smell sample was inhaled and the smell purging starts 100 seconds after the heater voltage is switched-back to 5 volts.

Figure 5-3 shows the temperature modulation function response of the sensors array to a VOM sample of Coca Cola. The zero pulse is sent when almost all the sensors have reached their steady states. The width of this pulse was set to 20 seconds. This time was selected because it is long enough to produce a change in the sensors response values and small enough to allow rapid recovery of their previous state.

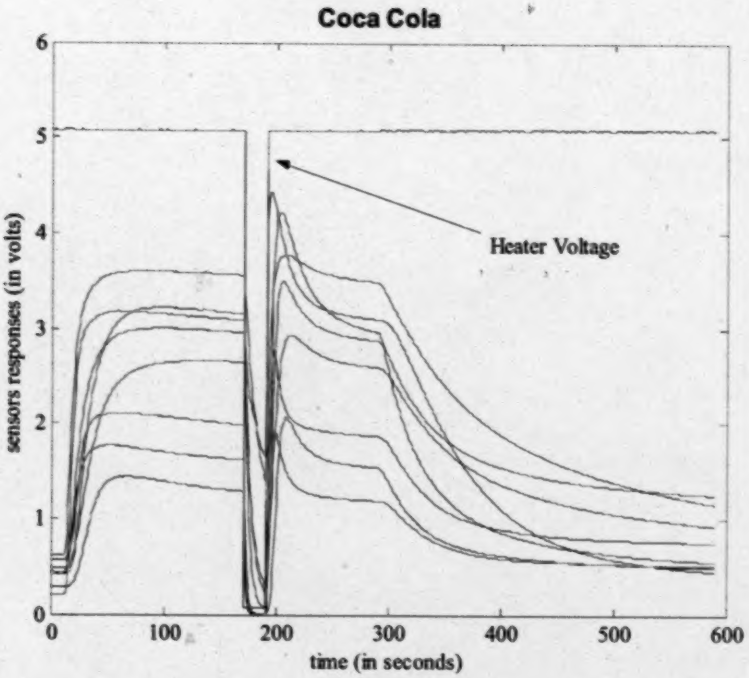

Figure 5-3 Array sensors response to the proposed modulation function

Table 5-4 describes the sniff-cycle settings used with the proposed temperature modulation function. The first and second columns describe each sniff-cycle state and its proposed duration time. The fourth column indicates the function generator activation/deactivation states. The zero volts voltage source is connected to the sensors heaters at the beginning of the Steady (**SS**) state and disconnected at the beginning of the Pre-Exhale (**PE**) state. Therefore, a zero volts voltage step is sent to the heaters and kept during 20 seconds. The fifth column indicates when the data acquisition engine is recording the sensor signals. The data acquisition engine starts recording at the beginning of the Baseline (**BL**) state and stops recording at the beginning of the Recovery (**R**) state. Therefore, the sensors signals are recorded for 580 seconds, from the beginning of the sniff-cycle until the end of the smell is purged out of the sensing chamber.

Table 5-4 Sniff Cycle settings for the proposed Temperature Modulation Function

SNIFF CYCLE STATE	DURATION	PUMPS	FUNCTION GENERATOR:	DATA ACQUISITION ENGINE
			ZERO PULSE	
Baseline (BL)	10s	--	--	Start
Inhale (I)	10s	Start	--	
Post-Inhale (PI)	150s	Stop	--	
Steady (SS)	20s	--	Start	
Pre-Exhale (PE)	100s	--	Stop	
Exhale (E)	300s	Start	--	
Recovery (R)	300s	Stop	--	Stop

i) Hybrid Technique TMWSD

The Hybrid technique TMWSD proposed in this thesis is a combination of the WSD technique with a TM technique that uses the proposed work-temperature modulation function. It applies the WSD technique to the signal region enclosing the transients induced in the sensors signal responses by the proposed modulation function.

The TMWSD computes the average of the derivative over seven equally sized time intervals on the signal region enclosing the induced transients. The size of each interval k_n is calculated using the following equation

$$k_n = \frac{(N_{SS} + N_{PE} - 1)}{N_f} \qquad (5\text{-}12)$$

where N_f is the number of features to be extracted from each sensor signal.

In the TMWSD technique, the number of features N_f extracted from each sensor is equal to seven (i.e., $N_f = 7$). Consequently, the total number of features N_m obtained from each observation of the $N_s = 8$ sensors array is $N_m = 56$. These 56 features are put together in order to assemble a feature-vector F_e. The features (coordinates) of the feature-vector F_e produced by the TMWSD preprocessing technique are calculated using SD algorithm with the value of constant $K_0 = N_{BL} + N_I + N_{PI} + 1$

ii) Hybrid Technique TMDFT

The Hybrid technique TMDFT proposed in this thesis is a combination of the DFT technique with a TM technique that uses the proposed work-temperature modulation function. It applies the DFT technique to the signal region enclosing the transients induced in the sensors signal responses by the work-temperature modulation function.

TMDFT extracts the first ten coefficients descriptors from the response of each sensor in the array. The descriptors are obtained after applying the Fourier transform to the transients induced in the sensors signal responses by the work-temperature modulation function. In this thesis, we chose the first ten coefficients because almost all the signal power is concentrated on these coefficients (see Figure 5-4 and Figure 5-5).

In the TMDFT technique, the number of features N_f extracted from each sensor is equal to ten (i.e., $N_f = 10$). Consequently, the total number of features N_m obtained from each observation of the $N_s = 8$ sensors array is $N_m = 80$. These 80 features are put together in order to assemble the feature-vector F_e extracted from each example e.

Figure 5-4 shows the plot of the first 30 coefficients obtained from the application of the DFT transform to the sensors array response signals obtained using TMDFT technique. A sample of VOM from Coca Cola is used in this eNose experiment. Note, that the first few coefficients have the greatest power values.

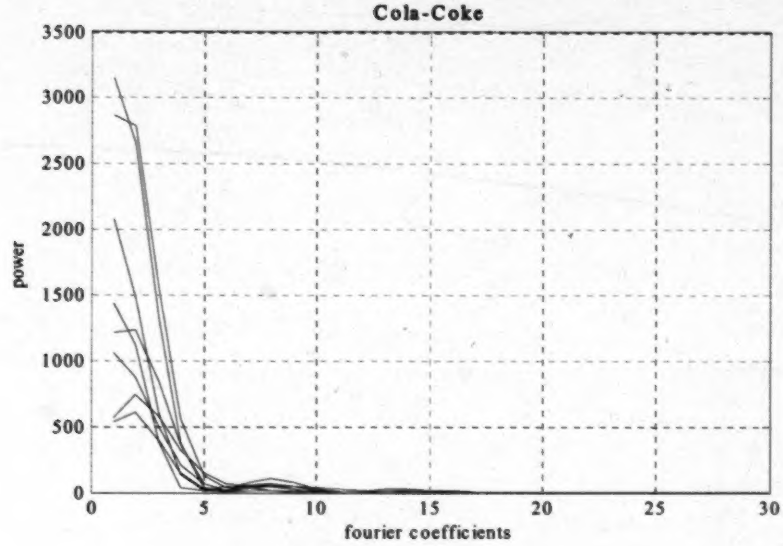

Figure 5-4 Power spectrum of the eight sensors signals responses to Coca Cola

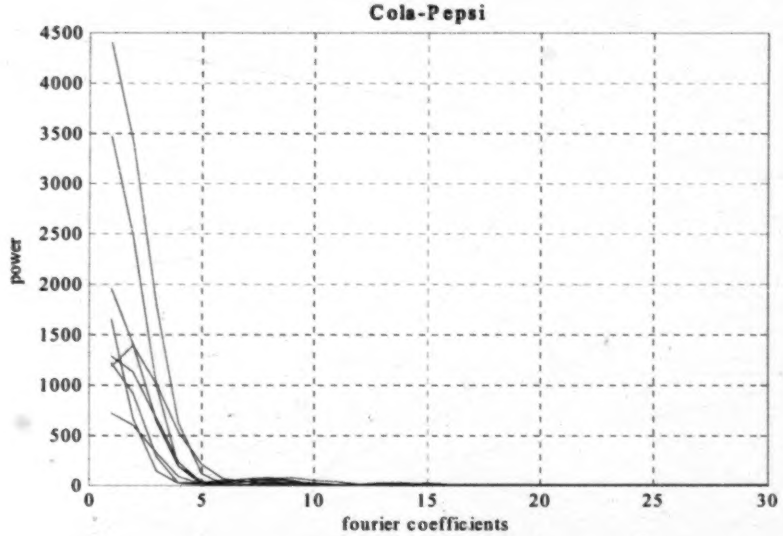

Figure 5-5 Power spectrum of the eight sensors signals responses to Pepsi Cola

Figure 5-5 shows the plot of the first 30 coefficients obtained from the application of the FFT transform to the sensors array response signals obtained using TMDFT technique. A sample of VOM from Pepsi Cola is used in this experiment. The maximum signal power is concentrated in the first few coefficients.

Note the differences between the power spectra from Coca Cola and Pepsi Cola. For example, coefficients 5 to 10 from the Coke spectrum plot are slightly greater that same coefficients from the Pepsi power spectrum plot.

5.2.3 Feature-Vector Normalization

In the previous section, several features have been proposed for smell recognition. Some of these features such as the steady state (SS) sensor response parameters, which are voltage values, are not comparable to features of the time-interval types such as $T_{on}X$ (see Section 5.2.2.2).

The feature-vector normalization techniques transform the distribution of the original values that the extracted features can take by adjusting them to fit into a new dynamic range ensuring that all the features magnitudes are comparable. Three commonly used feature-vector normalization techniques are implemented in the eNose (see Section 3.3.3): vector auto-scaling (VAS), dimension auto-scaling (DAS) and vector normalization (VNORM).

5.3 The eNose Software System

In this thesis, we propose an automated software platform to compute the combination of signal-processing techniques that achieves the highest classification rates for any given smell-space. The proposed system can extract several different types of feature-vectors from a given smell-database and then compute their detection efficiencies over two popular classifiers (see Sections 3.5.1 and 3.5.2): the Nearest Neighbor (NN) and the Nearest Mean (N-MEAN). In this software, the statistical re-sampling techniques (see Section 3.6.1) n-fold cross-validation (N-CV) and leave-one-out (LOO) are used in combination with these two classifiers in order to obtain more realistic estimations of the detection efficiency of each feature-vector type (see Section 3.6).

The automated software platform consists of three independent software modules: the Smell Signal Processing module, the Pattern Analyzer module and the Results Plotter module. The Smell Signal Processing module is used to automatically compute many combinations of signal processing techniques on a given smell-database. The Pattern Analyzer is used to automatically compute the smell detection efficiencies of the different combinations of signal-processing techniques. The Results Plotter module is used to produce bar plots and tables with the detection efficiencies scored by the different combinations.

The design strategy was to produce an expandable software platform with automatic processing capabilities. A simple design solution based on three independent applications is implemented here. These applications are developed over a similar backbone code and communicate between them using the disk file system. The backbone code supports the basic input/output file operations and the user interface operations of the application. The specific functionalities of each application are coded as independent subroutines inserted in the backbone code.

The software implementation is based on list boxes that are used to display the different tasks and configuration choices that the given application can perform. Each item in a list box is linked using a "CASE" instruction to the function subroutine that implements its functionality. The automatic processing capabilities are activated when more than one multiple items are selected in any given list box. The application will then automatically perform all possible combinations of the selected items in all the list boxes. The system functionality can be expanded performing the following two basic steps. First, the programmer must insert the name of the task into the proper list box and into the corresponding CASE instruction. Second, the programmer must insert the programming code that implements the functionality of the new task as a new subroutine into the main program module. All the software modules were implemented using MATLAB visual development environment.

5.3.1 Smell Signal Processing Module

The Smell Signal Processing Module is a software module designed to automatically compute many combinations of signal processing techniques on a given smell-database (see Figure 5-6). The Smell Signal Processing Module was developed with MATLAB visual environment and contains 2880 lines of source code. This software module opens the given smell-database and processes it in order to obtain at least one feature-vector per each smell-example contained in this database. Different types of feature-vectors can be extracted from the same smell-database. Each feature-vector type is extracted by applying a different combination of signal preprocessing techniques. The software generates one data file per each applied combination. This data file is called the Combination-File. The combination-file contains the feature-vectors produced with the given combination. Each combination-file contains as many feature-vectors (of same type) as smell-examples *e* are in the given smell-database. All the combinations of signal processing techniques selected by the researcher can be applied automatically to the given smell-database. Therefore, several combination-files can be automatically generated and saved in the disk for later use.

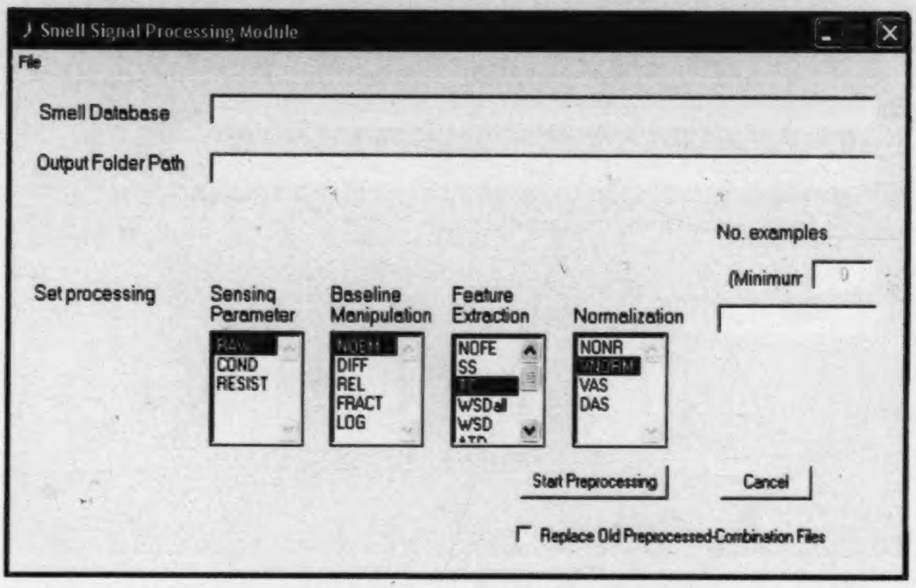
Smell Signal Processing Module
File
Smell Database
Output Folder Path
No. examples
(Minimum
0
Set processing
Sensing Parameter
RAW
COND
RESIST
Baseline Manipulation
DIFF
REL
FRACT
LOG
Feature Extraction
NOFE
SS
WSDall
WSD
Normalization
NONR
VAS
DAS
Start Preprocessing
Cancel
☐ Replace Old Preprocessed-Combination Files

Figure 5-6 The Smell-Signal Processing Module

Figure 5-6 shows the graphic user interface of the Smell Signal Processing module. All the smell-signal processing techniques implemented in the eNose (see Section 5.2) are listed in the three boxes in the center of this interface. The first box in the left is not working in this software version. This selection box is designed for future use with different choices of the sensing parameters (e.g., resistance, conductance and raw voltage). The implemented smell-signal processing techniques are organized in three stages: baseline manipulation, feature-vector extraction and feature-vector normalization. Each selection box corresponds to one of these processing stages. The user must select at least one item from each box depending on the preprocessing technique that will be applied in this stage. The smell-signal is then processed orderly according to these three selected techniques and a feature-vector per each smell-example in the database is computed. The user can also select multiple items in each box. Therefore, programming many different combinations of smell-signal processing techniques. These combinations will be automatically applied (one after the other) to the given smell-database.

5.3.2 Pattern Analyzer Module

The Smell-Pattern Analyzer Module is a software application designed to automatically compute many combinations of smell-pattern analysis techniques on a given combination-file (see Figure 5-7). The Smell-Pattern Analyzer Module was developed with MATLAB visual environment and contains 4700 lines of source code. This software module opens the selected combination-file and uses the smell-patterns to design and test the selected classifier. The smell-patterns are randomly divided into several subsets depending on the selected re-sampling technique. These subsets are alternatively used for designing (training) and testing the classifier. The classification rates obtained are averaged over all the iterations in order to compute the detection efficiency η of the given combination. The software also summarizes all the computed confusion matrices in one. The results are saved in a data file called the Statistics-File and this file is saved in disk for later use. There is one statistics-file per combination-file. The user can select more than one combination-file to be analyzed. The user can also select both classifiers as well as more than one re-sampling technique. Therefore, several statistics-files per combination-file can be automatically generated.

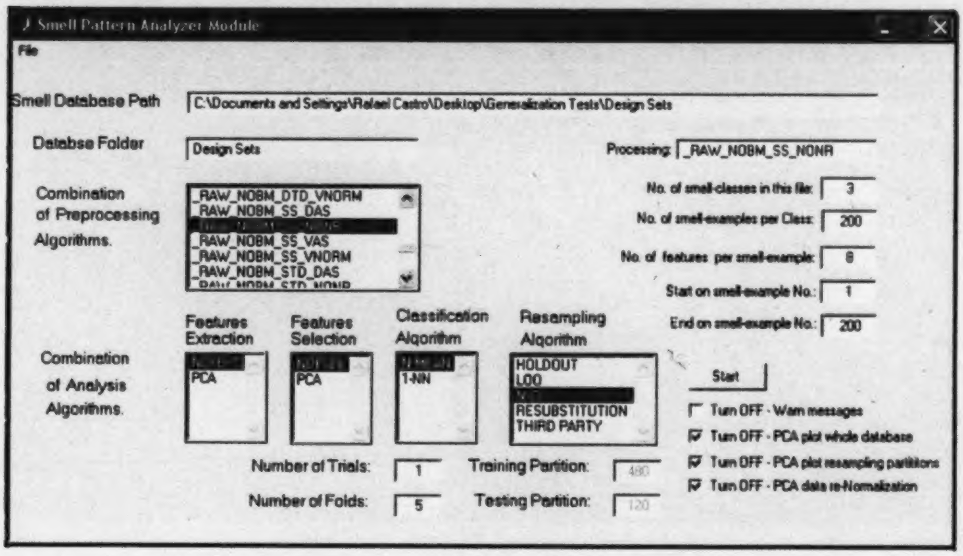
Smell Pattern Analyzer Module
File
Combination of Preprocessing Algorithms.
_RAW_NOBM_DTD_VNORM
_RAW_NOBM_SS_DAS
_RAW_NOBM_SS_VAS
_RAW_NOBM_SS_VNORM
_RAW_NOBM_STD_DAS
Combination of Analysis Algorithms.
Features Extraction
PCA
Features Selection
PCA
Classification Algorithm
1-NN
Resampling Algorithm
HOLDOUT
LOO
RESUBSTITUTION
THIRD PARTY
Start

Smell Database Path: C:\Documents and Settings\Rafael Castro\Desktop\Generalization Tests\Design Sets

Databse Folder: Design Sets

Processing: _RAW_NOBM_SS_NONR

No. of smell-classes in this file: 3

No. of smell-examples per Class: 200

No. of features per smell-example: 8

Start on smell-example No.: 1

End on smell-example No.: 200

Number of Trials: 1

Number of Folds: 5

Training Partition: 480

Testing Partition: 120

☐ Turn OFF - Warn messages

☑ Turn OFF - PCA plot whole database

☑ Turn OFF - PCA plot resampling partitions

☑ Turn OFF - PCA data re-Normalization

Figure 5-7 The Pattern Analyzer Module

Figure 5-7 shows the graphic user interface of the Smell Pattern Analyzer module. In this module we implemented the pattern recognition techniques (see Section 3.5): NN and N-MEAN, the statistical re-sampling techniques (see Section 3.6.1): N-CV and LOO and the dimensionality reduction technique PCA (see Section 3.4.1). These pattern analysis techniques are organized in three stages (boxes): dimensionality reduction (**Features-Extraction** box), pattern recognition (**Classification Algorithm** box) and re-sampling techniques (**Re-sampling Algorithm** box). The user must select at least one item from each box corresponding to the pattern analysis technique that will be applied in this stage. The smell-patterns are then processed orderly according to these three selected techniques and detection efficiency value η is scored per selected combination-file in the database. The user selects the combination-files to be processed from the list box in the center of the panel-window (**Combination of Preprocessing Algorithms**).

5.3.3 Results Plotter

The Results Plotter Module (see Figure 5-8) is a software application designed to organize and produce comparative bar plots and tables with the detection efficiencies scored by the different combinations-files. The Results Plotter Module was developed with MATLAB visual environment and contains 2060 lines of source code. This software module opens the selected statistics-files and organizes them in order to be able to produce bars plots or tables displaying the detections efficiencies η (or the error rates depending on the user selection) scored by each combination-file. The number of rows in this table corresponds to the number of statistics-files selected by the user. The table can be sorted in descending (or ascending order) therefore the first row corresponds to the combination that scored the highest detection efficiency among the selected combination-files (see Table 5-5). The table also displays additional information about the smell-pattern analysis techniques and the combination-files selected for display. The bars plot graph displays various subplots corresponding to the number of feature-vector extraction techniques selected for comparison (see Figure 5-9).

Figure 5-8 shows the graphic user interface of the Results Plotter module. The software of this application can produce comparative plots and tables with the detection efficiencies achieved by different combinations-files extracted from the selected smell-database. The comparison is constrained to only those combination-files that have been analyzed using the same smell-pattern analysis techniques. The user must then first define the constraining combination of smell-pattern analysis techniques. The user selects these techniques on the row of five boxes shown on the upper side of this interface. These five boxes list all the smell-pattern analysis techniques used with the selected smell-database. The statistics-files that comply with this constrain will be then automatically listed in the large box (**Select Combination of Preprocessing Algorithms**). The user selects from this box all the statistics-files that will be compared. The row of three boxes in the center of this interface list all the smell-signal processing techniques tested on the selected smell-database. These boxes define the smell-signal preprocessing techniques that are of interest in this comparison. The user can select one or more items in each of these boxes. This action will automatically adjust the statistics-files listed in the large box.

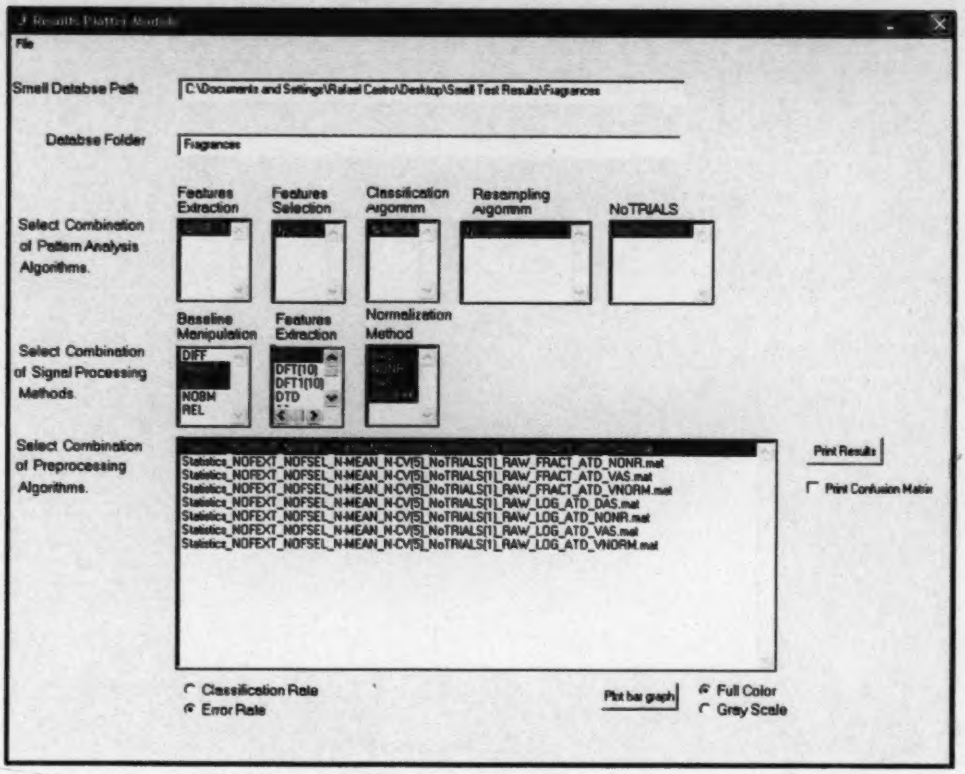

File
Features Extraction
Features Selection
Classification Algorithm
Resampling Algorithm
NoTRIALS
Baseline Manipulation
Features Extraction
Normalization Method
Print Results
☐ Print Confusion Matrix
Plot bar graph

Smell Databse Path: C:\Documents and Settings\Rafael Castro\Desktop\Smell Test Results\Fragances

Databse Folder: Fragances

Select Combination of Pattern Analysis Algorithms.

Select Combination of Signal Processing Methods.

Baseline Manipulation: DIFF, NOBM, REL

Features Extraction: DFT(10), DFT1(10), DTD

Select Combination of Preprocessing Algorithms.

```
Statistics_NOFEXT_NOFSEL_N-MEAN_N-CV[5]_NoTRIALS[1]_RAW_FRACT_ATD_NONR.mat
Statistics_NOFEXT_NOFSEL_N-MEAN_N-CV[5]_NoTRIALS[1]_RAW_FRACT_ATD_VAS.mat
Statistics_NOFEXT_NOFSEL_N-MEAN_N-CV[5]_NoTRIALS[1]_RAW_FRACT_ATD_VNORM.mat
Statistics_NOFEXT_NOFSEL_N-MEAN_N-CV[5]_NoTRIALS[1]_RAW_LOG_ATD_DAS.mat
Statistics_NOFEXT_NOFSEL_N-MEAN_N-CV[5]_NoTRIALS[1]_RAW_LOG_ATD_NONR.mat
Statistics_NOFEXT_NOFSEL_N-MEAN_N-CV[5]_NoTRIALS[1]_RAW_LOG_ATD_VAS.mat
Statistics_NOFEXT_NOFSEL_N-MEAN_N-CV[5]_NoTRIALS[1]_RAW_LOG_ATD_VNORM.mat
```

○ Classification Rate
● Error Rate

● Full Color
○ Gray Scale

Figure 5-8 The Results Plotter Module

Table 5-5 shows an example of a table printout produced by the Results Plotter module. In the first column of the bottom half are listed the names of the combination-files being compared. The name the combination-file corresponds to the techniques used in this combination. For example, the name _RAW_REL_WSD_DAS for the first file means that the smell-patterns in this file were produced with the baseline manipulation technique REL (Relative), the feature-vector extraction technique WSD (Whole Signal Derivative) and the normalization technique DAS (Dimension Auto Scaling). The upper half of this printout shows the smell-pattern analysis techniques used for this comparison.

Table 5-5 Example of a table printout produced by the Results Plotter

```
****************************************************
Smell Database Folder: C:\Smell Test Results\Coffee
Analysis Algorithms Used:      _NOFEXT_NOFSEL_N-MEAN_N-CV(5)_NoTRIALS(1)_
Feature Sel. Algorithm         = NOFSEL
Feature Ext. Algorithm         = NOFEXT
Classifier Algorithm           = N-MEAN
Resampling Algorithm           = N-CV
NoTestExamples                 = 120
NoTrainExamples                = 840

_Signal Processing
                                   ErrorRateAvg   NoFeatures
_RAW_REL_WSD_DAS                    0.05             64
_RAW_FRACT_WSD_DAS                  0.051667         64
_RAW_LOG_WSD_DAS                    0.058333         64
_RAW_DIFF_WSD_DAS                   0.061667         64
_RAW_REL_SS_VNORM                   0.13167          8
_RAW_LOG_SS_VNORM                   0.13667          8
_RAW_FRACT_SS_VNORM                 0.14333          8
_RAW_DIFF_SS_VNORM                  0.14667          8
_RAW_DIFF_SS_VAS                    0.18433          8
_RAW_LOG_SS_DAS                     0.17             8
_RAW_LOG_SS_VAS                     0.175            8
_RAW_LOG_WSD_VNORM                  0.17667          64
_RAW_DIFF_WSD_VAS                   0.18             64
_RAW_REL_WSD_VAS                    0.18167          64
***********************************************
```

Figure 5-9 shows an example of a bars-plot graph produced by the Results Plotter module. The bars-plot graph consists on one or more subplots depending of the number of feature-vector extraction techniques selected for comparison. Each subplot is a two-dimensional bars plot. In each subplot, one or more clusters of bars are drawn over the "x" axis and the error rate (or the detection efficiency as per the user selection) in the "y" axis. Each axis "x" cluster corresponds to one of the baseline manipulation techniques used in the selected combination-files. The bars in the cluster correspond to the feature-vector normalization techniques used in each combination. Each bar has a different color representing a different feature-vector normalization technique.

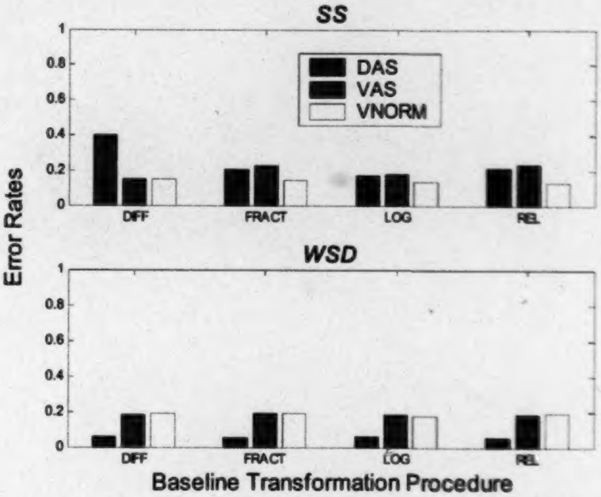

Figure 5-9 Example of a bars-plot graph produced by the Results Plotter

5.3.4 The eNose Data Flow

In this Section we present the data structure and the data exchange between the different components of the eNose software framework. The data processing and smell pattern analysis operations available in the eNose software platform are performed in four independent stages (see Figure 5-10).

In the first stage, the eNose Control Panel is programmed to acquire many sniff samples (in consecutive order) from a given smell source. This is to produce a large number of smell-examples from this smell-source. Each smell-example is saved on the disk in a data file called the smell-file. The smell-files corresponding to the same smell-source are consecutively numbered. The folder containing these smell-files is called the smell-class folder. This first stage must be repeated as many times as smell-classes are defined in the targeted smell-space. For each time this process is repeated a new smell-class folder will be created.

In the second stage, the smell-class folders must be manually assembled into a smell-database. A smell-database consists of one or more smell-class folders. The smell-database is itself a folder at a higher hierarchical level than the smell-class folders. The folders (smell-classes) that constitute a given smell-database are arranged in correspondence to the smell-classes in the targeted smell-space.

In the third stage, the Smell Signal Processing module is programmed to open the assembled smell-database in order to compute the smell-patterns (feature-vectors) corresponding to the smell-examples contained in this database. A data file is generated per each combination of signal preprocessing techniques applied to the smell-database. This data file is called the combination-file and it is automatically saved on the disk for later use. In general, more than one combination-file should be produced in order to compare the detection efficiencies of different combinations of signal processing techniques.

In the fourth stage, the Pattern Analyzer module is programmed to open a selected number of combination-files in order to compute their smell detection efficiencies. A data file with the achieved detection efficiency is generated per each combination-file. This data file also contains additional information such as the number of features in the smell-pattern, the re-sampling technique used, the classifier used and number of iterations performed. This data file is called the Statistics-File and it is automatically saved on the disk for later use.

Finally, the results of the different processing and pattern analysis stages performed over a given smell-database can be retrieved at any time by using the Results Plotter module. This module opens the selected statistics-files and produces bar plots and tables with the detection efficiencies scored by the different combinations of smell-signal processing techniques.

Figure 5-10 shows the schematic of the data structure and the data exchange between the different components of the eNose software framework. The data processing and smell pattern analysis operations available in the eNose software platform are performed in four independent stages: smell data collection, smell database preparation, smell signal processing and smell pattern analysis. Finally, the results with the smell detection efficiencies computed over all the smell-signal processing combinations applied to a given database can be printed or plotted with the Results Plotter module.

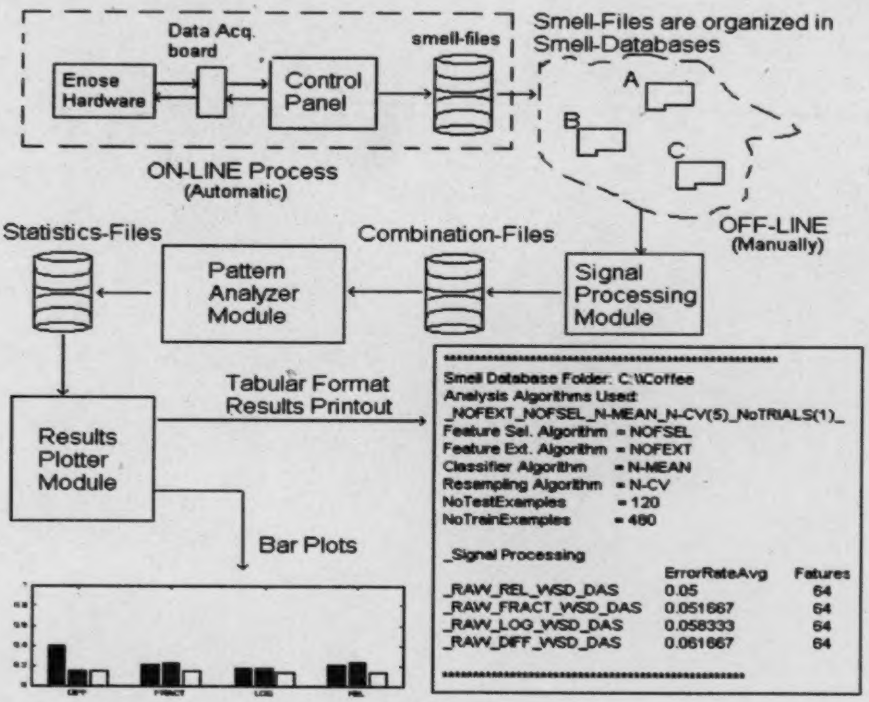
Smell-Files are organized in Smell-Databases
Data Acq. board
smell-files
Enose Hardware
Control Panel
A
B
C
ON-LINE Process
(Automatic)
OFF-LINE
(Manually)
Statistics-Files
Combination-Files
Pattern Analyzer Module
Signal Processing Module
Tabular Format Results Printout
Results Plotter Module
Bar Plots

```
****************************************************
Smell Database Folder: C:\\Coffee
Analysis Algorithms Used:
_NOFEXT_NOFSEL_N-MEAN_N-CV(5)_NoTRIALS(1)_
Feature Sel. Algorithm  = NOFSEL
Feature Ext. Algorithm  = NOFEXT
Classifier Algorithm    = N-MEAN
Resampling Algorithm    = N-CV
NoTestExamples          = 120
NoTrainExamples         = 480

_Signal Processing
                          ErrorRateAvg    Fatures
_RAW_REL_WSD_DAS          0.05              64
_RAW_FRACT_WSD_DAS        0.051667          64
_RAW_LOG_WSD_DAS          0.058333          64
_RAW_DIFF_WSD_DAS         0.061667          64

**********************************************
```

Figure 5-10 The eNose Software System data flow

5.4 Summary

In this chapter, we presented the signal processing techniques and the software system implemented in the eNose. First, the different transient regions of the smell signals produced by the eNose hardware were described. This was followed by a detailed explanation of the signal preprocessing techniques implemented in the eNose software system. Finally, the GUI software system that computes the signal processing and smell-pattern analysis in the eNose was described.

Chapter 6

Performance Evaluation

In chapters 4 and 5, we have presented the proposed electronic nose (eNose) and the software system for smell signal processing and smell pattern analysis. The eNose can collect many examples from a given smell-source, process these examples with up to 140 different combinations of signal processing techniques and estimate the detection efficiency of each combination using the analysis algorithms embedded in the eNose software system.

In this chapter, we evaluate the performance achieved by our eNose in various machine olfaction application areas. The organization of this chapter is as follows. In Section 6.1, we present the proposed smell experiments and the smell databases used in this performance evaluation. The smell database collection methods, the smell sampling methods and the different sniff cycles used are explained in great detail. In Section 6.2, we briefly introduce the evaluation procedures and discuss the results obtained in the proposed smell experiments and examine the influence of different combinations of signal processing techniques in the smell detection efficiency achieved by our eNose.

6.1 Experimental Setup

In this thesis we evaluate the performance achieved by our eNose in common machine olfaction applications such as discrimination of different smells, discrimination of very similar smells and smell discrimination under modulation of the sensors work-temperatures. We also test the feasibility of using eNose to detect smells in the open ambient (i.e., the concentration flask is not used) and the detection efficiency of a novel smell sniff mode proposed in this thesis (see Section 4.6).

In this section, we present the smell experiments, the smell-databases and the smell-sampling methods used to evaluate the performance of the eNose. Each experiment is based in one or more smell-databases specially designed to fulfill the objective of this experiment. The smell-databases are collected using the eNose automatic smell-sampling mode and several smell-sampling techniques are applied.

6.1.1 Proposed Smell Experiments

The proposed smell experiments are performed using a wide gamut of smells that occur in our daily life. The selected smells are commonly occurring smells produced by natural sources such as fresh lemon juice, fresh sliced onions, grounded coffees and grounded pepper. The smells produced by manufactured food products such as Beers, Colas and Cheeses are also used in our experiments.

The objective of the smell-experiments is to evaluate our eNose performance in different application areas. We also evaluate, the performance achieved with the modulation of the sensors work-temperatures and the performance achieved with the novel smart-sniff inhaling cycle. We have designed five sets of experiments to evaluate the performance of the eNose under different circumstances.

The Experiment #1 evaluates the discrimination capabilities of eNose for different smells. Four smell-databases are used in this experiment. These databases contain smells from natural sources such as spices, fruits and livestock manures. It also includes smell sources from manufactured foods such as cheeses. The smells in each database are widely different.

The Experiment #2 evaluates the discrimination capabilities of eNose for very similar smells. Four smell-databases are used in this experiment. These databases contain smells from natural sources that have been processed such as ground coffees, nuts and fruit juices, and smell sources from manufactured beverages such as beers and colas. The smells in each database are very similar.

The Experiment #3 evaluates the use of the eNose as an instrument capable of doing fieldwork and environmental tests. One factor that greatly affects fieldwork measurements with electronic noses is the high degree of variability in the concentration of VOM acquired between consecutive sniffs. Four smell-databases are used in this experiment. The databases were designed using an open ambient smell-sampling method. These databases contain smells from natural sources such as fruits and from manufactured beverages such as beers and colas. The smells in each database are very similar between them. These smells were collected from the atmospheric ambient and no concentration flask was used (see Section 6.1.3).

The Experiment #4 evaluates the novel eNose sniff technique called "smart-sniff" (see Section 4.6). Two smell-databases are used in this experiment. One of the databases contains miscellaneous smells from natural sources such as spices, fruits, flowers, herbs, vegetables, essential oils and fish oils. These smells range from very strong smells (that can poison the sensors) such as black pepper and sweet orange essential oils to very weak smells such as peanut butter. It also contains smells from manufactured beverages such as beers, colas, pops, wine and vinegar. The second database contains very concentrated smells (that can poison the sensors) from processed natural sources such as essential oils from flowers. The smells in each of these databases are in general not similar between them. These smells have been collected using smart-sniff-cycles A and B (see Section 6.1.4).

The Experiment #5 evaluates smell discrimination under modulation of the sensors work-temperatures. One smell-database is used in this experiment. This database contains smells from manufactured beverages such as colas. The smells in this database are very similar between them. These smells have been collected using the TM sniff-cycle (see Section 6.1.4).

Table 6-1 summarizes the five categories of smell experiments.

Table 6-1 Smell Experiments performed for the eNose performance evaluation

EXP. NO.	OBJECTIVES TESTED	SMELL DATABASES
1	Discrimination of widely different smells	Cheese (3 classes) Spice (3 classes) Livestock Manure (3 classes) Fruit Juice (5 classes)
2	Discrimination of similar smells	Coffees (6 classes) Beers (4 classes) Colas (4 classes) Nuts (3 classes)
3	Smell detection in the open ambient	Colas-from-Can (4 classes) Beers-from-Can (2 classes) Colas-no-Headspace (3 classes) Fruits-no-Headspace (3 classes)
4	Smart-sniff smell inhaling mode	Fragrances (3 classes) 25_Smells (25 classes)
5	Temperatures modulation	TM Cola (4 classes)

6.1.2 Smell-Database Collection Method

In this thesis we define a smell-database as a group of smell-examples that have been organized in one or more smell-classes (see Section 5.3.4). A smell-example is defined as the digitized response of the sensors array to a VOM sample from a given smell-source. The smell-class label is defined as the number that identifies each smell-source in a given smell-database.

The smell-source was deposited in the concentration flask and the VOM samples were collected (sniffed) from the headspace created on top of the concentration flask. The vacuum created in the concentration flask by each sniff is filled up with fresh air from the surroundings. This fresh air passed through the smell-source (liquid and grounded) producing a bubbling effect that helped to release more VOM. These VOM accumulated in the top of the flask for the next sniff (see Section 4.3.1).

The smell-examples of a given class are all sniffed from the same smell-source. The smell-source is consecutively sampled (sniffed) until the programmed number of examples has been reached. This operation typically lasted 24 hours in most of the experiments realized.

This collection method has several advantages. First, it is automatic and hence it frees the researcher from constant monitoring of the data collection process. Second, it produces a large smell database necessary to obtain more realistic performance estimates. Third, it reproduces a smell scenario that is closer to real life situations as many natural smell-sources do not smell exactly the same after several hours exposed to ambient but still the human nose is able to recognize them.

6.1.3 Smell Sampling Methods

The smell-source volume typically tested was 160 ml. However in some experiments (smart-sniff) this volume was set to 30 ml, and in the case of essential oils only two drops (on a cotton swab) of the smell-source was used.

The solid smell-sources such as cheese, fresh lemon and fresh onion are cut into two or three pieces of approximately 1cm^3 and then deposited in the concentration flask. The fresh air inlet tube was placed very close to the bottom and between the smell-source pieces.

The grounded smell-sources such as coffees, pepper, herbs and small beans were deposited into the concentration flask. The concentration flask was filled with the substance up to one third of its volume (i.e., a volume of approximately 160 ml). The fresh air inlet tube was buried into the substance.

The liquid smell-sources such as colas, beers, fruit juices and vinegar were deposited into the concentration flask. The concentration flask was filled with the liquid up to one third of its volume. The fresh air inlet tube was immerged into the liquid very close to the bottom.

The sampling bag method was used in the collection of the livestock manure smells. In this case, the eNose sampled the smells directly from Tedlar bags. The bags were filled in the field with the air coming out the exhaust vents in the barns. Each bag has a volume of approximately 20 liters, which allows for about 50 sniffs (10 seconds of inhaling draws approximately 333 ml of gas).

The open ambient method is used in the fieldwork feasibility (discrimination of smells in open ambient) experiments. The concentration flask was used but it was let open. The eNose sniffed over the smell source in the open. The eNose smell inlet was placed at approximately 10 centimeters above the smell-source. This method was applied to the "Fruits-no-Headspace" and the "Colas-no-Headspace". A slight modification of the open ambient method was also used. In this variant, the eNose sniffs above the smell-source original container. The eNose smell inlet was placed at approximately 2 centimeters above the can opening. This method was applied to the "Beers-from-Can" and the "Colas-from-Can".

6.1.4 The Smell Sniff Cycle Settings used

In preliminary smell experiments realized with the eNose we observed that the metal-oxide sensors responded smoothly and slowly to most sources of VOM. These sensors needed, in general, more than 60 seconds to reach 70% of their steady state response values. Therefore, a sampling rate of 1 Hz (i.e., one sample per second) was chosen for the remaining smell experiments because at this sampling rate the smell-signal is acquired without loosing any important information.

The eNose sniff-cycle is fully programmable (see Section 4.5). This characteristic allows defining many different configurations for sniffing the VOM from different smell sources. In this thesis we use four types of sniff-cycles namely: standard sniff-cycle, smart-sniff-cycle A, smart-sniff-cycle B and the TM-sniff-cycle. The Steady state of all the proposed sniff-cycles was set to 300 seconds. This duration time is chosen in order to guarantee that all the sensors will reach their steady states in all the smell experiments.

Table 6-2 shows in detail the settings for each of the sniff-cycle types used for collecting the smell databases used in the experiments. Each column represents a sniff-cycle type. The first seven rows represent the seven states that constitute any given sniff-cycle. The last row shows the portion of the sensors response signals that is recorded in the given sniff-cycle type whereas the row before shows the total length (i.e., including the recovery time) of the given sniff-cycle type. The Inhale duration time showed for the smart-sniff cycles A and B represents the dynamic range achieved by the different smells tested in the Experiment #4 (see Section 6.1.1). The Inhale duration time set for the smart-sniff cycle types A and B is 20 seconds. This setting is the maximum duration time that the Inhale state will last in case that none of the sensors reaches the threshold (see Section 4.6). In these cases the duration of the Inhaling state is variable and dependent of: the sensitivity of the sensors, the threshold specified, the concentration of the smell-source and the type of smell-source. A threshold of 0.1 volt was specified for all the smart-sniff experiments realized. The eNose did not reach the maximum duration time specified for the Inhaling state in any of the experiments performed to test the smart-sniff mode. However, note that, a smaller Inhaling duration time was generally needed for testing the first sample of a given smell-source than the last sample of the same source. For example, the first sample of VOM taken from English Rose fragrance oil was being inhaled for only 2.03 seconds while the last sample (example number 52) taken from the same smell-source scored 6.06 seconds.

The standard sniff-cycle settings (see second column of Table 6-2) were chosen after several preliminary tests with all smells selected for the eNose performance evaluation. The Duration times of Exhale and Recovery states are chosen to be 300 seconds each because these settings allow the fastest recovery of the eNose sensors when testing the selected smells. In general, the lowest baseline values can only be reached after having the sensors inactive for very long periods of time such as a 72 hours recovery time. However, it was observed that 300 seconds was in general enough time for the sensors to reach working baseline values. These working baselines are marginally higher than the bottom baselines but the sensors consistently reach them in each experiment.

Table 6-2 Sniff Cycle Settings for the eNose experiments (times are expressed in seconds)

SNIFF CYCLE TYPES / SNIFF CYCLE STATES	STANDARD SNIFF CYCLE	SMART SNIFF CYCLE A	SMART SNIFF CYCLE B	TM SNIFF CYCLE
Baseline	10	10	10	10
Inhale	10	0 – 10*	0 – 10*	10
Post-inhale	5	5	5	150
Steady	300	300	300	20
Pre-exhale	5	5	5	100
Exhale	300	700	300	300
Recovery	300	1000	900	300
Cycle length	930	2040	1540	890
Response recorded length	630	1040	640	590

* Depending on how fast the sensors respond

The smart-sniff-cycle-A is a generic type of sniffing cycle. These settings (see third column of Table 6-2) were chosen to fit a wide gamut of smell-source types. The smell-sources targeted with the "smart-sniff-cycle-A" range from smells that are easily flushed from the sensing chamber to smells characterized by their persistence (or stickiness), which make them very difficult to flush out of the sensing chamber. In a preliminary test realized with these "sticky" smells, the eNose delivery system got poisoned and it was very hard to clean it out. In these experiments VOM samples of grounded pepper and essential oil of sweet orange were inhaled for only 10 seconds but the sensors were not able to recover their baselines before approximately 10 hours of alternative cycles of flushing and recovery that were set at various different duration times. We also noticed that recovery times are in general dependent of the duration of the Exhaling state. In general, long recovery times are needed after long exhaling times. One of the causes of this dependency is the temperature of the sensors, which drops abruptly during long flushing times. Other causes can be found in the characteristics of the smell-source VOM. In general, the oily smell-sources release VOM that adhere strongly on the walls of the system and the sensing surfaces of the sensors. These VOM are hard to flush. However, setting long recovery time helps the sensors to burn completely these VOM.

The smart-sniff-cycle-B settings (see fourth column of Table 6-2) were chosen to fit the smells produced by fragrance oils. Fragrance oils are essential oils that have been diluted in non-odorous oils such as grape seed oil. Therefore, these smell-sources are less concentrated than pure essential oils and the risk of poisoning the eNose is smaller. However, fragrance oils still need a longer recovery time than the lighter smells that were collected using the standard sniff-cycle.

We observed that those smell sources that could poison the sensors such as ground pepper and sweet orange essential oils typically produce the strongest and fastest responses of the smell sensors and in general these substances are hard to flush out of the chamber. However, not all substances that produce strong and fast responses can be classified as sticky or hard to flush out substances for example alcohol and coffee produce very strong responses but the sensors are able to recover their baselines in a reasonable time.

The TM sniff-cycle (Temperature Modulation sniff-cycle) settings (see fifth column of Table 6-2) are tailored to fit the requirements of a zero-voltage pulse temperature modulation function (see Section 5.2.2.5). The settings for this sniff-cycle are selected in order to emulate as much as possible a standard sniff-cycle with an embedded zero-voltage pulse in the middle of the steady state. The objective is to visually compare the smell-signal produced from the same smell-source by a standard sniff-cycle and a TM sniff-cycle (see Figure 6-1).

Figure 6-1 shows the smell sensors responses to same smell-source (Coca Cola) produced by a standard sniff-cycle (a) and a TM sniff-cycle (b). Note that both response signals look very similar except for the smell-signal transitions induced by the zero-voltage pulse in the middle of the steady states reached by the sensors in (a).

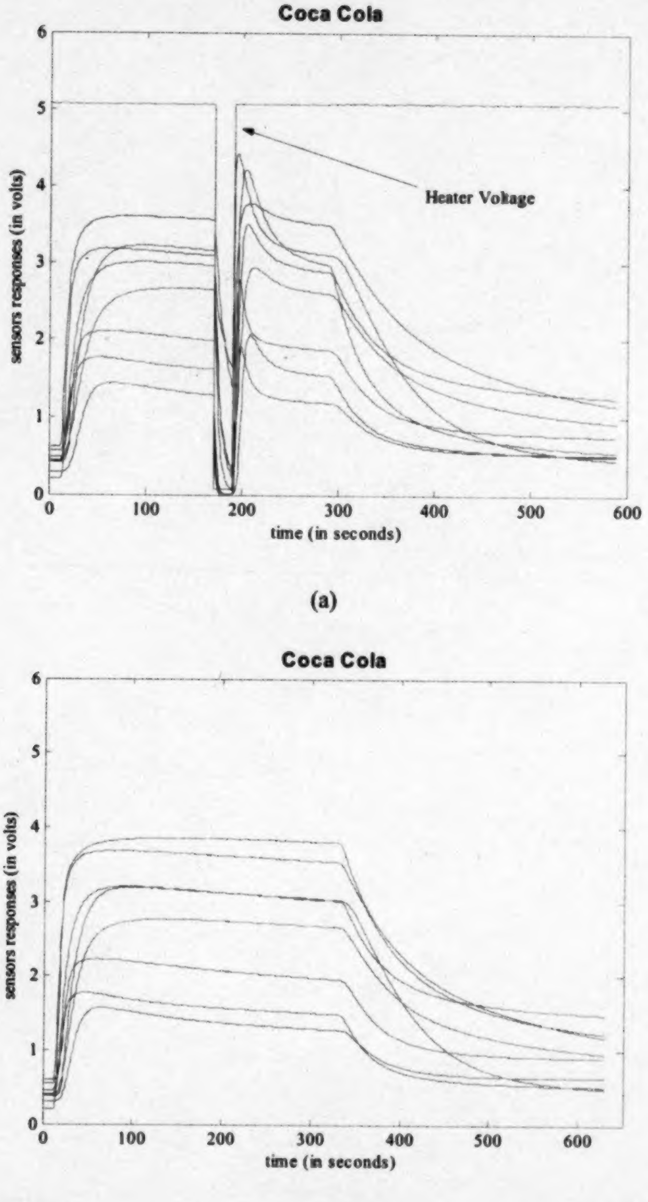

(a)

(b)

Figure 6-1 TM sniff-cycle (a) and standard sniff-cycle (b) responses to Coke VOM

6.1.5 The Collected Smell-Databases

The smell environments for the eNose experiments are simulated in fifteen different smell-databases collected in this thesis (see Table 6-3). Some of these databases represent characteristic smell types such as Coffee, Beer, Cola and Nut smell. In other cases the databases were assembled according to a specific sniff-cycle such as TM-sniff-cycle and smart-sniff-cycles. Some databases were also assembled according to a known property that the smells in the group share such as spicy smells, foul smells and hircine smells. In general, these smells do not smell similar. For example, clove and cumin belong to the spice category but they have very distinct smells. Finally, the smell-sampling method was the criteria used to assemble databases such as Colas-from-Can and Colas-no-Headspace in order to test the fieldwork feasibility of the eNose. A detailed explanation of each of the collected smell-databases follows.

Table 6-3 describes the fifteen smell-databases collected in this thesis. Entries in column 2 and 3 show the sniff- cycle type and the smell sampling method used to collect each of the described databases. The column 4 shows the number of smell-classes in the database and the column 6 shows the total number of smell-examples collected in each database.

Table 6-4, Table 6-5 and Table 6-6 describe the smell-classes contained in each of the collected databases. Table 6-4 contains the descriptions of the databases used in Experiment #1 and Experiment #2. Table 6-5 contains the descriptions of the databases used in Experiment #3. Table 6-6 contains the descriptions of the databases used in Experiment #5 and Experiment #4. In these tables, each column represents a smell-database and the rows correspond to the smell-classes contained in this database. The last column of Table 6-6 corresponds to the "25_Smells" database. This database contains 25 smell-classes and they are described together in only one row in order to save table space.

Table 6-3 Smell Databases

DATABASE	SNIFF CYCLE	SMELL SAMPLING METHOD	NO. OF CLASSES	NO. OF SAMPLES
Cheese	Standard	Headspace	3	300
Spice	Standard	Headspace	3	300
Manure	Standard	Tedlar Bag	3	150
Fruit Juice	Standard	Headspace	5	500
Coffee	Standard	Headspace	6	600
Beer	Standard	Headspace	4	400
Cola	Standard	Headspace	4	400
Nut	Standard	Headspace	3	300
Colas-from-Can	Standard	Open Ambient	4	32
Beers-from-Can	Standard	Open Ambient	2	16
Colas-no-Headspace	Standard	Open Ambient	3	48
Fruits-no-Headspace	Standard	Open Ambient	3	48
Fragrances	Smart-Sniff B	Headspace	3	156
25_Smells	Smart-Sniff A	Headspace	25	225
TM Cola	TM sniff-cycle	Headspace	4	400

The Cheese and Spice smell databases contain 300 smell-examples each. Each database consists of three different smell-classes (see Table 6-4). There are 100 smell-examples collected per smell-class. The cheese smell-source was sampled using the solid smell-source sampling method (see Section 6.1.3). Two pieces of approximately 1cm^3 each were deposited in the concentration flask. The spice smell-source was sampled as follows. The concentration flask was filled up to one third of its volume. The standard sniff-cycle settings were used in the collection of these databases.

Table 6-4 Database classes for Experiments #1 and #2

CHEESE	SPICE	MANURE	FRUIT JUICE	COFFEE	BEER	COLA	NUT
Blue	Clove	Dairy	Apple	Arabica	Becks	Coke	Almond
Italian	Oregano	Poultry	Grape	Brazil	Holsten	IGA	Hazelnut
Oka	Tabasco	Swine	Grapefruit	Colombia	Labatt	Pepsi	Peanut
			Orange	Sumatra	Molson	Safeway	
			Tomato	Cubita			
				Indiana			

Table 6-5 Database classes for Experiment #3

COLAS (FROM CAN)	BEER (FROM CAN)	COLAS (NO HEADSPACE)	FRUIT (NO HEADSPACE)
Coke	Labatt	Coke	Fresh Lemon
IGA	Molson	Pepsi	Apple Juice
Pepsi		Safeway	Orange Juice
Safeway			

The Livestock Manure database contains 150 smell-examples from three smell-classes: Swine manure, Poultry manure and Cattle manure. Fifty smell-examples per smell-class are collected. The eNose sampled the manure smells directly from Tedlar bags (see Section 6.1.3). The sampling of manure smells was possible thanks to the collaboration of Dr. John Feddes professor in the Department of Agriculture, Food & Nutritional Science of the University of Alberta.

Table 6-6 Database classes for Experiments #5 and #6

TM COLAS	FRAGRANCES	25_SMELL
Coke	English Rose	Alcohol, Fresh Onion, Corona Beer, Fresh Lemon, Lemon essential oil, Orange Juice, Cubita Coffee, Fish Oil, Sardines in water, Jasmine essential oil, Lavender essential oil, Mountain Ashes flower, Rosemary herb, Peanut butter, Coke, Pepsi, Sprite, Grounded Black Pepper, Cinnamon, Cocoa, Honey, Balsamic Vinegar and Red Wine
IGA	Lily of the Valley	
Pepsi	Violet	
Safeway		

The Fruit Juices smell database contain 500 smell-examples. This database consists of five different smell-classes (see Table 6-4). There are 100 smell-examples collected per smell-class. The juices were selected from brand name manufacturer Sun-Rype Products Ltd. with the exception of the tomato juice that was selected from Heinz Company. The fruit juices were sampled using the liquid smell-source sampling method (see Section 6.1.3). The standard sniff-cycle settings were used in the collection of this database.

The Coffee, Beer, Cola and Nut smell databases contain respectively 600, 400, 400 and 300 smell-examples from six, four, four and three different smell-classes each. Each database represents a different type of smell but its constituent classes smell very similar between them (see Table 6-4). There are 100 smell-examples collected per smell-class. The standard sniff-cycle settings were used in the collection of these databases.

The Coffees smells are selected from four blends of Nabob Coffee Co. and two Cuban coffee brand names: Cubita and Indiana. The Cola smell-classes are selected from three brand names colas: Coca Cola, Pepsi Cola and IGA cola. The three nut smell-sources selected are: Almond butter, Hazelnut butter and Peanut butter.

The Beer smells selected are from four brand name beers: Becks, Holsten, Labatt and Molson. Low alcohol content beers were selected in order to diminish the interference that alcohol produces in the response of the sensors.

The Colas-from-Can and Beers-from-Can databases contain only eight smell-examples per smell-class. The reason of such small amount of examples is due to the low volume of VOM released by the colas after being more than 2 hours in the open ambient. The Colas-from-Can database contains four smell-classes whereas Beers-from-Can contains two smell-classes (see Table 6-5). The smell-examples were sampled directly from the can and no concentration flask was used. The smell inlet tube was held near the opening of the can (see the open ambient sampling method in Section 6.1.3). The objective of these databases is to help evaluate the fieldwork feasibility of the eNose.

The Colas-no-Headspace and Fruits-no-Headspace databases contain only eight smell-examples per smell-class (see Table 6-5). The smell-examples were sampled in the open ambient (see Section 6.1.3). The concentration flask was used but it was let open. The eNose sniffed the VOM at 10 centimeters above the smell-source. The objective of these databases is to help evaluate the fieldwork feasibility of the eNose.

The Temperature Modulated Colas (TM Colas) database contains the same smell-classes than the Colas database (see Table 6-6). The objective of this database is to evaluate the performance of smell-patterns extracted with the modulation of the sensors work-temperature.

6.2 Results and Discussion

The previous sections of this chapter provided details of the experimental setup used to evaluate the performance of the eNose in several application areas. In these sections, we explained in great detail the characteristics of each smell database, the smell sampling and collection methods used and the proposed smell experiments. This section begins with an explanation of the general evaluation procedure used in this thesis and then we start discussing the results obtained in the smell-experiments. First, we discuss the results achieved by the eNose using the standard signal processing combination DIFF_SS_VNORM. Secondly, we examine the results achieved by all possible combinations of the signal processing techniques implemented in the eNose software system. For each database, the best and worst performing combination are selected and their performances compared to the performance achieved by the standard combination. Finally, the results of each combination are graphically analyzed trying to find trends that could be important for the smell discrimination.

6.2.1 Evaluation Procedure

In this thesis, we use the smell detection efficiency η defined in Section 3.6 to evaluate the eNose performance. The smell detection efficiency η is computed in each of the collected smell-databases and averaged over the databases that belong to each particular experiment. These averages are then used to rank the performance of the eNose in each of the proposed tests.

The detection efficiency η is calculated based in the classification rates obtained with the Nearest Neighbor (NN) and the Nearest-Mean (N-MEAN) classifiers. These classifiers are designed and tested using five-fold cross-validation (5-CV) or leave-one-out (LOO) statistical re-sampling methods. The 5-CV re-sampling method is applied to the smell-databases with more than 50 examples per smell-class otherwise the LOO method is used.

The smell-signal processing combination DIFF_SS_VNORM (see Section 5.2) was selected in order to comparatively evaluate the performance achieved by the eNose in each experiment. This combination is chosen because it is the most commonly used combination of signal processing techniques in machine olfaction. This combination was used to evaluate eNose in all except two of the proposed smell-experiments. The smell discrimination under modulation of the sensors work-temperatures uses the DIFF_TMWSD_VNORM and DIFF_TMDFT_VNORM combinations.

6.2.2 Performance of DIFF_SS_VNORM combination

The results of the eNose performance evaluation using the standard combination DIFF_SS_VNORM are summarized in Table 6-7. In this table, we present a comparative list of the detection efficiencies computed using the N-MEAN and the NN classifiers. The detection efficiency values shown here are the averages of the detection efficiencies computed over all the databases selected in each smell experiment. As expected the NN classifier shows better performance than N-MEAN classifier. The NN classifier can generate highly nonlinear classification boundaries in contrast to the N-MEAN classifier that can only be used successfully when the smell-patterns are very well separated (see Section 3.5.1 and Section 3.5.2). In order to better assess the eNose performance we chose to do the evaluations based in the results produced by the N-MEAN classifier.

Table 6-7 Experiment Results

EXP. #	OBJECTIVE TESTED	AVERAGED DETECTION EFFICIENCY (DIFF_SS_VNORM)	
		N-MEAN	NN
1	Discrimination of different smells	95.4 %	99.9 %
2	Discrimination of similar smells	91.1 %	99.2 %
3	Smell detection in the open ambient	76.6 %	88.3 %
4	Smart-sniff smell inhaling mode	87.0 %	97.5 %
5	Temperatures modulation	84.0 %	99.7 %

Table 6-7 shows the general detection efficiencies achieved by the eNose in each of the five smell experiments. These values are obtained after averaging the detection efficiencies scored over all the databases used in each smell experiment.

The general detection efficiency achieved by the eNose in all the experiments is between 76 – 95 % (see Table 6-7). This performance can be considered superior even in comparison to expensive commercial electronic noses. The best results were obtained in the Experiment #1. In this experiment we used odor-sources that smelled very different and they were easily discriminated by our eNose. The results obtained in the Experiment #2 are second in the ranking but still are very good. The smells used in this case were very similar and it was very difficult to discriminate even by a human subject. However, our eNose discriminated theses similar smells very well achieving more than 90% of smell detection efficiency. The result obtained in the Experiment #3 was the lowest detection efficiency (76%). However, due to the variability in the concentration of the VOM samples sniffed by eNose in this experiment, the achieved efficiency is very good. In the Experiment #4, we evaluated the smart-sniff inhaling technique proposed in Section 4.6. A detection efficiency of an 87% was obtained in this experiment. This is a very good result considering the large number and diverse types of smell-sources tested. These sources ranged from very weak and almost imperceptible smells such as an open can of coke to very strong ones such as lemon and sweet orange essential oils. Finally, the results obtained with the temperature modulation techniques in the Experiment #5 were lower than expected. A better result was expected because in almost all the reviewed literature this kind of techniques has been used with very good results. We believe that this result can be improved further. However, more detailed study regarding modulation functions, the features to characterize the smell and the smells tested is necessary to achieve a better performance.

Table 6-8 shows the details of the detection efficiencies obtained for each database in the smell experiments. The standard combination DIFF_SS_VNORM is used for the computations of the detection efficiencies in these databases. The N-MEAN and the NN classifiers are used to compute two different values of the detection efficiency per database. In this evaluation, we used only the values computed by the N-MEAN classifier to evaluate the eNose performances (see Section 6.2.2). The Spice, the Cheese and the Fruit Juice databases score the highest detection efficiencies. These three databases contain different smells. The Colas-from-Can database scored the lowest detection efficiency with a 53.1 %. The Colas-no-Headspace scored much better with an 80%. However, in the case of the Colas-no-Headspace the smell-source has a larger surface area in contact with the ambient than the case of Colas-from-Can which surface area is limited to the small opening in the can (see section 6.1.3).

Table 6-8 Detailed Results of the eNose Performance Evaluation Experiments

EXP. #	OBJECTIVES TESTED	DATABASES	DETECTION EFFICIENCY (DIFF_SS_VNORM)	
			N-MEAN	NN
1	Discrimination of different smells	Cheese (3 smells)	100 %	100 %
		Spice (3 smells)	100 %	100 %
		Manure (3)	85.3 %	100 %
		Fruit Juice	96.6 %	99.6 %
2	Discrimination of similar smells	Coffees (6 classes)	85.3 %	98.8 %
		Colas (4 classes)	87.7 %	99.0 %
		Beers (4 classes)	99.5 %	100 %
		Nuts (3 smells)	92.3 %	99.3 %
3	Smell detection in the open ambient	Colas-from-Can	53.1 %	75.0 %
		Beers-from-Can	90.0 %	95.0 %
		Colas-no-Headspace	80.0 %	93.3 %
		Fruits-no-Headspace	83.3 %	90.0 %
4	Smart-sniff smell inhaling mode	Fragrances	79.3 %	100 %
		25_Smells	92.8 %	95.1 %
5	Temperatures modulation	TM Colas:		
		DIFF_TMDFT_VNORM	84.5 %	99.7 %
		DIFF_TMWSD_VNORM	84.0 %	99.7 %

6.2.3 Performance of other combinations

In this section, we evaluate 140 different combinations of signal processing techniques over each of the collected smell-databases. The best and worse performing combinations in each smell-database are selected and their performances compared to those achieved by the standard combination presented in the previous section. We also apply the well-known feature extraction method PCA (see Section 3.4.1) to each of the best performing combinations aiming to reduce the dimensionality of the features-vectors produced by these combinations. Reducing the dimensionality of the extracted smell-patterns is very important in order to avoid over-fitting the classifier on the training patterns (see Section 3.4).

These 140 combinations are the maximum number of possible combinations that can be made using the entire set of signal processing techniques implemented in the eNose software system. The smell-examples are processed in three preprocessing stages: a) baseline manipulation, b) feature-vector extraction and c) feature-vector normalization. In this software system, we implemented four baseline manipulations techniques, seven feature-vector extraction techniques and three feature-vector normalization techniques (see Section 5.2). Hence, the number of total combinations can be calculated as $(4 \times 7 \times 3) = 84$. However, we also take into account the cases when no technique is applied in the two preprocessing stages: baseline manipulation and feature-vector normalization. Therefore, the total number of combinations is $((4+1) \times (7) \times (3+1)) = 140$.

The name of each combination of signal processing techniques is composed by three acronyms separated by underscores. Each acronym position in this name corresponds to one of the three preprocessing stages (see Table 5-2 in Section 5.2) applied to the smell-examples. Therefore, a combination name represents: a) the baseline manipulation technique, b) the feature-vector extraction technique and c) the feature-vector normalization technique applied to produce the smell-patterns used in each of the given tests. In the cases where "no technique is applied" the acronyms used are: NOBM (for no baseline manipulation) and NONR (for no feature-vector normalization). For example: the combination name DIFF_STD_VNORM represents the patterns extracted using a) the difference (DIFF) baseline manipulation technique, b) the steady transient derivatives (STD) feature-vector extraction technique and c) the vector array normalization (VNORM) feature-vector normalization technique.

The features extracted with the PCA method are used to assemble a new feature-vector to represent the smells under test. These new smell-patterns are then re-sampled and the smell detection efficiency η is calculated again using the N-MEAN classifier. The final number of features extracted with each PCA analysis is defined by the number of principal components that accounted for at least 98% of the total variance of the patterns from the database under analysis. For example (see Table 6-9), the feature-vectors extracted with the combination

DIFF_STD_VNORM from the **Cheese** database were reduced from a dimension of 16 coordinates (features) to only 6 new coordinates (new features or scores obtained with the PCA analysis). This means that these 6 new features account for at least the 98 % of the total variance of the new features-vectors. On the other hand, the feature-vectors extracted with the combination DIFF_STD_VNORM from the **Manure** database were reduced to an even smaller dimension of only 4 coordinates because these four principal components account for at least 98% of the total variance.

Table 6-9 and Table 6-10 show the best and worst performing combinations in each database. They were selected from 140 different combinations of signal processing techniques that were applied to each smell database. The combination displayed in the first column is the combination that scored higher in the given database. In case of more than one combination with same higher score, we chose the combination which feature-vector extraction technique appears with more frequency. The column "ALL FEATURES" displays the number of features extracted and the detection efficiencies scored on the N-MEAN classifier by the selected combinations displayed in the second column. The column "PCA" displays the number of features extracted after applying Principal Component Analysis (PCA) to the selected combinations and the detection efficiencies scored by these features (the extracted features in the new coordinated system) evaluated on the same classifier. Finally, the seventh column shows the smell-databases that correspond to the best and worse combinations from the same row.

Table 6-9 The best and worst performing combination for Experiments #1 and #2

EXP. #	COMBINATION NAME (SECTION 6.2.3)	ALL FEATURES		PCA		DATABASE
	(+) BEST (-) WORSE	NO. FEAT.	DETECTION EFFICIENCY	NO. FEAT.	DETECTION EFFICIENCY	
1	(+) DIFF_STD_VNORM	16	100 %	6	99.6 %	Cheese
	(-) DIFF_DFT_VAS	80	88.6 %			
	(+) DIFF_STD_VNORM	16	100 %	5	99.6 %	Spice
	(-) FRACT_DFT_NONR	80	59.3 %			
	(+) DIFF_STD_VNORM	16	100 %	4	100 %	Manure
	(-) DIFF_SS_VNORM	8	84.6 %			
	(+) NOBM_SS_VAS	8	100 %	3	100 %	Fruit Juice
	(-) FRACT_DFT_NONR	80	52.2 %			
2	(+) DIFF_STD_DAS	16	98.1 %	6	97.6 %	Coffees
	(-) DIFF_DFT_NONR	80	48.8 %			
	(+) LOG_STD_VNORM	16	100 %	5	99.7 %	Beers
	(-) REL_DFT_NONR	80	75.2 %			
	(+) LOG_WSD_VAS	56	92.2 %	7	83.5 %	Colas
	(-) REL_DFT_NONR	80	38 %			
	(+) DIFF_ATD_VAS	24	96.3 %	6	98 %	Nuts
	(-) FRACT_DFT_NONR	80	68.3 %			

Table 6-9 and Table 6-10 corroborate the performance evaluation results obtained with the standard combination (see Table 6-7). Table 6-9 and Table 6-10 also show that the general detection efficiency of the eNose can always be improved by selecting the appropriate combination of signal processing techniques. Note that for each one of the 15 smell-databases analyzed with the standard combination (see Table 6-8) there exists a combination (in Table 6-9 and Table 6-10) that produces a higher detection efficiency score.

Table 6-10 The best and worst performing combination for Exp. #3, #4 and #5

EXP. #	COMBINATION NAME (SECTION 6.2.3)	ALL FEATURES		PCA		DATABASE
	(+) BEST (-) WORSE	NO. FEAT.	DETECTION EFFICIENCY	NO. FEAT.	DETECTION EFFICIENCY	
3	(+) NOBM_SS_VNORM	8	71.8 %	5	71.8 %	Colas-from-Can
	(-) REL_DFT_DAS	80	21.8 %			
	(+) DIFF_TC_NONR	32	100 %			Beers-from-Can
	(-) REL_STD_NONR	16	45 %			
	(+) NOBM_SS_VAS	8	100 %	5	96.6 %	Colas-no-Headspace
	(-) REL_DFT_DAS	80	30 %			
	(+) LOG_ATD_VAS	24	100 %	7	96.6 %	Fruits-no-Headspace
	(-) NOBM_DFT_NONR	80	46.6 %			
4	(+) DIFF_STD_VNORM	16	100 %	5	96.7 %	Fragrances
	(-) FRACT_ATD_NONR	24	56.1 %			
	(+) DIFF_WSD_VAS	56	97.7 %			25_Smells
	(-) REL_DFT_NONR	80	44.4 %			
5	(+) NOBM_TMDFT_VNORM	80	85 %	5	66.2 %	TM Colas
	(-) LOG_TMWSD_VAS	56	41 %			

6.2.4 Graphical Analysis of different combinations

In this section we analyze graphically the results of each combination in order to find which characteristics dominate the relations between a smell-database and the signal processing techniques used to extract the smell-patterns.

We use a row of small bars plot graphics to represent the smell detection efficiency achieved by the different combinations of signal processing techniques applied to a given smell-database. There are one or more subplots aligned along the same row. The number of sub-plots corresponds to the number of feature-vector extraction techniques displayed. Each subplot is itself a two-dimensional bars plot. In this subplot, one or more clusters of bars are drawn along the "x" axis. Each cluster corresponds to a different baseline manipulation technique and each bar in the cluster corresponds to a different feature-vector normalization technique. The height of each bar represents the detection efficiency achieved by a particular combination of signal processing techniques. The bars are drawn between 0 and 1 corresponding to 0% and 100% smell detection efficiency respectively.

In order to produce a better visual comparison, we put together in the same Figure all the bars plots corresponding to a particular experiment. Therefore, each row in this figure represents all the combinations applied to one of the smell-databases selected for this particular experiment. Each column of bars plots in the figure represents one of the feature-vector extraction techniques applied in this experiment. In order to compact these graphics, we do not show those combinations involving any dummy application of processing techniques. For example, the combination DIFF_SS_NONR is not showed because NONR means "no normalization" was applied, even though the feature-vector extraction technique SS and the baseline manipulation technique DIFF were applied. This constrain reduces the number of combinations showed from 140 to only 84 (see Section 6.2.3). However, in our experiments we tested all the possible combinations including the dummy ones and in some cases the absence of any processing technique leads to better results (see fourth row "NOBM_SS_VAS" in Table 6-9).

Figure 6-2 shows graphically the performance achieved by the 24 out of the 40 different combinations of signal processing techniques tested in Experiment #5. In this experiments we tested smell-sources that are sampled using the temperature modulation (TM) feature-vector extraction techniques proposed in this thesis. A quick glance to this figure reveals a general good performance achieving in general more than 80% detection efficiency. The TMDFT feature-vector extraction techniques produced the one greatest detection efficiency value (see Table 6-9) but the TMWSD technique scored in general better. To arrive to this conclusion could have taken more time if we have not used this graphical evaluation method. The normalization techniques: VNORM and VAS together and the baseline manipulation techniques: DIFF, FRACT and REL are used in almost all the combinations that produced the best smell detection efficiencies for these two feature-vector extraction techniques (TMDFT and TMWSD).

Figure 6-3 shows graphically the performance achieved by 84 out of the 140 different combinations of signal processing techniques tested in Experiment #1. A quick glance to this figure reveals that in general a good performance could have been achieved using any of the 140 combinations. This result was expected considering the fact that all the smells tested in this experiment are very different between each other. The worse performances were achieved with the Fruit Juice database. The WSD, STD and ATD (in this order) feature-vector extraction techniques produced the best results while the DFT, DTD, SS and TC techniques produced in general the worse results. The baseline manipulation techniques performed evenly in almost all combinations.

Figure 6-4 shows graphically the performance achieved by 84 out of the 140 different combinations of signal processing techniques tested in Experiment #2. In this experiments we tested different smell-sources that produce very similar smells that are very difficult to discriminate by a human nose. A quick glance to this figure reveals that in general the performance was not as good as the performance achieved in the Experiment #1. The Colas database as expected presented the most difficult smell discrimination followed by the Coffees database. The WSD, SS and STD (in this order) feature-vector extraction techniques produced the best results. The normalization techniques VNORM and VAS were almost always present in the combinations that produced the best smell detection efficiencies. The baseline manipulation techniques performed evenly in almost all combinations.

Figure 6-5 shows graphically the performance achieved by 84 out of the 140 different combinations of signal processing techniques tested in Experiment #3. In this experiments we tested smell –sources that are sampled in open ambient conditions. The performance achieved is worse than in the two previous experiments. This is an expected result due to the fact that the concentration of the VOM inhaled, even from the same smell-source, varies greatly from one sniff to the next. It is well known that the sensors response is dependent of the concentration of VOM inhaled (see Equation 4-1). The WSD, STD and SS (in this order) feature-vector extraction techniques produced the best results. The normalization techniques:

VNORM and VAS were almost always present in the combinations that produced the best smell detection efficiencies. The baseline manipulation techniques performed evenly in almost all combinations.

Figure 6-6 shows graphically the performance achieved by 84 out of the 140 different combinations of signal processing techniques tested in Experiment #4. In this experiments we tested smell –sources that are sampled using the smart-sniff inhaling mode proposed in this thesis. The two databases tested have very different characteristics. The Fragrances database is constituted by a few but very strong smells produced by essential oils. The 25_Smells database is constituted by a wide gamut of smells ranging from very weak smells to very strong ones. A quick glance to this figure reveals a general good performance achieving between 60% and 70% detection efficiency in the worse cases. The STD, ATD and WSD (in this order) feature-vector extraction techniques produced the best results. The normalization techniques: VNORM and VAS together with the baseline manipulation techniques: DIFF and LOG were almost always present in the combinations that produced the best smell detection efficiencies.

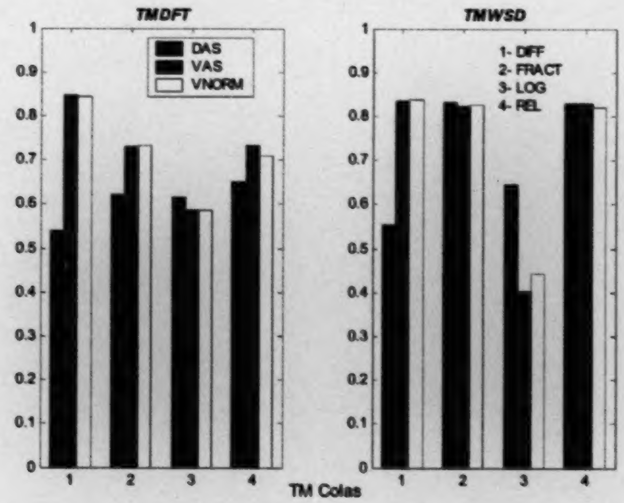

Figure 6-2 Bars plot of the detection efficiencies achieved in Experiment #5

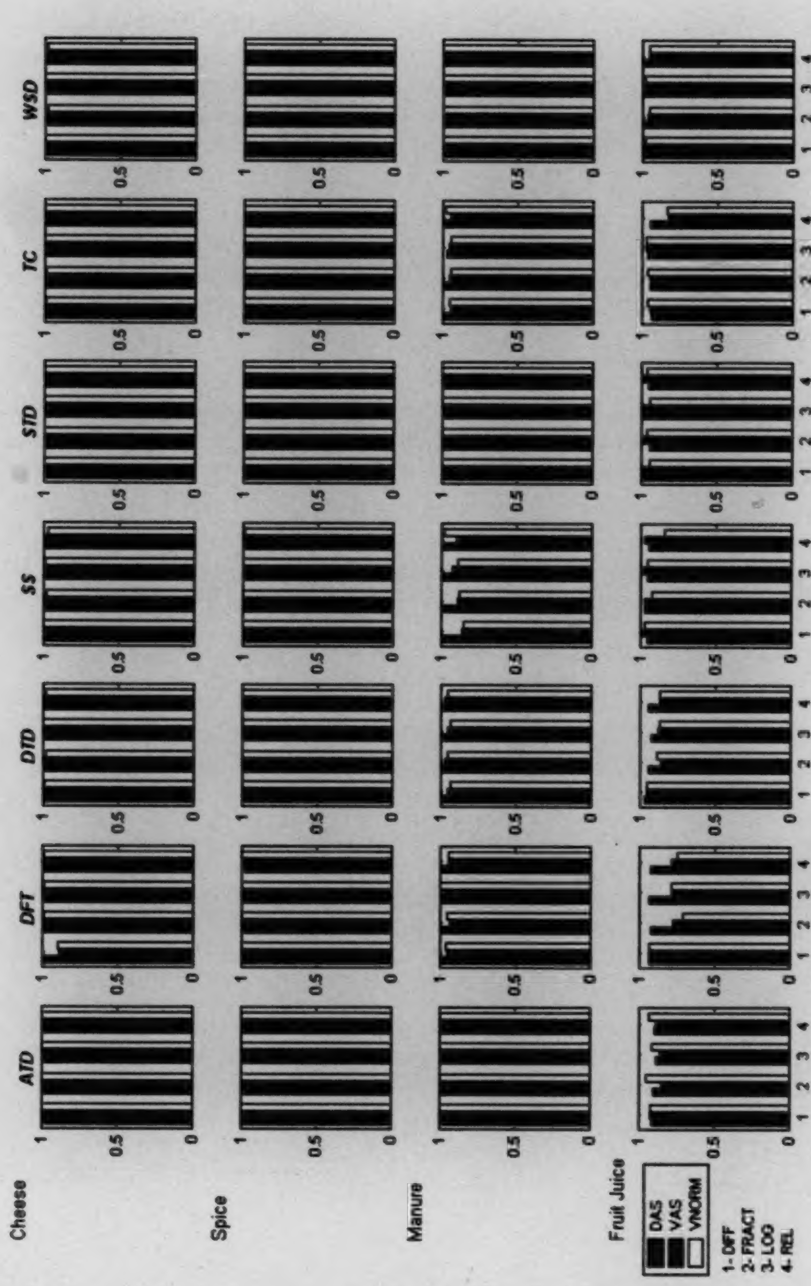

Figure 6-3 Bars plot of the detection efficiencies achieved in Experiment #1

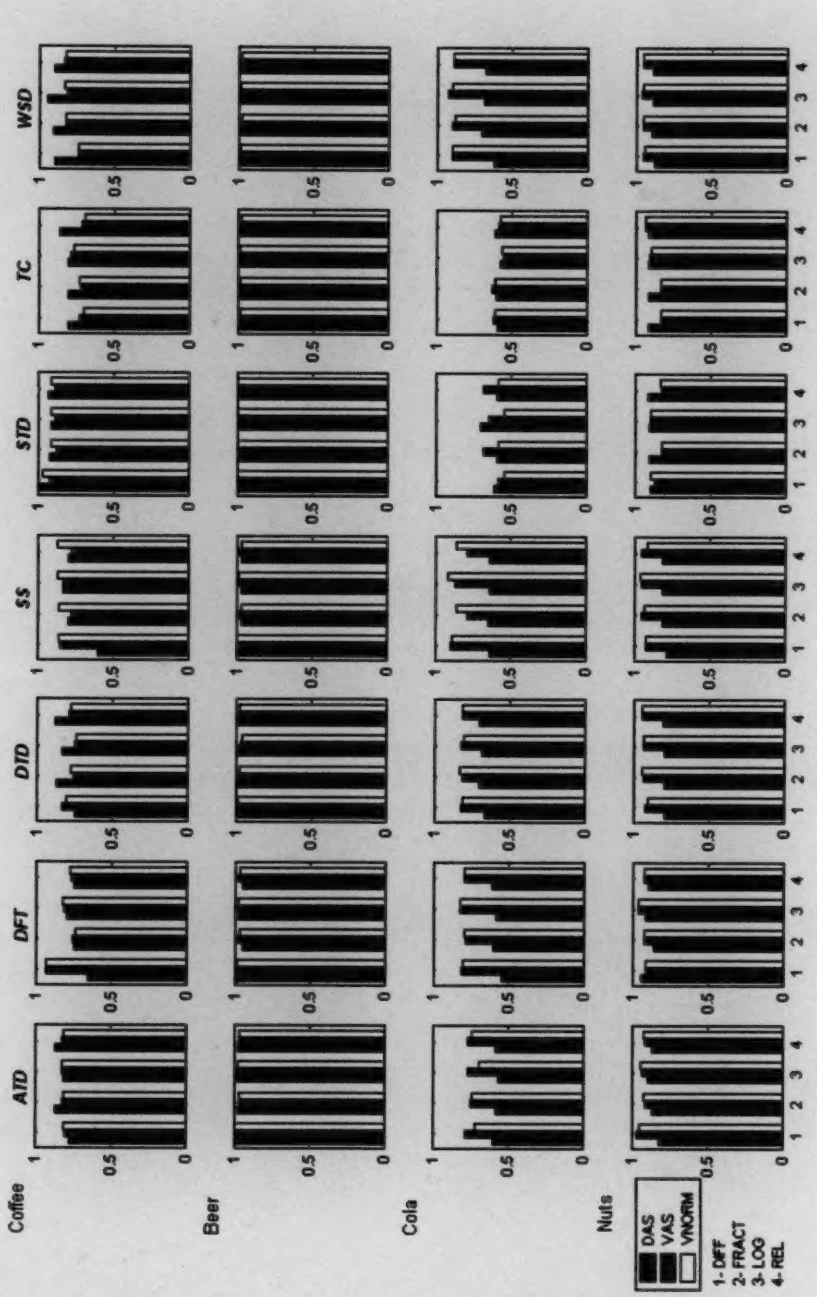

Figure 6-4 Bars plot of the detection efficiencies achieved in Experiment #2

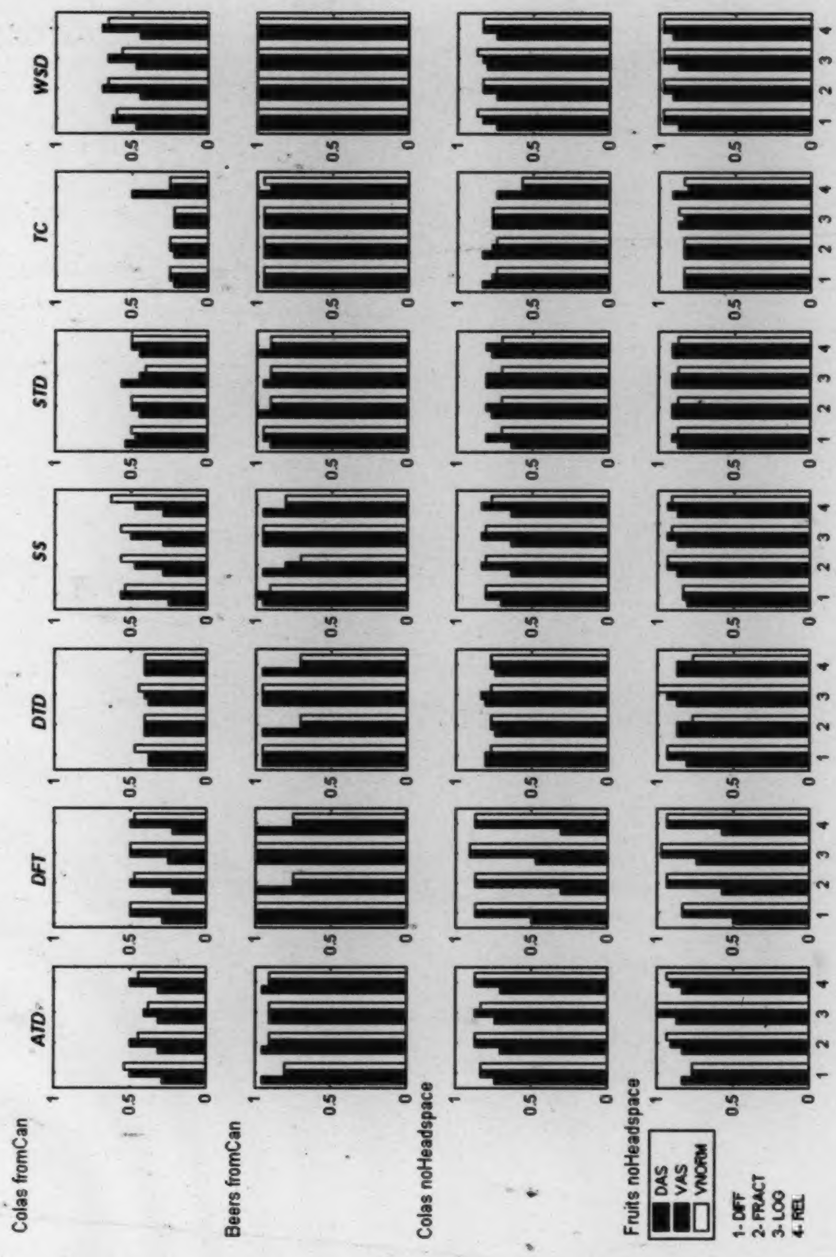

Figure 6-5 Bars plot of the detection efficiencies achieved in Experiment #3

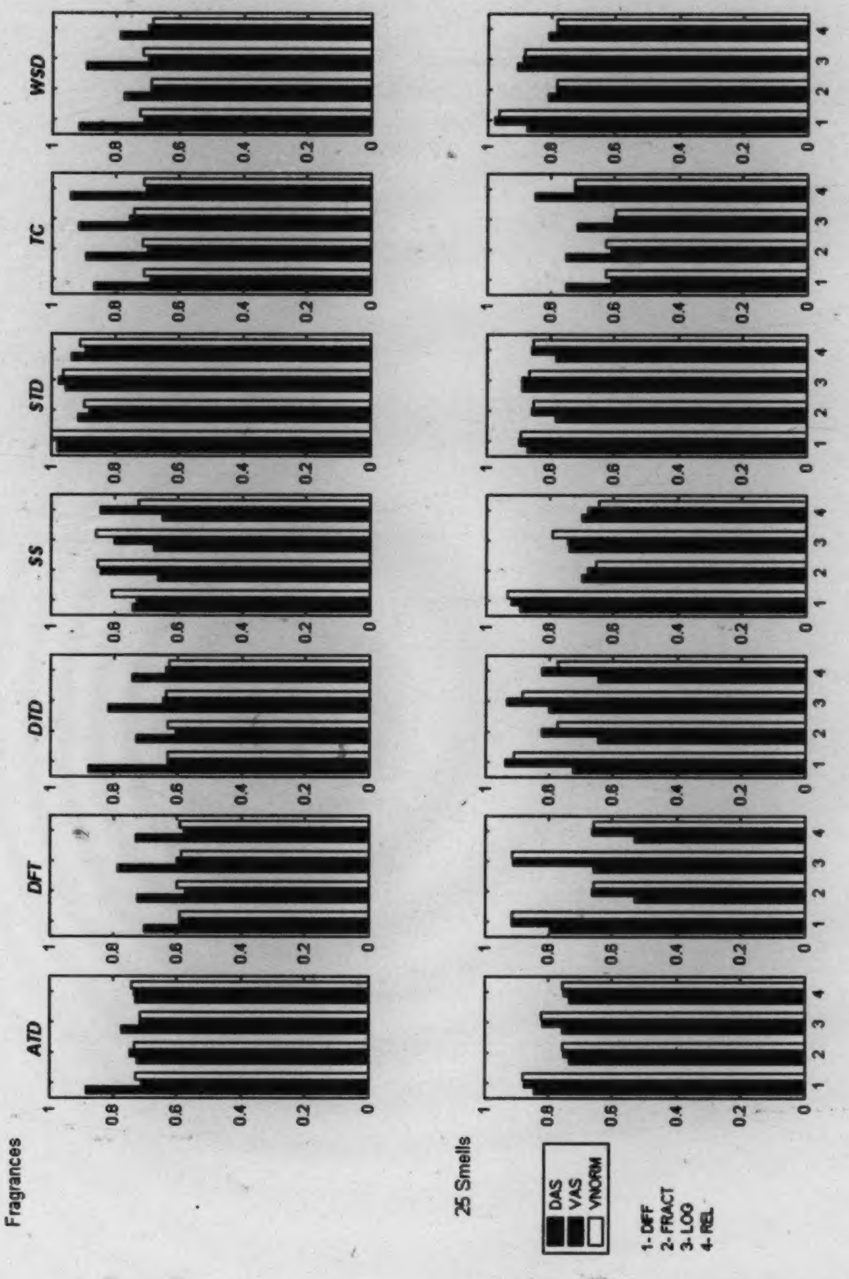

Figure 6-6 Bars plot of the detection efficiencies achieved in Experiment #4

6.2.5 Conclusions

In this chapter we have analyzed the performance of eNose with many different combinations of signal processing techniques. After applying these techniques an a variety of smell databases, we can conclude that the smell environment (i.e., the smell-database) targeted by a particular application must be matched with a specific combination of signal processing techniques in order to achieve maximum performance.

We found that the feature-vector extraction techniques STD, proposed in this thesis (see Section 5.2.2.3.3), provided in general very good performance. On the other hand, the feature-vector extraction techniques: DFT and TC produced poor performance.

The STD technique is based on the WSD signal derivatives extraction technique. The STD technique achieved superior or similar smell detection efficiency in 10 out of the 14 databases where it was used. The smell detection efficiency scored in these four databases was just slightly smaller than the values scored with the WSD technique (see Colas-From-Can and Fruit-No-Headspace in Figure 6-5 and Colas and Nuts in Figure 6-4). The STD technique is also 3.5 times less compute intensive than WSD due to a smaller number of features extracted with this feature-vector (16 features) compared to that of WSD (56 features). Finally, the fact that fewer features constitute the smell-pattern produced with STD helps to reduce the risk of over-fitting the classifier [47], [48] on the small size training sets that are typical in machine olfaction applications.

The smart-sniff technique, proposed in this thesis (see Section 4.6), also produced very good performances with 87% averaged detection efficiency for two different smell-databases. This is a very good result considering the large number and diverse types of smell-sources tested. These smell-sources ranged from almost imperceptible to very strong smells.

We also found that the use of any of the normalization techniques is a primary factor for a good smell detection efficiency score. For example, the combinations using the normalization techniques: "VNORM" and "VAS" consistently produced good detection efficiency scores. On the other hand, almost all the worse scores achieved in our experiments were based in combinations that did not use a normalization technique (look in Table 6-9 and Table 6-10 for combinations that end with the acronym "NONR").

Finally, the Baseline Manipulation Techniques do not seem to have great influence in the results scored in our performance evaluation experiments. For example, three out of the seven winner combinations in Table 6-10 do not use any Baseline Manipulation techniques (acronym "NOBM"). Observing bar plots in Figure 6-3 to Figure 6-2, we also cannot find any general and clear tendency where Baseline Manipulation technique produces better or worse detection efficiency as almost all of them produce relative same performance. However, a small tendency can be noticed in Figure 6-2, where the logarithmic (LOG) technique diminishes the performance in the two cases compared. A weak tendency can also be noticed in the database "25_Smells" in Figure 6-6, where it seems that the difference (DIFF) technique and the logarithmic (LOG) technique produce the best results in the seven cases compared.

6.3 Summary

In this chapter, we presented the performance evaluation of our eNose. First, we introduced the objectives of this performance evaluation, the evaluation procedure and a detailed explanation of the proposed smell experiments. Following we presented the proposed methods for collecting the smell databases, sampling the VOM from the smell sources and the smell sniff settings used. We then presented the results of the performance evaluation experiments and examined the influence of different combinations of signal processing techniques in the smell detection efficiency.

Chapter 7

Conclusions and Future Work

Electronic noses have been around for more than twenty years and the research in this field has been growing steadily during all this time. In recent years an exponential jump has taken place and electronic noses reached the commercial markets targeting several sectors of the world global economy such as food, perfumery health and environmental applications. However, these devices are designed for specific applications and they are still too expensive for acquisition by the general consumer. As a result these enoses are not yet suitable for integration with multimedia systems.

In this thesis, we have presented the design and implementation of an electronic nose using inexpensive off-the-shelf components: as is shown in Chapter 4 a low electronic nose suitable for integration into multimedia systems that can detect tens of commonly occurring smells have been developed. We have also developed a software system to allow the analysis, testing and performance evaluation of several smell signal processing techniques and pattern recognition algorithms (see Section 5.3). This software system is expandable allowing the addition of more smell-signal processing techniques and smell-pattern analysis methods into the currently developed framework.

A simple solution for the poisoning problem that typically affects the electronic noses when strong smells are sniffed has been proposed and tested (see Section 4.6).

We have found that each different smell environment must be matched to a specific combination of signal processing techniques in order to achieve maximum smell discrimination performance: as shown in Section 6.2.3.

We also found that using the derivative values from the signal steady state transient region (STD) produce in general better smell discrimination efficiency than using derivative values from the whole signal (see Section 6.2.5).

7.1 Summary of Contributions

There are four main contributions of this thesis into the area of machine olfaction:

- A low cost electronic nose suitable for integration with multimedia systems has been implemented and tested.

- A complete software system to allow the analysis, testing and performance evaluation of several smell signal processing techniques and pattern recognition algorithms has been implemented and tested. This software infrastructure can be also used as a development platform for further research in the area of smell detection (see Section 5.3).

- A novel smell sniffing technique for machine olfaction applications has been proposed, implemented and tested (see Section 4.6).

- An improvement to the whole smell-signal derivatives (WSD) feature-extraction technique has been proposed and successfully tested. The proposed technique (STD) produces equal or better performances than WSD extracting only two derivative values from each smell-signal in contrasts to the seven values extracted by the WSD technique (see Section 5.2.2.3.3).

7.2 Future Work

To reduce the recovery time between two consecutive smell sniffs is an important goal to address in future research. Reducing this recovery time will allow the use of the eNose in online applications such as quality control in production lines, etc. The speed of the sniff-cycle can be improved by reducing the size and number of the smell sensors and the volume of the smell-sensing chamber. Therefore, more research is needed to identify which sensors are redundant in most smell environments and try to keep the smaller sensors in the array.

More research is needed regarding the TM feature-vector extraction techniques implemented in the eNose. In this thesis, we tested a simple temperature modulation function combined with two conventional feature-vector extraction techniques (see Section 5.2.2.5). However, more complex voltage modulation functions can be used such as sinusoidal, square or triangle at several frequencies and amplitudes [44].

It is well known in the machine olfaction field that the water vapor in the ambient has huge impact in the sensors response and degrades considerably the smell detection efficiency of electronic noses. We did not address these issues because our experiments were realized in stable lab conditions. This is definitively a line for future research with the eNose.

The response of the smell sensors is in general dependent on the concentration of VOM. In most of the smell experiments, we used same volume of the smell source aiming to keep similar concentration levels among the smells tested. It would be an interesting future work to test the eNose performance using variable concentration of VOM.

Another factor of consideration for future work is the background-smells in the ambient. The background-smell is a source of interference and noise that can degrade considerably the performance of the electronic nose devices. A solution typically implemented in expensive devices is to flush out the sensors chamber with an inert gas such as nitrogen before each sniff. In the eNose, the exhaust pipes were placed far from the smell inlet and the smell source was kept isolated in the concentration flask to avoid the background smells from mixing with the air used for flushing out the chamber.

Finally, an important future line of work is the design and construction of a portable electronic nose for smell data collection in the field, which could be used in applications such as environmental monitoring and other agricultural applications.

References

[1] R.W. Moncrieff, "An instrument for measuring and classifying odours", *J. Appl. Physiol.*, no. 16, pp. 742-749, 1961.

[2] J. W. Gardner, "Pattern recognition in the Warwick Electronic Nose", *8th International Congress of European Chemoreception Research Organization*, July, 1987.

[3] R. Castro, M. K. Mandal, P. Ajemba, and M. Istihad, "A Low Cost Smell Detection System for Multimedia Applications," *IEEE Transactions on Consumer Electronics*, Vol. 49, No. 4 (2003), pp. 1431-1437.

[4] Cyrano Sciences, http://www.cyranosciences.com/. Note that Cyrano Sciences web site was taken down recently. The Smiths Group, www.smithsdetection.com, acquired Cyrano Sciences on May 2004.

[5] Q. Guogliang, "The measurement of odor concentration", Ph.D thesis, University of Alberta Bruce Speel Special Collections, 00D QUG, 2000.

[6] R. Harper, E. C. B. Smith, and D. G. Land, Odour Description and Odour Classification, New York, American Elsevier Pub. Co., 1968.

[7] W. Göpel, "Chemical Imaging: I. Concepts and visions for electronic and bioelectronic noses," Sensors and Actuators B, vol. 52, pp. 125-142, 1998.

[8] R. Olafsson, E. Martinsdottir, G. Olafdottir, S. I. Sigfusson and J. W. Gardner, "Monitoring of fish freshness using tin oxide sensors," *Sensors and sensory systems for an electronic nose,* Kluwer Academic, ISBN 0792316932, pp. 257-272, 1992.

[9] T. Tan, Q. Lucas, L. Moy, J. W. Gardner and P. N. Bartlett, "The electronic nose - a new instrument for sensing vapours," *LC – GC Int.*, no. 8, pp. 218-225, 1995.

[10] T. Aishima, "Aroma discrimination by pattern recognition analysis of responses from semiconductor gas sensors array," *Journal of Agricultural and Food Chemistry,* vol. 39, pp. 752-756, 1991.

[11] T. Aishima, "Discrimination of liqueur aromas by pattern recognition analysis of responses from a gas sensor array," *Analytica Chimica Acta*, vol. 243, 1991.

[12] J. W. Gardner, H. V. Shurmer and T. T. Tan, "Application of an electronic nose to the discrimination of coffees," *Sensors and Actuators B,* vol. 6, pp. 71-75, 1994.

[13] I. Simon, N. Barsan, M. Bauer, and U. Weimar, "Micromachined metal oxide gas sensors: opportunities to improve sensor performance," *Sensors and Actuators B,* vol. 73, pp. 1-26, 2001.

[14] J. W. Gardner and P. N. Bartlett, "Electronic noses: principles and applications", *Oxford University Press*, New York, 1999.

[15] A. Hierlemann, U.Weimar, G. Kraus, M. Schweizer-Berberich, W. Göpel, "Polymer-based sensor arrays and multicomponent analysis for the detection of hazardous organic vapors in the environment", *Sensor and Actuators B*, vol. 26-27, pp. 126-134, 1995.

[16] M. Bicego, G. Tessari, G. Tecchiolli and M. Betinelli, "A comparative analysis of basic recognition techniques for the development of small size electronic nose," *Sensors and Actuators B,* vol. 85, pp. 137-144, 2002.

[17] J. W. Gardner, T. C. Pearce, P. N. Bartlett and N. Blair "A multisensor system for beer flavour monitoring using an array of conducting polymers and predictive classifiers", *Sensors and Actuators B,* vol. 18, pp. 240-243, 1994.

[18] T. Nakamoto, A. Iguchi and T. Moriizumi, "Vapor supply method in odor sensing system and analysis of transient sensor responses", *Sensors and Actuators B,* vol. 71, pp. 155-160, 2000.

[19] J. V. Hatfield, P. Neaves, P. J. Hicks, K. C. Persuad and P. Travers, "Towards and integrated electronic nose using conducting polymer sensors," *Sensors and Actuators B,* vol. 26-27, pp. 221-228, 1994.

[20] L. Ratton, T. Kunt, T. McAvoy, T. Fuja, R. Cavicchi and S. Semancik, "A comparative study of signal processing techniques for clustering microsensor data (a first step towards an artificial nose)," *Sensors and Actuators B,* vol. 41, pp. 105-120, 1997.

[21] H.Miwa, T. Umetsu, A. Takanishi and H. Takanobu, "Human-like Robot Head that has Olfactory Sensation and Facial Color Expression," *Proc. of the 2001 IEEE. International Conference on Robotics & Automation,* Seoul, Korea, May 21-26, 2001.

[22] Y. Kunugi, K. Nigorikawa, Y. Harima and K. Yamashita, "A selective organic vapour sensor based in simultaneous measurements of changes in mass and resistance polypyrrole thin film", *J. Chem. Soc., Chem. Commun.*, pp. 873-874, 1994.

[23] P. Ingleby, J. Covintong, J. W. Gardner and P. N. Bartlett, "Dual resistance-mass polymeric sensor for improved gas sensing", *10th Eur. Conf. Solid-State Transducers (Eurosensors X), Leuven, Belgium*, Sept., 1996.

[24] Figaro Engineering Inc., www.figarosensor.com.

[25] W. F. Wilkens, J. O. Hartman, "An electronic analog for the olfactory processes," *Ann. N. Y. Acad. 116*, pp. 608-612, 1964.

[26] J. W. Gardner and P. N. Bartlett, "A brief history of electronic noses," *Sensors and Actuators B*, vol. 18-19, pp. 211 - 220, 1994.

[27] D. C. David and J W. Gardner, "High-precision intelligent interface for a hybrid electronic nose," *Sensors and Actuators A*, vol. 62, pp. 724-728, 1997.

[28] H.T. Chueh and J. V. Hatfield, "A real-time data acquisition system for a hand-held electronic nose (H2EN)," Sensor *and Actuators B*, vol. 83, pp. 262 - 269, 2002.

[29] J. Mizsei and S. Ress, "Chemical images by artificial olfactory epithelia," *Sensor and Actuators B*, vol. 83, pp. 164-168, 2002.

[30] S. Roussel, G. Forsberg, V. Steinmetz, P. Grenier and V. Bellon-Maurel," Optimisation of electronic nose measurements. Part I: Methodology of output feature selection", *Journal of Food Engineering*, Vol. 37, pp. 207-222, 1998.

[31] E. Llobet, J. Brezmes, X. Vilanova, J.E. Sueiras and X. Correig, "Qualitative and quantitative analysis of volatile organic compounds using transient and steady-state responses of a thick-film tin oxide sensor array", *Sensors and Actuators B*, vol. 41, pp. 13–22, 1997.

[32] F. Hossein-Babaei and M. Orvatinia "Gas diagnosis based on selective diffusion retardation in an air filled capillary", *Sensors and Actuators B*, vol. 96, pp. 298-303, 2003.

[33] C. Distante, M. Leo, P. Siciliano, K. C. Persaud, "On the study of feature extraction

methods for an electronic nose", *Sensors and Actuators B,* vol. 87, pp. 274-288, 2002.

[34] R. G. Osuna and H. T. Nagle, "A Method for Evaluating Data-Preprocessing Techniques for Odor Classification with an Array of Gas Sensors", *IEEE Transactions on System, Man, and Cybernetics – Part B: Cybernetics,* vol. 29, pp. 189-202, 1999.

[35] J. W. Gardner, M. Craven, C. Dow, and E. L. Hines, "The prediction of bacteria type and culture growth phase by an electronic nose with a multi-layer perceptron network," *Meas. Sci. Technol.*, vol. 9, pp. 120–127, 1998.

[36] T. Eklöv, P. Mårtensson and I. Lundström, "Enhanced selectivity of MOSFET gas sensors by systematical analysis of transient parameters", *Analytica Chimica Acta,* vol. 353, pp. 291-300, 1997.

[37] H. E. Endres, W. Göttler, H. D. Jander, S. Drost, G. Sberveglieri, G. Faglia and C. Perego, "A systematic investigation on the use of time-dependent sensor signals in signal-processing techniques", *Sensors and Actuators B,* vol. 25, pp.785-789, 1995.

[38] E. Llobet, J. Brezmes, R. Ionescu, X. Vilanova, S. Al-Khalifa, J. W. Gardner, N. Bârsan and X. Correig, "Wavelet transform and fuzzy ARTMAP-based pattern recognition for fast gas identification using a micro-hotplate gas sensor", *Sensors and Actuators B,* vol. 83, pp. 238-244, 2002.

[39] J. Samitier, J. M. López-Villegas, S. Marco, L. Cámara, A. Pardo, O. Ruiz and J. R. Morante, "A new method to analyze signal transients in chemical sensors", *Sensors and Actuators B,* vol. 18, pp. 308-312, 1994.

[40] R. G. Osuna, H. T. Nagle, S. S. Schiffman, "Transient response analysis of an electronic nose using multi-exponential models", *Sensors and Actuators B*, vol. 61, pp. 170-182, 1999.

[41] A. P. Lee and B. J. Reedy, "Temperature modulation in semiconductor gas sensing", *Sensors and Actuators B,* vol. 60 (1999), pp. 35-42.

[42] W. M. Sears and K. Colbow, "Algorithms to improve the selectivity of thermally-cycled tin oxide gas sensors", *Sensors and Actuators,* vol. 19, pp. 333-349, 1989.

[43] A. Heilig, N. Bârsan, U. Weimar, M. Schweizer-Berberich, J. W. Gardner and W. Göpel,

"Gas identification by modulating temperatures of SnO_2-based thick film sensors", *Sensors and Actuators B,* vol. 43, pp. 45-51, 1997.

[44] X. Huang, J. Liu, D. Shao, Z. Pi and Z. Yu, "Rectangular mode of operation for detecting pesticide residue by using a single SnO2-based gas sensor", *Sensor and Actuators B,* article in press available on line at www.sciencedirect.com, 2003.

[45] T. Eklöv, P. Mårtensson and I. Lundström, "Selection of variables for interpreting multivariate gas sensor data", *Analytica Chimica Acta,* vol. 381, pp. 221-232, 1999.

[46] R. G. Osuna, "Pattern Analysis for Machine Olfaction: A Review", *IEEE Sensors Journal,* vol. 2, pp. 189-202, 2002.

[47] A. K. Jain, R. P. W. Duin, and J. Mao, "Statistical Pattern Recognition: A Review", IEEE Transactions on Pattern Analysis and Machine Intelligence, vol. 22, pp. 4-37, 2000.

[48] S. M. Weiss and C. A. Kulikowski, "Computer systems that learn: classification and prediction methods from statistics, neural nets, machine learning, and expert systems", *Morgan Kaufmann Publishers Inc.*, 1990.

[49] J. Edward Jackson, "A user's guide to principal components", *John Wiley & Sons, Inc., New York,* 1991.

[50] W. Gardner, "Detection of vapours and odours from a multisensor array using pattern recognition Part 1. Principal component and cluster analysis", *Sensors and Actuators B,* vol. 4, pp. 109-115, 1991.

[51] M. Penza and G. Cassano, "Application of principal component analysis and artificial neural networks to recognize the individual VOCs of methanol/2-propanol in a binary mixture by SAW multi-sensor array", Sensors and Actuators B, Vol. 89, pp. 269-284, 2003.

[52] T. M. Cover and P. E. Hart, "Nearest neighbor pattern classification", *IEEE Transactions on Information Theory,* vol. 13, pp. 21-27, 1967.

[53] K. Fukunaga and P. E. Hart, "Bias of Nearest Neighbor Error Estimates", *IEEE Transactions on Pattern Analysis and Machine Intelligence,* vol. 9, pp. 103-112, 1987.

[54] S. J. Raudys and A. K. Jain, "Small Sample Size Effects in Statistical Pattern Recognition: Recommendations for Practitioners", *IEEE Transactions on Pattern Analysis and Machine Intelligence,* vol. 13, pp. 252-264, 1991.

[55] K. Fukunaga and R. R. Hayes, "Estimation of Classifier Performance", *IEEE Transactions on Pattern Analysis and Machine Intelligence,* vol. 11, pp. 1087-1101, 1989.

[56] S. M. Weiss, "Small Sample Error Rate Estimation for k-NN Classifiers", *IEEE Transactions on Pattern Analysis and Machine Intelligence,* vol. 13, pp. 285-289, 1991.

[57] Bernardin Ltd., www.homecanning.com

[58] J. Brezmes, E. Llobet, X. Vilanova, G. Saiz and X. Correig, "Fruit ripeness monitoring using an Electronic Nose", *Sensors and Actuators B,* vol. 69, pp. 223-229, 2000.

[59] Ishizuka Electronics Corporation, www.semitec.co.jp/english/indexe.htm

[60] Bukert Fluid Control Systems, www.burkert.com

[61] Hagen, www.hagen.com

[62] National Instruments, www.ni.com